Service Altimetrie & Localisation Precise

CalVal Saral/ Altika

SARAL/Altika validation and cross calibration activities

Annual report 2017

Contract No 14026/00 – 160182 - lot 1.6.3

Reference : -

Nomenclature : SALP-RP-MA-EA-23188-CLS

Issue : 1rev 2

Date : February 20, 2018

CLS - 11 Rue Hermès - Parc Technologique du Canal - 31520 Ramonville St-Agne - FRANCE
Telephone 33 5 61 39 47 00 / Fax 33 5 61 75 10 14

Chronology Issues:		
Issue:	Date:	Reason for change:
1.0	Jan 08, 2018	Creation
1.1	Jan 31 , 2018	Delivery
1.2	Feb 20, 2018	Revised version

People involved in this issue :	AUTHORS	COMPANY	DATE	INITIALS
Written by:	G. Jettou; P. Prandi	CLS		
Checked by:	S. Labroue	CLS		
Approved by:	J.-P. Dumont	CLS		
Application authorised by:				

Index Sheet :	
Context:	
Keywords:	
Hyperlink:	

Distribution:		
Company	Means of distribution	Names
CLS/DOS	electronic copy	mablain@cls.fr slabroue@cls.fr
CNES	electronic copy	thierry.guinle@cnes.fr nicolas.picot@cnes.fr Gerald.Dibarboure@cnes.fr Nadege.Queruel@cnes.fr dominique.chermain@cnes.fr delphine.vergnoux@cnes.fr aqgp_rs@cnes.fr

List of tables and figures

List of Tables

List of Figures

List of items to be defined or to be confirmed

Applicable documents / reference documents

Contents

1. Introduction

1.1. Executive summary

This document presents the synthesis report concerning validation activities of SARAL/AltiKa GDRs in 2017 under SALP contract supported by CNES at the CLS Space Oceanography Division.

The present report covers different topics, which are investigated either as part of routine Cal/Val activities, or following mission events:

- mono-mission validation and monitoring,
- cross-calibration between SARAL/AltiKa and Jason-2 / Jason-3,

Results presented in this document are mainly based on the current version of GDR data (GDR-T Patch2). Sometimes results using IGDR, OGDR, or updated GDR data are also shown. This is mentioned in the text when needed. The content of the Patch2 reprocessing of SARAL/AltiKa data can be found at chapter 10.2.. A detailed evaluation of the impacts of Patch 2 on mission performance was performed in 2014 when the reprocessing occured by [22, Philipps and Pignot]. Hereafter a brief summary of the main results presented in this report.

Data coverage and parameters monitoring

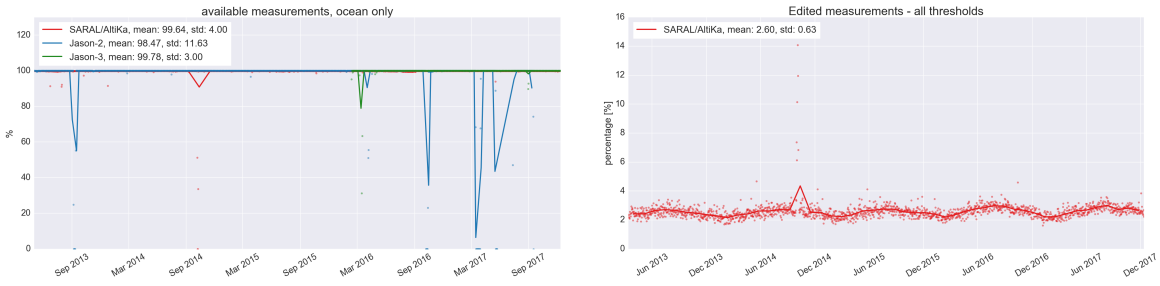

Figure 1: *Monitoring of GDR data since the beginning of mission (cycles 1 to 114). Percentage of available (left) and edited (right) measurements (on thresholds critiria).*

Considering all surface types, SARAL/AltiKa has an average of 96.82% of available data over its lifetime (March 2013 - January 2018). When considering only the ocean surface, the mean value of available measurements for SARAL/AltiKa is around 99.6%. SARAL/AltiKa had some periods with reduced data availability. All these events are described in table 3.
In any case, these figures largely exceeds the specifications for SARAL/AltiKa, which were 95% of all possible over-ocean data during a 3-year period with no systematic gaps plus the specific Ka-band limitation (5% of measurements may be not achieved due to rain rates > 1.5 mm/h according to geographic areas).
As for edited measurements, on average 20.08% of ocean measurements are edited, the majority of which are removed due to the sea ice flag $\approx 17.5\%$ while only $\approx 2.5\%$ are removed by threshold

Figure 2: *Monitoring of along track averages of standard deviation of range measurements (left), of retracking and platform mispointing (right), and latitude weighted box average of significant wave height(bottom).*

editing criteria. Statistics for the main parameters of SARAL/AltiKa are routinely monitored since the beginning of the mission and have been updated until cycle 114. Note that because of the several SHM periods that has been experienced by Jason-2 in 2017, the monitorings of parameters will include Jason-2 and Jason-3 to cover up for Jason-2's gaps and have a continuous comparisons over SARAL/AltiKa's lifetime. This systematic monitoring aims at detecting changes in parameter statistics, that would indicate a problem on the mission. No significant change has been noticed in 2017.

Crossovers analysis

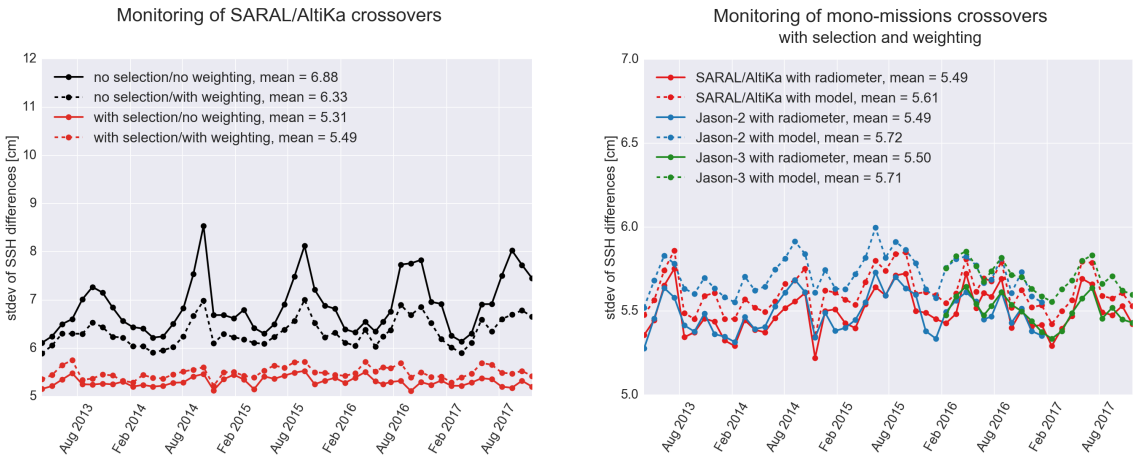

Figure 3: *Cycle per cycle monitoring of standard deviation of SSH differences at mono-mission crossovers - cycles 1 to 114.*

At each crossover, the observed difference of SSH measurements between ascending and descending arcs results from the sum of errors in the system and ocean variability. In order to reduce the impact of ocean variability, an additional selection can be applied to remove shallow waters (bathymetry above -1000 m), areas of high ocean variability (variability above 20 cm rms) and high latitudes ($|lat| < 50$ deg). To account for the uneven distribution of crossover points, we estimate weighted statistics (figure 3) where the weights applied are based on the crossovers density. This allows to better compare two missions that do not share the same ground track. Similar results are obtained with these weighted statistics: depending on the chosen wet troposphere correction, SARAL/AltiKa's performance is equivalent to Jason's.

Sea level anomaly

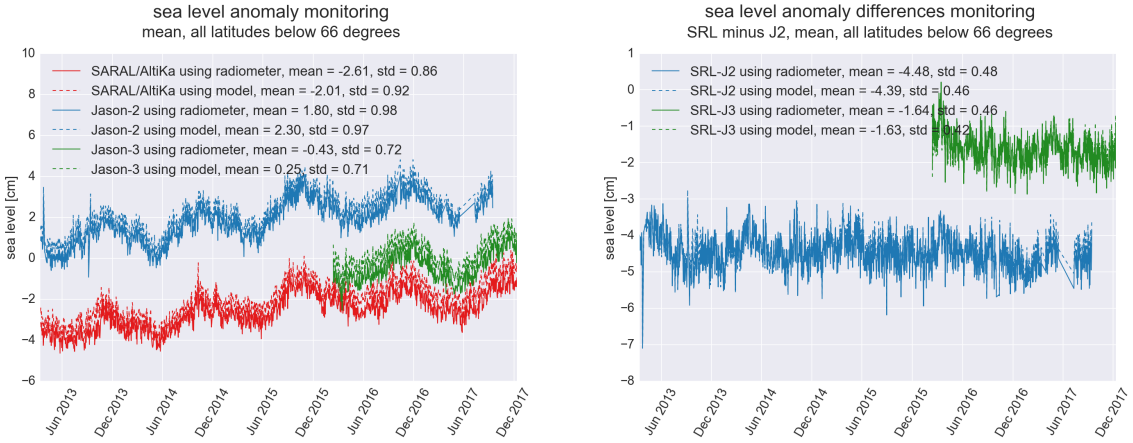

Figure 4: *Monitoring of daily mean (left) of SLA of GDR data using the radiometer (plain lines) and the model (dotted lines) wet tropospheric corrections. Global statistics are estimated for all latitudes between* -66 *and* 66 deg

Looking at along-track SLA provides additionnal metrics to estimate the altimetry system performances. The evolution of the mean SLA allows the detection of shifts, drifts or geographically correlated biases, while looking at the SLA variance may also highlight changes in the long-term stability of the altimeter's system performance.
SARAL/AltiKa Jason-2 and Jason-3 daily mean of SLA show similar signals and evolution.The standard deviation of daily averages of SLA differences is below 5 mm. No statistically significant drift is observed between the missions and switching from the radiometer to the model wet tropospheric correction has little impact on daily averages of SLA differences between SARAL/AltiKa and Jason-2 or Jason-3.

1.2. SARAL/AltiKa: a brief history

SARAL/AltiKa is a joint CNES/ISRO mission which was successfully launched on February, 25th, 2013. The spacecraft reached its operationnal orbit on March, 13th, and cycle 1/pass 1 started on March 14th. At this time, the satellite was not exactly on the expected ground track (the historical ERS and Envisat ground track), with a difference up to 2 km at high latitudes. After inclination maneuvers, SARAL/AltiKa reached its nominal ground track on October, 7th 2013 (cycle 6).

During September 2014, several mispointing events occured, attributed to variations of reaction wheel friction. The reaction wheel eventually failed, resulting in SARAL/AltiKa going into safe-hold mode (SHM) from October 6th to 9th. Since then, the satellite has been experiencing occasional mispointing events.

Following the loss of the reaction wheel, station keeping maneuvers have been less accurate, and SARAL/AltiKa's ground track has been drifting (eastward and westward) from its nominal ground track, which has been loosely maintained (from March 2015 onward). On June, 29th, 2016, CNES and ISRO announced that the mission would enter a new phase after a last maneuver: the drifting phase (SARAL-DP). On July 4th, 2016, this last maneuver was performed to raise the spacecraft's altitude by 1 km, and leave him flying free of station keeping maneuvers. This new phase comes with a new numbering of cycles, starting at 100.

1.3. SARAL/AltiKa Cal/Val activities

Since the beginning of the mission, SARAL/AltiKa data have been analyzed and monitored in order to assess the quality of SARAL/AltiKa products. Cycle per cycle reports summarizing mission performance are generated and made available through the AVISO web page (http://www.aviso.altimetry.fr/en/data/calval/systematic-calval/validation-reports.html). Main performance metrics were also summarized in a paper published in the Marine Geodesy special issue on SARAL/AltiKa in 2015 [8]. Each year, the Cal/Val activity is described in a yearly report, which are also available through the AVISO website ([29] and [10]).

The present report documents the activities undertaken in the framework of the SALP contract to assess and monitor Saral/AltiKa data quality. Depending on the sections the period considered may vary slightly. In general, all data from cycle 1 to 114 are considered (corresponding to March 2013 to January 2018). This period might be reduced (to end at cycle 112 or 113) for some plots. We present a detailed description of the main performance metrics of the mission including:

- monitoring of missing and edited parameters,
- analysis of geophysical parameters and corrections,
- accuracy and stability of SLA measurements.

We also present the results of cross-calibration analysis performed between SARAL/AltiKa, Jason-2 and Jason-3. Even if the three satellites are on different ground tracks comparisons remain possible, and necessary, to ensure the continuity of ocean observations through high precision altimetry.

Routine validation of SARAL/AltiKa mission and cross-calibration with Jason-3 activities generate

a large number of graphs, plots and figures. The purpose of the present report is to give the reader a useful and as much as possible reader-friendly summary of the most important results of the daily monitoring of the mission performed at CLS.

This report also presents the results of particular investigations undertaken this year on SARAL/AltiKa, either to better characterize mission performance or as a consequence of mission events.

2. Processing status

2.1. Processing history

Four months after launch, SARAL/AltiKa OGDR and IGDR data were available to all users beginning of July 2013. They were first released under the version T label, with some flaws (unit problem for liquid cloud water,...), some corrections voluntarily disabled (atmospheric attenuation set at default value) or with disclaimers of product fields (ice_flag, altimeter wind not to use, ...).

Some of these issues were addressed by Patch 1, whose content is recalled in 10.1.. Beginning of September 2013 the GDR products were released with consistent Patch 1 standards since the beginning of the mission.

A second processing upgrade, labeled Patch 2, containing several improvements for SARAL/AltiKa data, was applied on February 2014. The content of this Patch 2 is recalled in chapter 10.2. This included a full reprocessing of previous GDR cycles.

Further on, orbit standard changed from GDR-D to GDR-E from June 30th, 2015 onwards on IGDR and from cycle 25 (July 3rd) on GDR. To date, previous GDR cycles were not reprocessed. The mean sea surface was also updated from July 4th, 2016 onwards on IGDR data and from cycle 34 (May 12th) on GDR data. Again, previous GDR cycles were not reprocessed to date.

Table 1 summarizes the processing history of SARAL/AltiKa products through the application dates of main product versions.

Data version	Ogdr	Igdr	Gdr
Version T	till cycle 4 segment 0609	till cycle 4 pass 394	-
Version T with Patch1 (chapter 10.1.)	from cycle 4 segment 0611 onwards (2013-07-18 13h44m04)	from cycle 4 pass 0395 onwards (2013-07-10 23h56m18)	from cycle 1 pass 0001 onwards
Version T with Patch2 (chapter 10.2.)	from cycle 10 segment 0407 onwards (2014-02-06 10h46m58)	from cycle 10 pass 0566 onwards (2014-02-11 23h17m37)	from cycle 8 onwards (cycles 1 to 7 have been reprocessed)

Table 1: *Product versions*

2.2. Payload history

2.2.1. Acquisition/tracking modes

Table 2 shows the acquisition/tracking modes used since the beginning of the SARAL/AltiKa mission.

cycle	pass	start time	stop time	altimeter mode
1	0001-0200	2013-03-14	2013-03-21	DIODE acquisition / median tracking
1	0201-0400	2013-03-21	2013-03-28	DIODE acquisition / EDP tracking
1	0401-0600	2013-03-28	2013-04-04	DIODE acquisition / median tracking
1	0601-0800	2013-04-04	2013-04-11	DIODE / DEM tracking
1	0801-1002	2013-04-11	2013-04-18	DIODE acquisition / EDP tracking
2	0001-1002	2013-04-18	2013-05-23	DIODE acquisition / median tracking
3	0001-0400	2013-05-23	2013-06-06	DIODE acquisition / median tracking
3	0401-0800	2013-06-06	2013-06-20	DIODE acquisition / EDP tracking
3	0801-1002	2013-06-20	2013-06-27	DIODE acquisition / median tracking
4 to 9	0001-1002	2013-06-27	2014-01-23	DIODE acquisition / median tracking
10	0001-0127	2014-01-23	2014-01-27	DIODE acquisition / median tracking
10	0128-0135	2014-01-27	2014-01-27	autonomous DIODE / median tracking
10	0136-1002	2014-01-27	2014-02-27	DIODE acquisition / median tracking
11 to 16	0001-1002	2014-02-27	2014-09-25	DIODE acquisition / median tracking
17	0001-0324	2014-09-25	2014-10-06	DIODE acquisition / median tracking

.../...

cycle	pass	start time	stop time	altimeter mode
17	0414-0457	2014-10-09	2014-10-11	autonomous DIODE / median tracking
17	0457-1002	2014-10-11	2014-10-30	DIODE acquisition / median tracking
18 to 113	0001-1002	2014-10-30	2017-11-6	DIODE acquisition / median tracking
114	0001-0531	2017-11-06 15:58:04	2017-11-25 04:11:25	DIODE acquisition / median tracking
114	0532-0540	2017-11-25 04:13:19	2017-11-25 11:05:25	Autonomous acquisition / median tracking
114	0540-1002	2017-11-25 11:07:14	2017-12-11 15:06:21	DIODE acquisition / median tracking

Table 2: *Acquisition and tracking modes*

2.2.2. List of events

Table 3 summarizes the major events of the SARAL/AltiKa mission.

cycle	pass	start time	stop time	event
1		2013-03-14	2013-03-17	X-band stations acquisition problems (a few missing data)
1	0172-0175	2013-03-20 05:10:03	08:30	calibration I2+Q2 and I&Q for expertise
1	0266	2013-03-23 12:13:52	12:13:55	semi major axis maneuver
1	0372, 0374	2013-03-27		CAL2 long calibrations at 04:51 (28min missing data) and 06:40 (11min missing data)
1	0801	2013-04-11 04:42:00	04:59:45	altimeter gain calibration I2+Q2 (mostly over land)
1	0868	2013-04-13 12:53:52	12:53:54	station keeping maneuver
1	0898	2013-04-14 13:42:00	13:59:45	altimeter gain calibration I&Q (mostly over land)

.../...

cycle	pass	start time	stop time	event
1	0984	2013-04-17 13:47:00	14:04:45	altimeter gain calibration I2+Q2 (mostly over land)
2	0034, 0035	2013-04-19 9:37	10:25	cross calibration test over S-band station Biak (Indonesia)
2	0057	2013-04-20 04:53	05:12	altimeter gain calibration I&Q (over land)
2	0127	2013-04-22 15:26	15:54	cross calibration maneuver
2	0206	2013-04-25 9:53		pitch maneuver (0.045°) to correct the PF/RF alignment (alignment between the platform and the radiofrequency axis)
2	0355	2013-04-30 14:35	15:03	cross calibration maneuver
2	0782	2013-05-15 12:48:23	12:48:26	station keeping maneuver
3	0438	2013-06-07 12:25:11	12:25:13	station keeping maneuver
3	0887-0890	2013-06-23 05:06:55	06:56:57	no O/I/GDR product due to PLTM lost
3	0926	2013-06-24 13:31:11	13:31:13	station keeping maneuver
4	0498	2013-07-14 14:42:44	14:42:47	station keeping maneuver
4	0556	2013-07-16 15:01:01	15:19:00	altimeter gain calibration I&Q (mostly over land)
4	0586	2013-07-17 16:13:01	16:30:45	altimeter gain calibration I2+Q2 (mostly over land)
4	0911	2013-07-29 00:54:25	00:58:26	inclination maneuver (1 burn on Y and Z axis)
4	0984	2013-07-31 14:08:03	14:08:11	station keeping maneuver
5	0182	2013-08-07 13:48:06	13:48:09	station keeping maneuver
5	0726	2013-08-26 13:51:02	13:51:05	station keeping maneuver

.../...

cycle	pass	start time	stop time	event
5	0958	2013-09-03 16:02:01	16:20:00	altimeter gain calibration I&Q (mostly over land)
6	0038	2013-09-06 12:44:01	13:01:45	altimeter gain calibration I2+Q2 (over land)
6	0812	2013-10-03 13:55:39	13:57:17	1st inclination maneuver to reach the Envisat ground track (1 burn on Z axis)
6	0926	2013-10-07 13:29:45	13:31:25	2nd inclination maneuver to reach the Envisat ground track
6	0984	2013-10-09 14:07:52	14:07:57	station keeping maneuver
7	0526	2013-10-28 14:11:24	14:11:26	station keeping maneuver
7	0586	2013-10-30 16:11	16:28:45	altimeter gain calibration I2+Q2
7	0812	2013-11-07 13:57:01	13:57:03	station keeping maneuver
8	0326	2013-11-25 14:31:29	14:31:32	station keeping maneuver
8	0812	2013-12-12 13:56:58	13:57:01	station keeping maneuver
9	0240	2013-12-27 14:25:41	14:25:44	station keeping maneuver
10	0128	2014-01-27 16:15	16:32:45	altimeter gain calibration I2+Q2 (mostly over land)
10	0152	2014-01-28 12:38:43	12:38:45	station keeping maneuver
11	0126	2014-03-03 14:50:53	14:50:56	station keeping maneuver
11	0782	2014-03-26 12:47:17	12:47:20	station keeping maneuver
12	0438	2014-04-18 12:24:16	12:24:19	station keeping maneuver
12	0728	2014-04-28 15:12:55	15:30:45	expertise calibration CAL1

.../...

cycle	pass	start time	stop time	event
13	0326-0327	2014-05-19 14:31:18	14:31:21	station keeping maneuver with two consecutive mispointing events between 14:38 and 14:43 and between 15:03 and 15:12
14	0782	2014-07-09 12:47:10	12:47:12	station keeping maneuver
15	0356	2014-07-29 15:22:00	15:39:45	altimeter gain calibration I2+Q2 (mostly over land)
15	0782	2014-08-13 12:47:06	12:47:08	station keeping maneuver
16	0539	2014-09-09		No TM from 01:02:30 to 01:06:16 and from 01:09:25 to 01:14:08 due to the update of MNT onboard parameters
16	0640	2014-09-12 13:44:34	13:44:36	station keeping maneuver
16	0406 0474 0690	2014-09-04 09:44:24 2014-09-06 18:38:32 2014-09-14 07:36:44	09:47:15 18:41:55 07:38:50	several platform mispointing events caused by a rise in reaction wheel friction due to movement of lubricant. Only the 3 largest events are shown.
17	0324	2014-10-06 12:40:00	12:40:02	station keeping maneuver
17	0324-0414	2014-10-06 13:03:22	2014-10-09 16:27:46	safe hold mode
17	0438	2014-10-10 12:14:14	12:14:34	station keeping maneuver
17	0610	2014-10-16 12:26:26	12:26:35	station keeping maneuver
17	0958	2014-10-28 16:02:00	16:19:45	altimeter gain calibration I2&Q2
18	0152	2014-11-04 12:26:39	12:26:41	station keeping maneuver
18	0640	2014-11-21 13:39:10	13:39:12	station keeping maneuver

.../...

cycle	pass	start time	stop time	event
19	0182	2014-12-10 13:47:02	13:47:04	station keeping maneuver
19	0640	2014-12-26 13:44:42	13:44:45	station keeping maneuver
20		2015-01-12 11:30		software patch applied by ISRO in order to avoid zero-crossings of RW speed
20		2015-01-17	2015-01-18	platform pointing disturbance (fluctuations in RW friction)
20	0412	2015-01-22 14:31:03	14:31:06	station keeping maneuver
20	0586	2015-01-28 16:11		CNG calibration
21	0268	2015-02-21 13:47:56	13:47:58	station keeping maneuver
22	0354	2015-03-31 13:50:16	13:50:18	station keeping maneuver. Delta_Vy twice more than expected.
22	0610	2015-04-09 12:28:10	12:28:14	station keeping maneuver to stop the westward drift.
22	0986	2015-04-22 15:30		CNG calibration
23	0954	2015-05-26 12:51:07	12:51:12	station keeping maneuver. Delta_V applied twice less than expected. thruster firing has taken place between 10:00 to 10:04 UT to control a reaction wheel error guidance has been performed with thrusters (instead of RW)
24	0554	2015-06-16 13:23	13:39	station keeping maneuver (to calibrate satellite rotation with thrusters). The main objective is not to recover the nominal ground track but to calibrate this new way of performing satellite rotation
24		2015-06-30		introduction of a leap second =¿ UTC = TAI-36s The sequence of dates of the UTC second markers is: 2015 June 30, 23h 59m 59s 2015 June 30, 23h 59m 60s 2015 July 1, 0h 0m 0s
24		2015-06-30		First MOE with GDR-E orbit standard
25				Orbit standard = GDR-E

.../...

cycle	pass	start time	stop time	event
25	0182	2015-07-08 13:40:55	13:40:58	station keeping maneuver (only with thrusters). Thruster activity is expected from 13:31:50 UT to 13:50 UT
25	0758	2015-07-28 16:22		Altika quarterly expertise CNG calibration
26	0152	2015-08-11 12:32:56	12:32:59	station keeping maneuver (to stop western drift and stay in the +/-1km ground track window) only with thrusters
26	0524	2015-08-24 12:24:12	12:24:14	station keeping maneuver, performed only with thrusters.
26		2015-09-05	2015-09-06	mispointing events attributed to sudden changes in friction torque of reaction wheel (RW-4).
27		2015-09-15		Update of CoG historic file: the initial value of Zcog value has been updated by POD team and propagated to IDS teams through CoG historic file ; new value -0.6105 (instead of -0.6583)
28	0182	2015-10-21 13:41:40	13:41:43	station keeping maneuver
28	0195	2015-10-22		mising data due to issues on X-band stations network and the amount of TM_gaps
28	0614	2015-11-05 15:39		CNG Calibration
28	0812	2015-11-12 13:40:32	13:59:33	station keeping maneuver (3 bursts)
29	0210	2015-11-26 13:08:18	13:24:57	station keeping maneuver
30	0412	2016-01-07 14:28:48	14:44:39	station keeping maneuver
30	0986	2016-01-27 15:30:00	15:47:45	CNG calibration
31	0441-0442	2016-03-18 15:08:55	15:25:40	collision avoidance maneuver
33	0010	2016-04-07 13:18:44	13:34:31	station keeping maneuver
33	0528	2016-04-25 15:33:00	15:50:45	CNG Calibration

.../...

cycle	pass	start time	stop time	event
35	0522	2016-07-04 12:13:35	12:31:15	orbit change maneuver, cycle 35 ends at pass 522
101	0090	2016-08-11 15:54:00	16:11:45	CNG Calibration
103	0290	2016-10-27 15:47:00	16:04:45	CNG Calibration
105	0862	2017-01-25 15:43:00	16:00:45	CNG Calibration
108	0432	2017-04-25 15:38:00	15:55:45	CNG Calibration
111	0202	2017-07-31 15:11:00	15:28:45	CNG Calibration
113	0660	2017-10-25 15:30:00	15:47:45	CNG Calibration
114	0742	2017-12-02 12:32:08	12:48:47	collision avoidance maneuver

Table 3: *Main SARAL/AltiKa mission events (red rows indicates safe hold mode event)*

2.3. Models and Standards

Table 4 summarizes the contents regarding altimeter standards and geophysical correction models of the current version (T, Patch 2) of SARAL/AltiKa products.

Model	Product version "T" Patch2
Orbit	Based on Doris onboard navigator solution for OGDR DORIS tracking data for IGDR DORIS+SLR tracking data for GDR. Using POE-D, and POE-E from cycle 25
Altimeter Retracking	"Ocean MLE4" retracking: MLE4 fit from 2nd order Brown analytical model: MLE4 simultaneously retrieves 4 parameters from the altimeter waveforms: • Epoch (tracker range offset) → altimeter range • Composite Sigma → SWH • Amplitude → Sigma0 • Square of mispointing angle "Ice 1" retracking: Geometrical analysis of the altimeter waveforms, which retrieves the following parameters: • Epoch (tracker range offset) → altimeter range • Amplitude → Sigma0 "Ice 2" retracking: The aim of the ice2 retracking algorithm is to make the measured waveform coincide with a return power model, according to Least Square estimators. Retrieval of the following parameters: • Epoch → altimeter range • Width of the leading edge → SWH • Amplitude → Sigma0 • Slope of the logarithm of the waveform at the trailing edge → Mispointing angle/surface slope • the thermal noise level (to be removed from the waveform samples)

.../...

Model	Product version "T" Patch2
	"Sea Ice" retracking: In this algorithm, waveform parameterization based on peak threshold retracking is applied to the Ka-band waveform. From this parameterization, a tracking offset and backscatter estimate are determined. Tests are made on the extent of the tracking offset, and extreme values are flagged as retracking failures. The sea-ice waveform amplitude is determined by finding the maximum value of the waveform samples and the tracking offset is determined by finding the point on the waveform (by interpolation) where the waveform amplitude exceeds a threshold determined from the above sea-ice amplitude. A tracking offset is determined. The Centre Of Gravity offset correction must be included in the range measurement as the correction is not available separately in the L2 product. • Amplitude → Sigma0 • Tracking offset → altimeter range • Centre Of Gravity offset correction → correction to altimeter range measurement N.B.: the Ice2 retracking algorithm has been tuned to Ka-band since Patch2, but not the Ice1 nor the Sea Ice algorithms
Altimeter Instrument Corrections	consistent with MLE4 retracking
Saral/AltiKa Radiometer Parameters	Using on-board calibration
Dry Troposphere Range Correction	From ECMWF atmospheric pressures and model for S1 and S2 atmospheric tides
Wet Troposphere Range Correction from Model	From ECMWF model
Ionosphere correction	Based on Global Ionosphere TEC Maps from JPL
Sea State Bias Model	Hybrid SSB model from [23]
Mean Sea Surface	MSS_CNES-CLS11 (related to a 7-years mean) , MSS_CNES_CLS15 from cycle 34
Mean Dynamic Topography	MDT_CNES-CLS09
Geoid	EGM96
Bathymetry Model	DTM2000.1
Inverse Barometer Correction	Computed from ECMWF atmospheric pressures after removing S1 and S2 atmospheric tides
	.../...

Model	Product version "T" Patch2
Non-tidal High-frequency De-aliasing Correction	Mog2D high resolution ocean model on (I)GDRs. None for OGDRs. Ocean model forced by ECMWF atmospheric pressures after removing S1 and S2 atmospheric tides.
Tide Solution 1	GOT4.8
Tide Solution 2	FES2012 + S1 and M4 ocean tides. S1 and M4 load tides ignored
Equilibrium long-period ocean tide model.	From Cartwright and Taylor tidal potential.
Non-equilibrium long-period ocean tide model.	Mm, Mf, Mtm, and Msqm from FES2004
Solid Earth Tide Model	From Cartwright and Taylor tidal potential.
Pole Tide Model	Equilibrium model
Wind Speed from Model	ECMWF model
Altimeter Wind Speed	wind speed model from [20]
Trailing edge variation Flag	Derived from Matching Pursuit algorithm (from J. Tournadre, IFREMER)
Ice flag	Initialized in climatological areas based on wind speed values and updated by comparing the model wet tropospheric correction and the dual-frequency wet tropospheric correction retrieved from radiometer brightness temperatures

Table 4: *Models and standards adopted for the SARAL/AltiKa version T Patch 2 products. Adapted from [15].*

3. Data coverage and edited measurements

This section details the SARAL/AltiKa mission performance regarding data availablity. The ratio of missing and edited measurements is carefully monitored through routine Cal/Val analysis to detect any anomalies, either on the instrument itself or on ground processing.

3.1. Missing measurements

Determination of missing measurements relative to the theoretically expected orbit ground pattern is an essential tool to detect missing telemetry or satellite events for instance. It also permits to measure the tracking performances of the altimeter, especially over non ocean surfaces that remain more challenging for the signal acquisition by radar. The number of missing measurements is routinely monitored by Cal/Val tools. SARAL/AltiKa's performance regarding the number of missing measurements was so far compared to Jason-2.
Note that the interleaved phase that started in October 2016 along with several SHM periods experienced in 2017 (15-30 Mars , 17 May-12 July , 14 Sept-13 Oct) have severely impacted the number of available measurements for Jason-2 (see [5] for more details). To have suitable comparisons over SARAL/AltiKa's lifetime and to cover up the gaps of Jason-2's datased, all the monitoring will from now on include Jason-3's data over its whole available period.
SARAL/AltiKa's performance regarding the number of missing measurements through the comparison of the percentage of missing measurements is estimated in a consistent manner for all the missions.

3.1.1. Over land and ocean

Missing 1 Hz measurements are estimated by comparing actual measurements to the theoretical ground track, resampled from the ENVISAT one. From cycle 100 onward, the actual ground track is drifting and the theoretical track from the repetitive phase can't be used any more. Missing measurements are then estimated using a theoretical ground track generated from predicted orbit files. As long as a record exists for a given date, the measurement is accounted as present, even if there is no useful science data.

SARAL/AltiKa can use several on board tracking modes: median, Earliest Detectable Part (EDP) and Diode/DEM (see chapter 2.2.1.). The median mode is similar to the one used by Envisat and for most cycles of Jason-2. EDP tracker should improve the tracker behavior above continental ice surfaces and hydrological zones. Finally, Diode/DEM mode is a technique using information coming from Diode and a digital elevation model available on board. It was already tested on Jason-2. For more information about the different on board tracker algorithms see [17]. The information about the acquisition / tracking mode used is available in the GDR (fields alt_state_flag_acq_mode_40hz and alt_state_flag_tracking_mode_40hz).

From cycle 4 onwards, SARAL/AltiKa used the **DIODE acquisition / median tracking mode**, except for two short periods of autonomous DIODE acquisition at cycles 10 and 17:

- at cycle 10, the altimeter switched to autonomous DIODE acquisition mode after a CNG I2+Q2 calibration, this mode was used for about 6 hours before switching back to the nominal DIODE acquisition mode,
- at cycle 17, the altimeter switched to the autonomous DIODE acquisition mode after it was turned on again after the SHM, this acquisition mode was used for a day and a half before switching back to the nominal DIODE acquisition mode.

Considering all surface types, SARAL/AltiKa has more data available than Jason-2 (which also uses most of the time the median tracker), independently from the tracker mode used for Saral. Figure 5 shows the percentage of available measurements for SARAL/AltiKa, Jason-2 and Jason-3 over all surfaces. The interleaved phase and the many SHM periods experienced in 2017 have clearly dropped the mean number of available measurements for Jason-2 (see [5] for more details) which ultimately lowers the performances of the mission. On the other hand, SARAL/AltiKa has around 2% less available data than Jason-3, however one should bear in mind that unlike Jason-3, SARAL/AltiKa has also experienced one SHM period in October 2014.

The main differences between the three missions appear over land surfaces as shown in figure 6. The missing data are highly correlated with the mountains location. Note that the routine calibrations for SARAL/AltiKa are mainly done over desert regions (Sahara, Australia, south of Africa and Mongolia), the percentage of available data is therefore low in these regions. When excluding these calibration areas and the highest mountains, SARAL exhibits an improved coverage compared to Jason-2. This can be noted over the Amazonian region (see figure 5) for instance where the percentage of available observations is 10% higher than Jason-2's. In periods when the ground track was loosely maintained, and at the beginning of the drifting phase, routine calibrations also drifted and some of them were performed over ocean, resulting in short track sections missing.

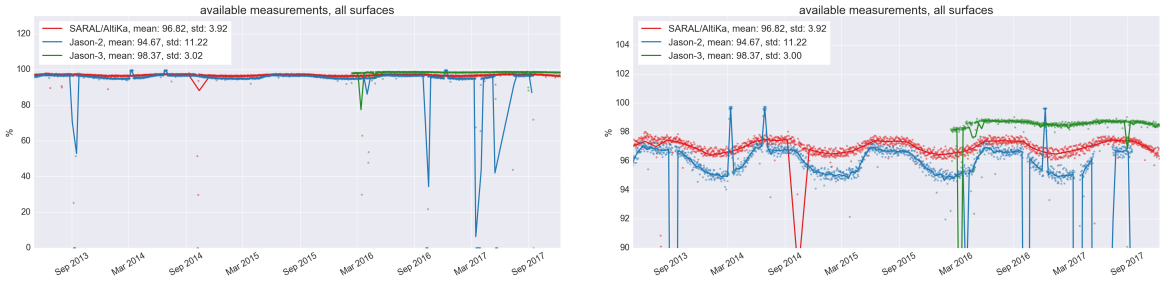

Figure 5: *Percentage of available measurements over all surfaces for SARAL/AltiKa, Jason-2 and Jason-3. Dots are daily averages while solid lines correspond to cycle averages.*

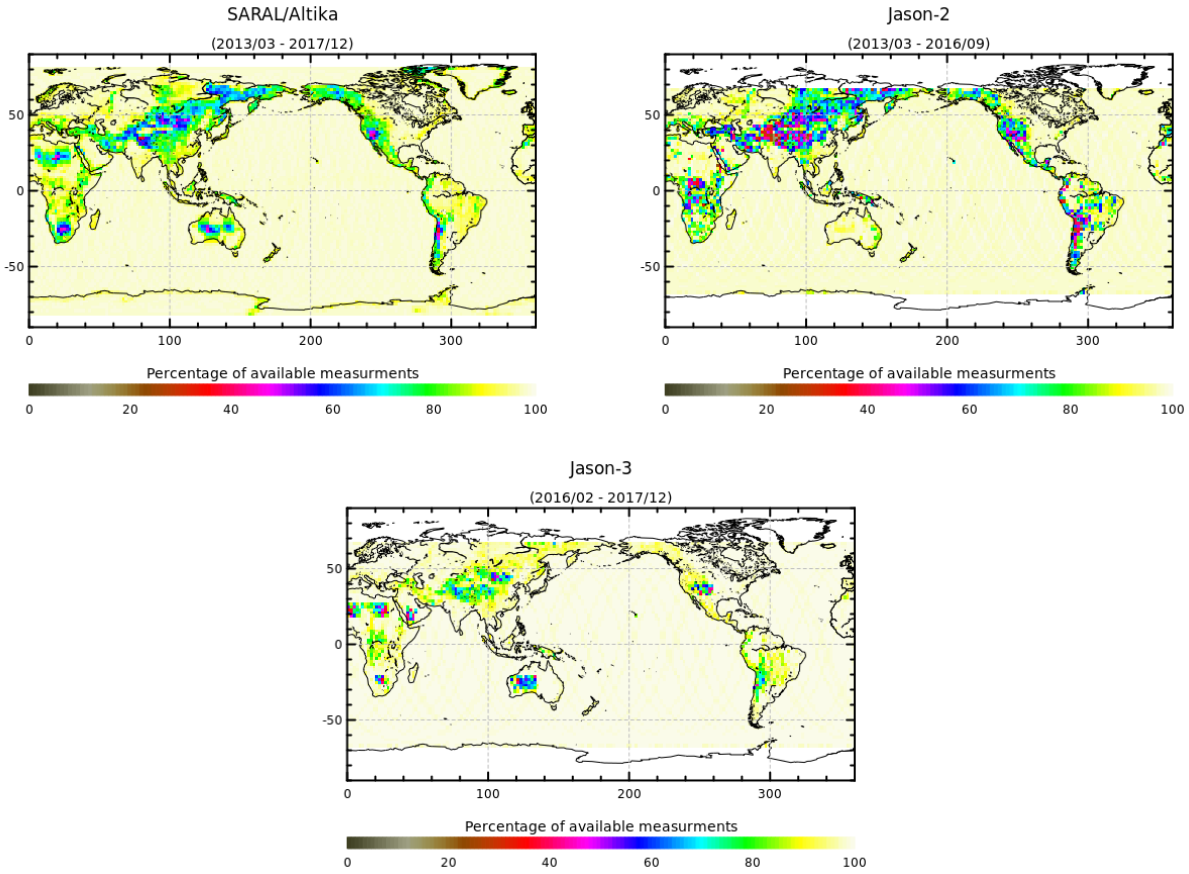

Figure 6: *Map of the percentage of available measurements over land for SARAL/AltiKa (left) Jason-2 (right) and Jason-3 (bottom).*

3.1.2. Over ocean

When considering only the ocean surface, the same analysis method leads generally to slightly less available data for SARAL/AltiKa compared to Jason-2 and Jason-3 data coverage, as shown on figure 7, which represents the percentage of available measurements limited to ocean surfaces. Over the shown periods, the mean value is about 98.5% for Jason-2, 99.8% for Jason-3, and 99.6% for SARAL/AltiKa, and we can still see the impact of SHM periods over Jason-2's globally lower value. SARAL/AltiKa had other periods with reduced data availability. All these events are described in table 3.

In any case, these figures largely exceeds the specifications for SARAL/AltiKa, which were (see [25]) 95% of all possible over-ocean data during a 3-year period with no systematic gaps plus the specific Ka-band limitation (5% of measurements may be not achieved due to rain rates > 1.5 mm/h according to geographic areas).

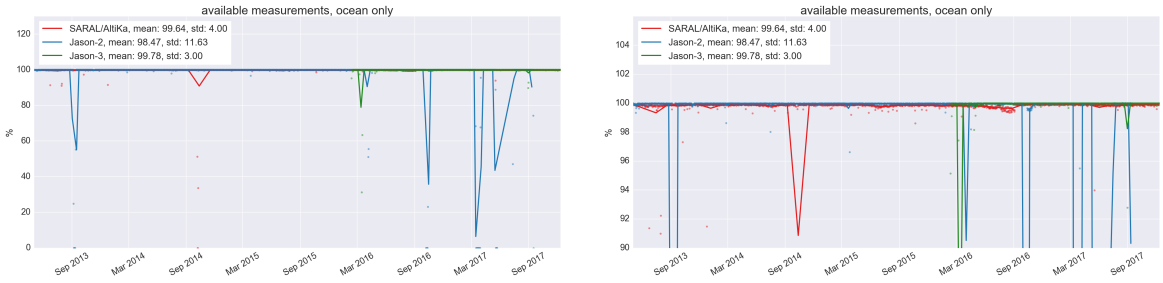

Figure 7: *Percentage of available measurements over ocean for SARAL/AltiKa Jason-2 and Jason-3. Dots are daily averages while solid lines correspond to cycle averages.*

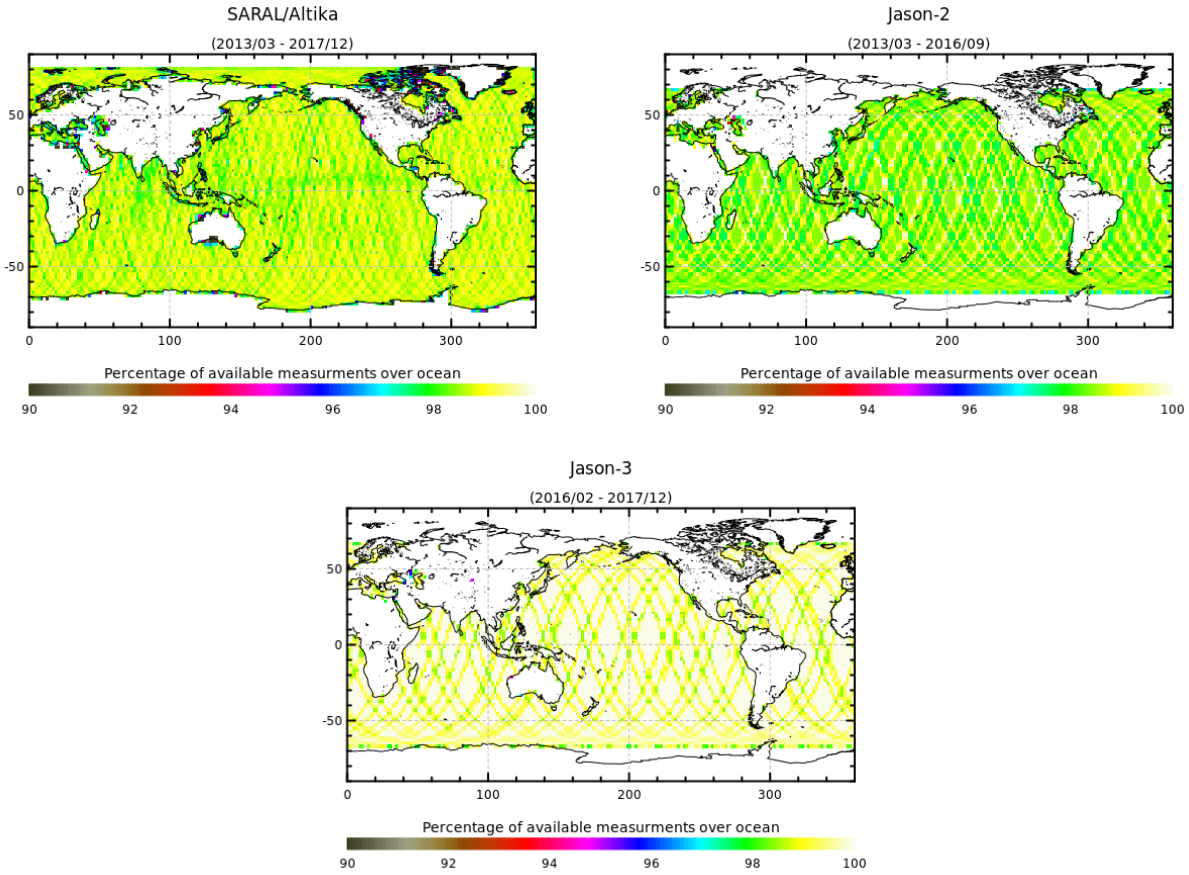

Figure 8: *Map of the percentage of available measurements over ocean for SARAL/AltiKa (left) Jason-2 (right) and Jason-3 (bottom).*

3.2. Edited measurements

The editing step of the Cal/Val process intends to remove from further analysis any measurement that is considered as erroneous. The definition of an erroneous measurement, and of the accepted error level on the final sea level anomaly is of course a trade off between accuracy and data coverage.

3.2.1. Editing criteria definition

Editing criteria are used to select valid measurements over ocean. The editing process is divided into 3 main parts:

- removal of all measurements affected by sea-ice (see section 3.2.2.),
- removal of all measurements which exceed given thresholds on different parameters (see section 3.2.3.),
- further checks on along-track sla consistency (see section 3.2.17.).

For each step of the editing process, the number of edited measurements, per track, per day and per cycle are routinely monitored at Cal/Val level. This allows the detection of anomalies through the number of removed data, which could come from instrumental, geophysical or algorithmic changes.

The editing performed here (and more generally SARAL/AltiKa Cal/Val activities) are dedicated to ocean applications. All data over land are removed using a land/water mask prior to the analysis described in this section. There are some variations over time (mainly at the beginning of the mission's life) of the number of measurements over land. These variations are directly related to the tracking mode used: when the DEM mode is used, more measurements are acquired over land compared to the median tracking periods.

Furthermore, as a very first step of the editing process, all passes are checked for latitude monotony (either increasing or decreasing). On SARAL/AltiKa this has not led to the removal of a single measurement yet.

Figure 9 gives an overview of the behavior of the edited measurements (all criteria combined) over the mission's lifetime. On average 20.08% of ocean measurements are edited, the majority of which are removed due to the sea ice flag. Results of the different editing steps applied to the data are presented below.

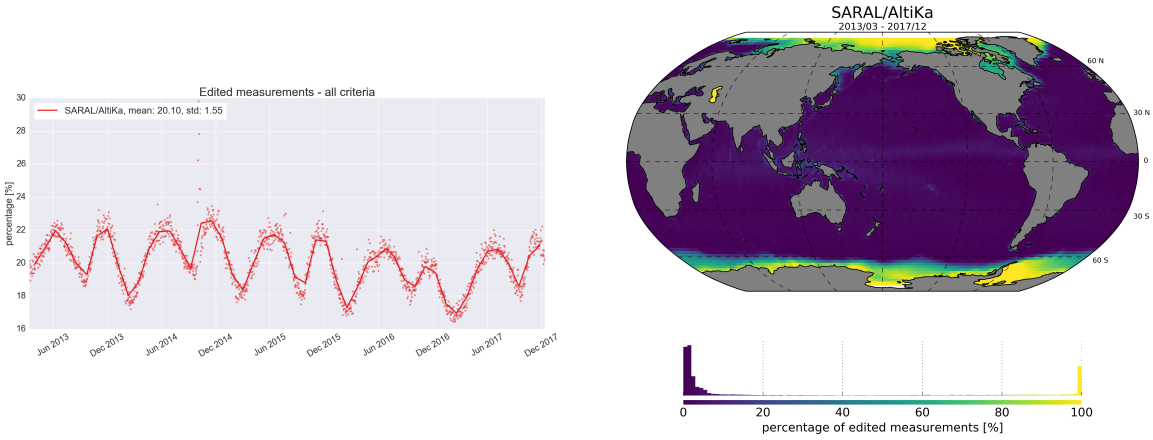

Figure 9: *Total percentage of SARAL/AltiKa edited measurements. [left] monitoring for GDR data and [right] map since the beginning of mission (cycles 1 to 114).*

3.2.2. Flagging quality criteria: Ice flag

The ice flag (ice_flag in the GDR products) is used to remove measurements affected by sea ice in the altimeter footprint. Left panel of figure 10 shows the evolution of the percentage of measurements edited by this criterion. Over the shown period, several characteristics are visible:

- a large seasonal cycle, due to annual growth and retreat of sea ice extent,
- two yearly minimums of the percentage of edited SARAL/AltiKa data (∼16% of edited data) are observed in February and September, corresponding respectively to periods where the Antarctic and Arctic sea ice extension are minimum,
- maximums (∼20% of edited data) are reached around June/July and November/December,
- a general decreasing trend, related to the global variation of sea ice extent.

The spatial distribution of the percentage of measurements edited by ice flag is plotted in the right panel of figure 10, over the whole mission lifetime.

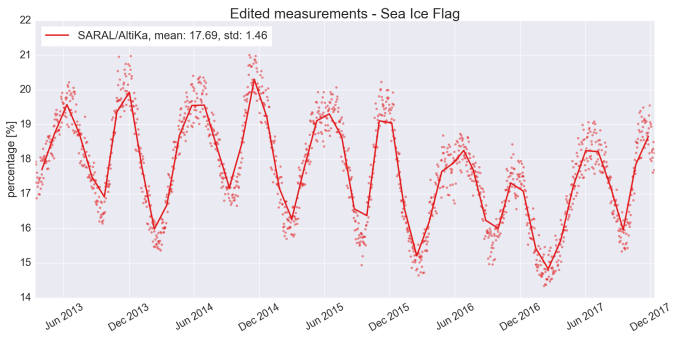

Figure 10: *Percentage of edited measurements by ice flag criterion. Monitoring for GDR data (all latitude).*

Please note that an improved ice flag algorithm is available through the PEACHI products. As it is not yet in the GDR products, we do not consider this flag here.

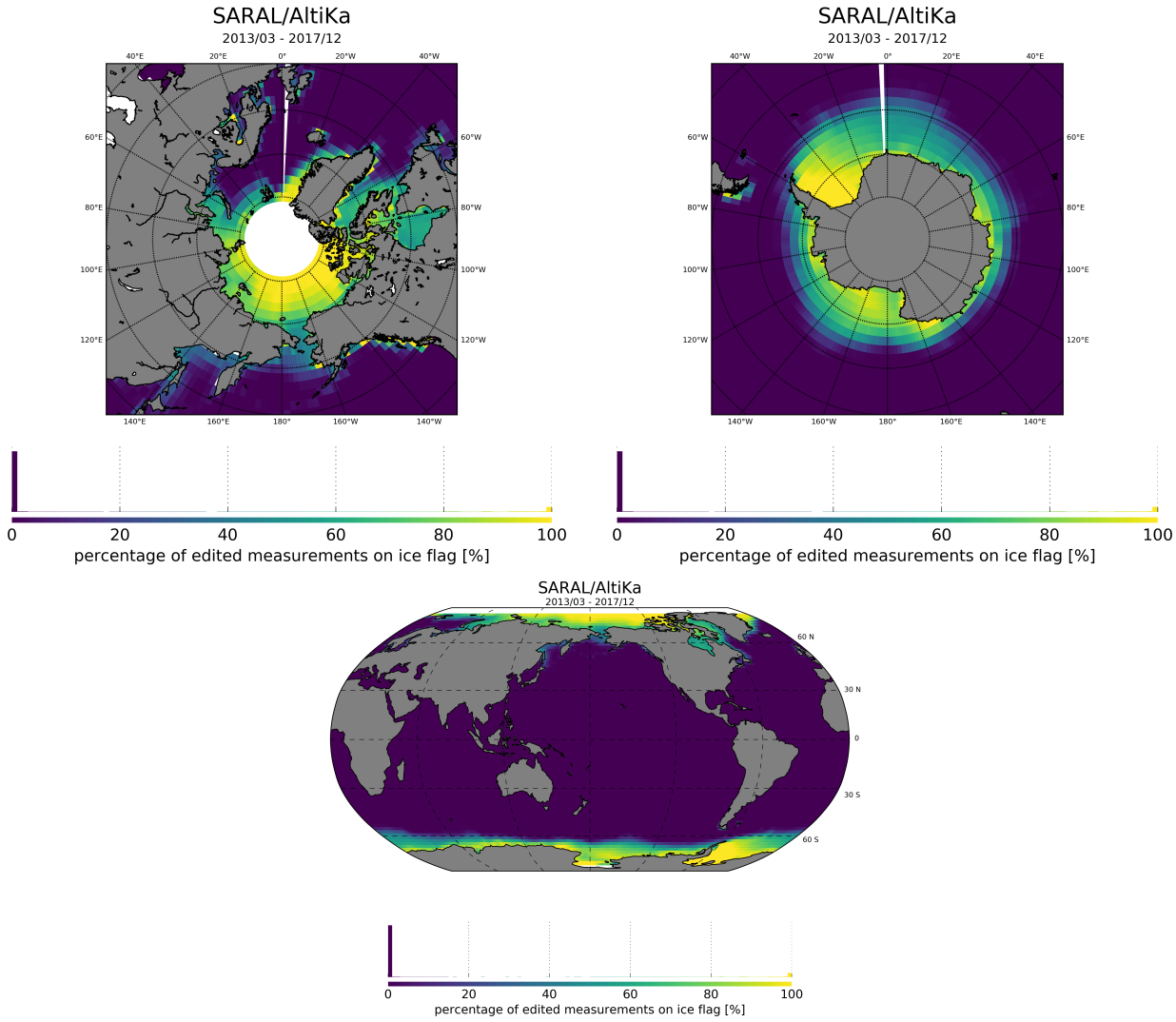

Figure 11: *Percentage of edited measurements by ice flag criterion. Maps since the beginning of the mission (cycles 1 to 114).*

3.2.3. Threshold criteria: Global

Parameter	Min thresholds	Max thresholds	mean edited
Sea surface height	$-130\,m$	$100\,m$	0.47%
Sea level anomaly	$-2\,m$	$2\,m$	0.84%
Number of range measurements	20	*Not applicable*	1.11%
Standard deviation of range	0	$0.2\,m$	1.48%
Squared off-nadir angle	$-0.2\,deg^2$	$0.0625\,deg^2$	0.36%
Dry troposphere correction	$-2.5\,m$	$-1.9\,m$	0.00%
dynamical atmopsheric correction	$-2\,m$	$2\,m$	0.00%
Radiometer wet troposphere correction	$-0.5m$	$0\,m$	0.06%
Significant wave height	$0\,m$	$11\,m$	0.39%
Sea State Bias	$-0.5\,m$	$0.0025\,m$	0.29%
Number measurements of Ka-band Sigma0	20	*Not applicable*	1.04%
Standard deviation of Ka-band Sigma0	0	$1\,dB$	0.93%
Ka-band Sigma0	$3\,dB$	$30\,dB$	0.34%
Ocean tide	$-5\,m$	$5\,m$	0.18%
Equilibrium tide	$-0.5\,m$	$0.5\,m$	0.00%
Earth tide	$-1\,m$	$1\,m$	0.00%
Pole tide	$-0.15\,m$	$0.15\,m$	0.00%
Altimeter wind speed	$0\,m.s^{-1}$	$30\,m.s^{-1}$	0.29%
All together	-	-	2.59%

Table 5: *Editing thresholds, statistics obtained for cycles 1 to 114*

The quality of instrumental and geophysical parameters is checked with respect to thresholds, after having selected only ocean measurements and having removed sea ice. Thresholds used are summarized in table 5, along with the average percentage of edited data for each parameter/threshold pair.

Note that no measurements are edited by the following corrections:

- dry troposphere correction,
- dynamical atmospheric correction,
- equilibrium tide,
- earth tide,
- and pole tide.

Indeed these parameters are all derived from models, and are only checked in order to detect default values, which would point to a processing anomaly.

For each parameter and threshold, the percentage of edited data are monitored on a cycle per cycle, day per day and pass per pass basis by Cal/Val routines. Figure 12 presents the monitoring of the percentage of data points edited on all thresholds combined. Considering all parameters and thresholds, the mean percentage of edited measurements is 2.6%. The editing rate is steady over time and shows a large seasonal signal, due to annual growth and retreat of sea ice extent. The rise of this parameter around October 2014 is a result of the mispointing events before the SHM. Note that one measurement can be edited by several different thresholds, so the sum of individual criterion percentages does not equal the all thresholds combined percentage.

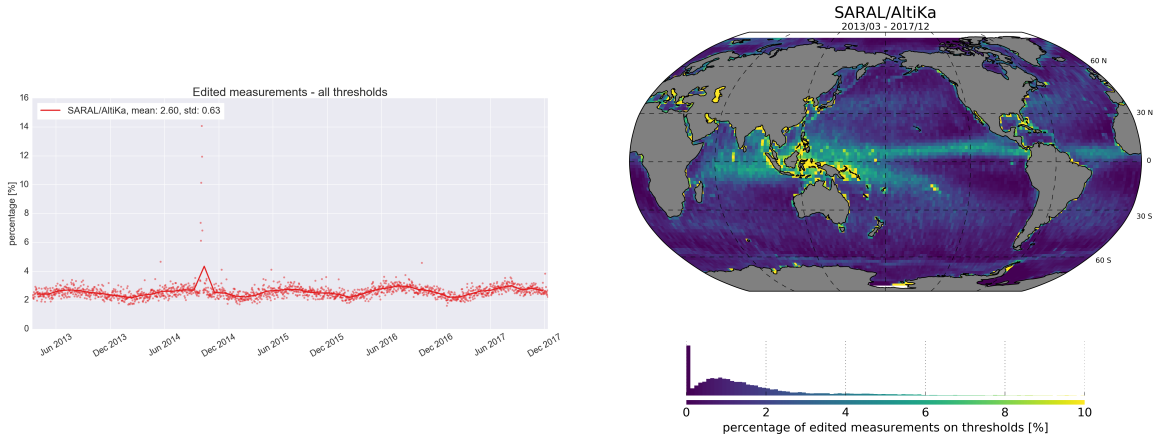

Figure 12: *Percentage of edited measurements on all thresholds combined. [left] monitoring for GDR data and [right] map since the beginning of mission (cycles 1 to 114).*

3.2.4. Number of 40-Hz measurements

The percentage of edited measurements because of a too low number of 40-Hz measurements is represented on the left side of figure 13. On SARAL/AltiKa all the 1 Hz measurements resulting from the compression of less than 20 high rate waveforms are discarded from further analysis. No trend nor any anomaly has been detected.

The map of measurements edited by 40-Hz measurements number criterion is plotted on the right panel of figure 13 and shows a correlation with wet and heavy rain areas (in general regions with disturbed sea state), as well as regions close to sea ice. Indeed waveforms are distorted by rain cells or sigma bloom events, which makes them often meaningless for SSH calculation. As a consequence, edited measurements due to several altimetric criteria are often correlated with wet areas (rain cells/sigma bloom events). Coastal regions are also impacted due to land contamination within the altimeter footprint.

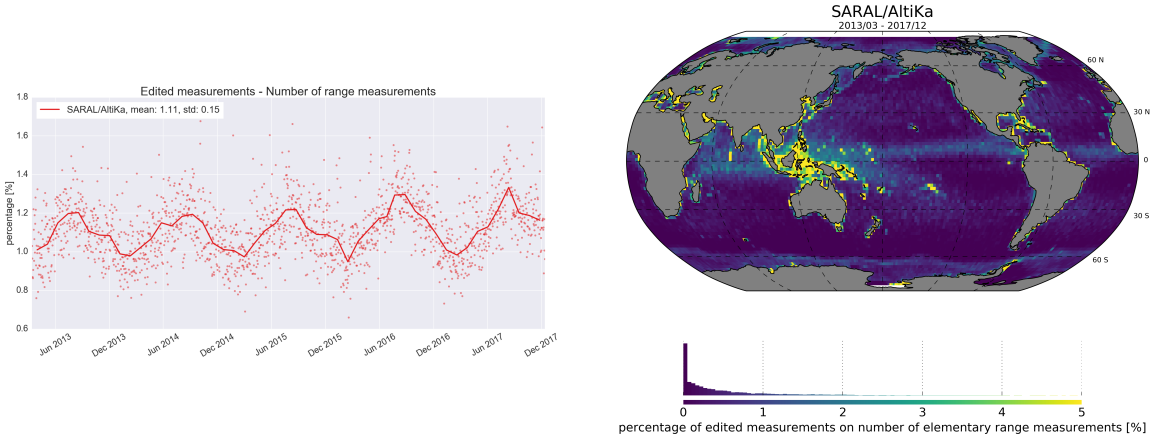

Figure 13: *Percentage of edited measurements on the number of 40-Hz measurements criterion. [left] monitoring for GDR data and [right] map since the beginning of mission (cycles 1 to 114).*

3.2.5. Standard deviation of 40-Hz range measurements

The percentage of edited measurements due to a high standard deviation (of the 40-Hz measurements) of the range is shown in figure 14. On average, 1.48% of the measurements are edited on this criterion.

Several days show a slight increase in the percentage of data edited by this criterion. These can mostly be related to mispointing episodes (before the SHM or around maneuver burns). In the latter case, the data a few minutes before and after the maneuver are edited (in general several parameters are out of thresholds) as a consequence of the lower platform pointing accuracy. Since cycle 24, platform pointing during maneuvers is achieved by the thrusters instead of the reaction wheels. The impact of this change on the number of edited GDR data is small.

The right panel of figure 14 shows a map of the percentage of measurements edited by the 40-Hz measurements standard deviation criterion. As in section 3.2.4., edited measurements are correlated with wet and costal areas.

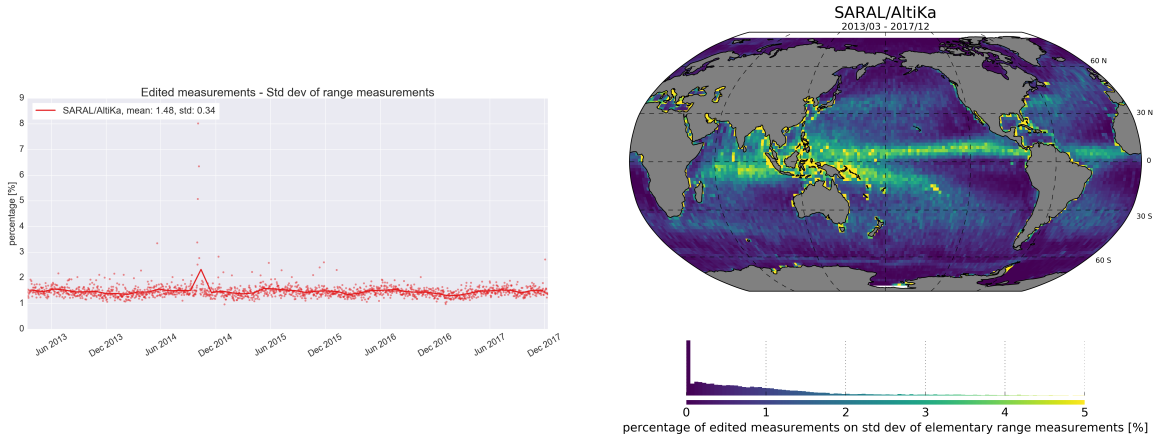

Figure 14: *Percentage of measurements edited due to high standard deviation of 40-Hz range measurements . [left] monitoring for GDR data and [right] map since beginning of mission (cycles 1 to 114).*

3.2.6. Significant wave height

The percentage of edited measurements due to significant wave height out of thresholds is represented on figure 15. On average, 0.39% of the measurements are edited on this criterion.

As for the 40 Hz range standard deviation, several days show an increased number of edited data. Again, this is mostly due to mispointing events and maneuver burns.

Figure 15 (right panel) shows that measurements edited by the SWH criterion are especially found in wet regions where heavy rains and sigma bloom events can occur, as well as in high sea state regions and costal areas.

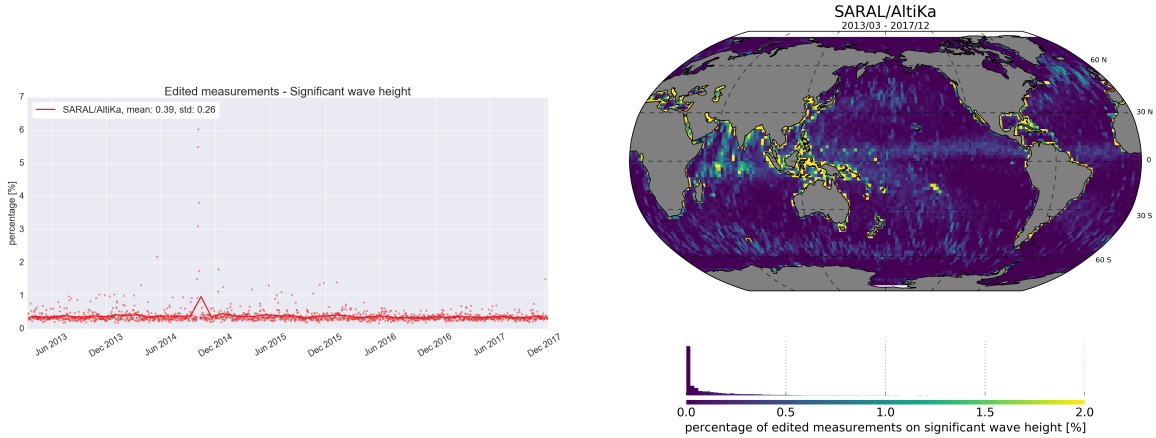

Figure 15: *Percentage of edited measurements by SWH criterion. [left] monitoring for GDR data and [right] map since the beginning of mission (cycles 1 to 114).*

3.2.7. Backscatter coefficient

The percentage of edited measurements due to backscatter coefficient out of thresholds is represented on figure 16. On average, 0.34% of the measurements are edited on this criterion.

High editing rates (see right panel of figure 16) are generally found at the coast, and in rain areas. Again, this quantity is affected by mispointing events, and high editing rates are generally observed close to maneuvers.

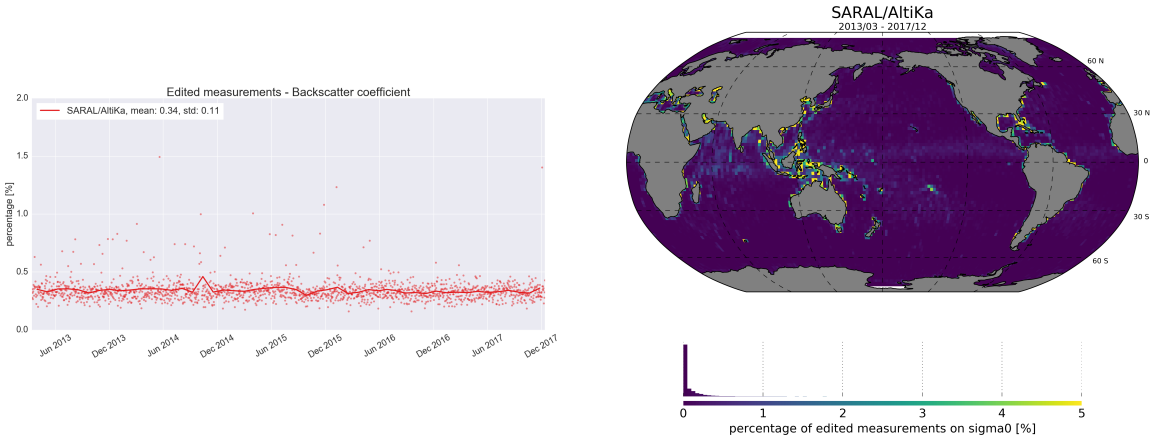

Figure 16: *Percentage of edited measurements by Sigma0 criterion. [left] monitoring for GDR data and [right] map since the beginning of mission (cycles 1 to 114).*

3.2.8. Number of backscatter coefficient measurements

The percentage of edited measurements due to too few 40 Hz measurements for each 1 Hz measuremet is represented on figure 17. On average, 1.04% of the measurements are edited on this criterion.

High editing rates (see right panel of figure 17)are generally found at the coast, and in rain areas. This quantity is also affected by mispointing events which lead to high editing rates (close to maneuvers for example). The number of elementary measurements of backscatter is closely related to the number of elementary range measurements, and metrics are very similar.

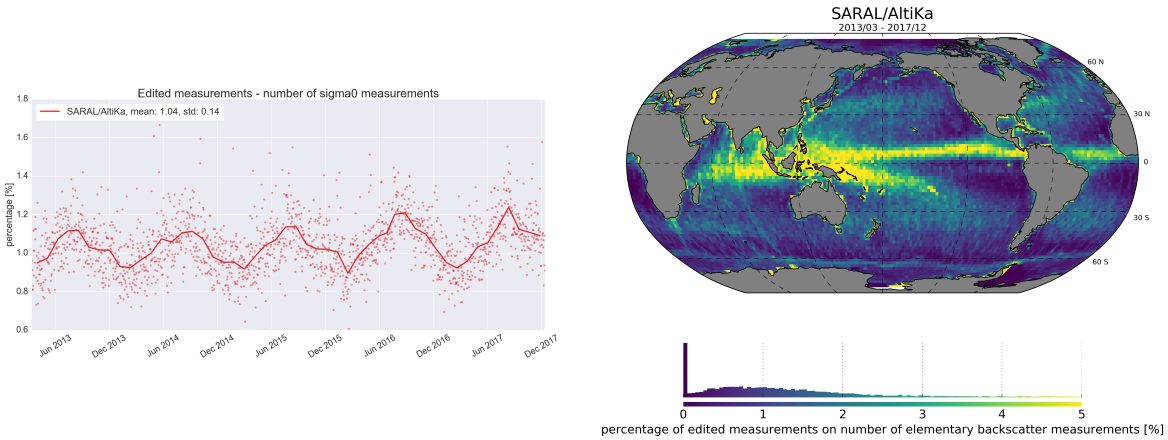

Figure 17: *Percentage of edited measurements by number of high rate backscatter coefficient measurements. [left] monitoring for GDR data and [right] map since the beginning of mission (cycles 1 to 114).*

3.2.9. Standard deviation of backscatter coefficient

The percentage of edited measurements on the 40 Hz backscatter coefficient standard deviation criterion is represented on figure 18. On average, 0.93% of the measurements are edited on this criterion.

The right panel of figure 18 shows that measurements edited on 40 Hz backscatter coefficient standard deviation criterion are found in coastal areas, and in regions affected by rain events, which can be either related to the contribution of the Ka backscatter attenuation that depends on atmospheric water content, or related to the high variability of the backscatter coefficient in theses regions. The spatial distributions of edited measurements due to high standard deviation of backscatter and of range measurements are very similar.

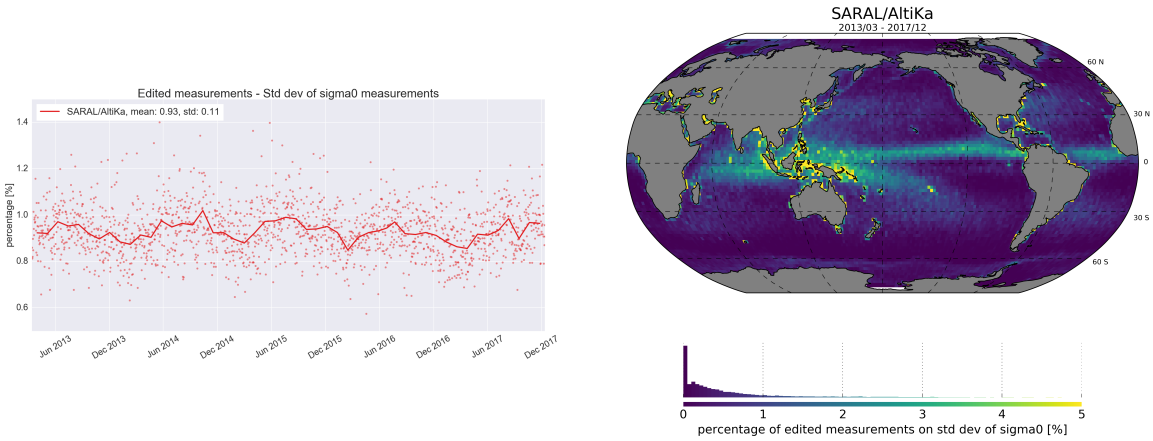

Figure 18: *Percentage of edited measurements by 40 Hz Sigma0 standard deviation criterion. [left] monitoring for GDR data and [right] map since the beginning of mission (cycles 1 to 114).*

3.2.10. Radiometer wet troposphere correction

The percentage of edited measurements due to radiometer wet troposphere correction criterion is represented in figure 19. On average, only 0.06% of the measurements are edited on this criterion. The edited data for Saral/AltiKa are generally due to wet troposphere path delay values that are larger than the tolerated -0.5 m threshold. Large editing percentages are mainly observed in coastal regions suggesting that some land effects on radiometer measurements impacts the quality of the wet troposphere path delay retrievals. Other editing events happen in known wet areas in the inter tropical band where the retrieval algorithm may be less efficient in some cases of high rain rates or unusal sea states (sigma blooms).

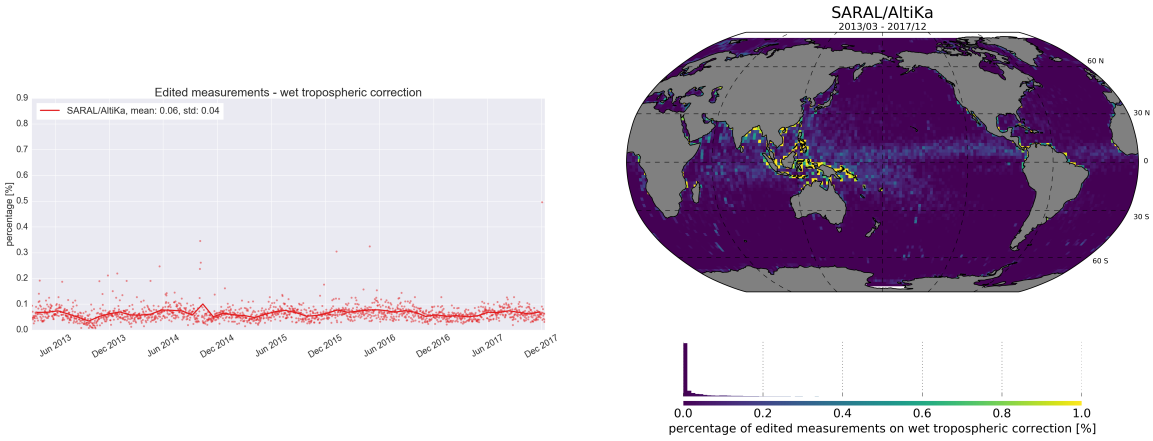

Figure 19: *Percentage of edited measurements due to radiometer wet tropospheric correction out of thresholds. [left] monitoring for GDR data and [right] map since the beginning of mission (cycles 1 to 114).*

3.2.11. Square off-nadir angle

The percentage of edited measurements due to square off-nadir angle criterion is represented in figure 20. On average, 0.36% of all measurements are edited due to high mispointing values. Maneuvers have a strong impact on mispointing values because the platform has to rotate from nadir to geodetic pointing before thrusters activity. As a result, nearly all maneuvers are edited due to high mispointing values. This is visible both on the monitoring (daily points slightly higher around 0.5 to 2 % values) and on the map as all maneuvers where performed in the Indian Ocean, within view on Indian ground stations. After the SHM, systematic mispointing were observed at zero-crossings of reaction wheel (RW) speed, resulting in a slightly higher percentage of edited points. This was corrected and the percentage of measurements edited due to high mispointing values came back to normal values. SARAL/AltiKa is still impacted by random fluctuations in RW friction which explains that several days show a higher percentage of edited measurements.

The spatial distribution of the percentage of edited values (right panel of figure 20) appears very noisy at first. There are several features visible in this map, such as:

- editing due to maneuvers in the Indian Ocean,
- a patch in the North Atlantic Ocean, resulting from zero crossings of RW speed over the regions between Greenland and Svalbard,
- several track-like patterns due to RW friction fluctuations,
- a pattern similar to the one observed for several other parameters: coastal areas and wet areas, as off-nadir angle estimation is based on the waveform trailing edge slope which is impacted by rain cells and surface roughness.

Since the SHM, mispointing is a carefully monitored parameter on SARAL/AltiKa. More information on mispointing events can be found in section 4.3. of this report .

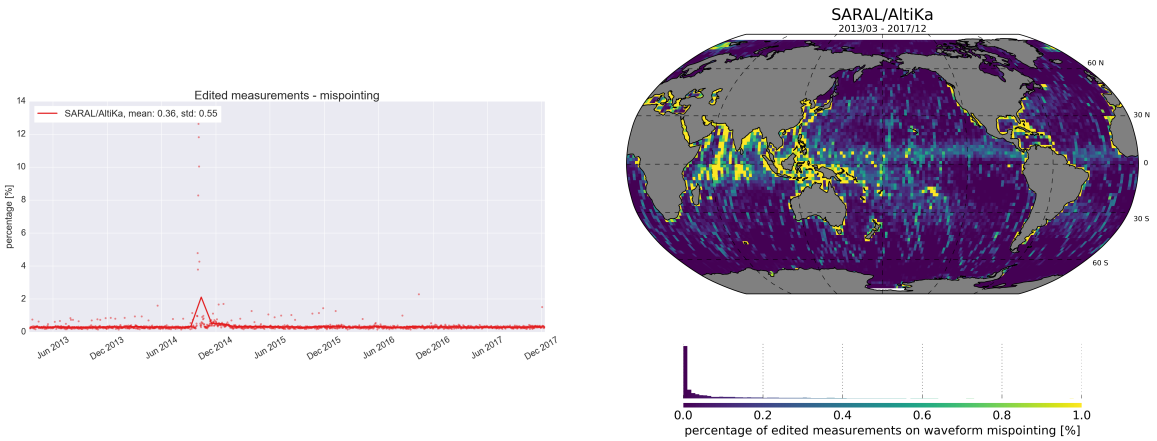

Figure 20: *Percentage of edited measurements by square off-nadir angle criterion. [left] monitoring for GDR data and [right] map since the beginning of the mission (cycles 1 to 114).*

3.2.12. Sea state bias correction

The percentage of edited measurements due to sea state bias correction criterion is represented in figure 21. On average, 0.29% of measurements are edited due to sea state bias values out of thresholds. The percentage of edited measurements is stable over time, although with several days with higher values, mainly due to maneuvers. The spatial distribution is consistent with what is observed regarding editing on SWH values: areas with low sea states may be edited due to erroneous sea state bias estimation. This does not happen for high sea states (high northern and southern latitudes) where no measurements are edited on the sea state bias threshold criterion.

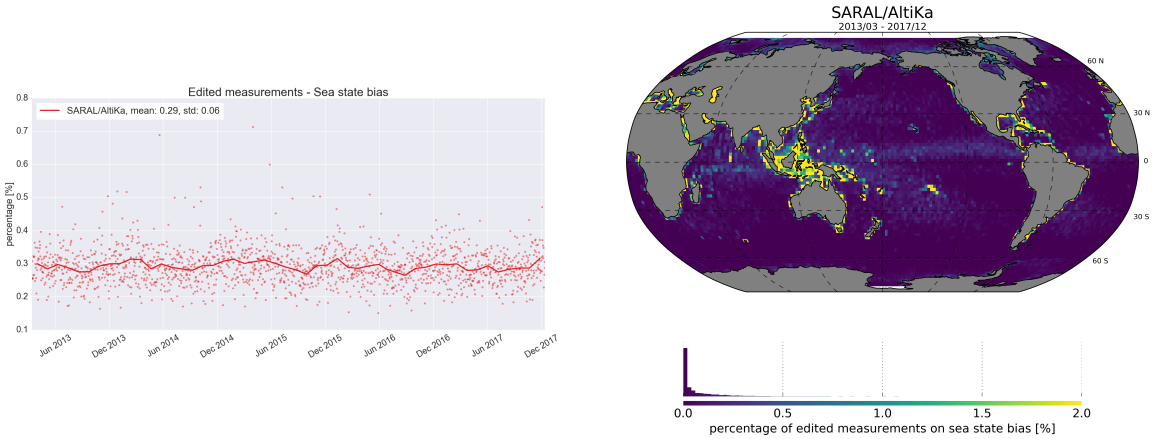

Figure 21: *Percentage of edited measurements by sea state bias criterion. [left] monitoring for GDR data and [right] map since the beginning of the mission (cycles 1 to 114).*

3.2.13. Altimeter wind speed

The percentage of edited measurements due to altimeter wind speed criterion is represented in figure 22. On average 0.29% of measurements are edited. This map exhibits the same patterns as the one related to the backscatter coefficient (which is used to derive the wind speed).

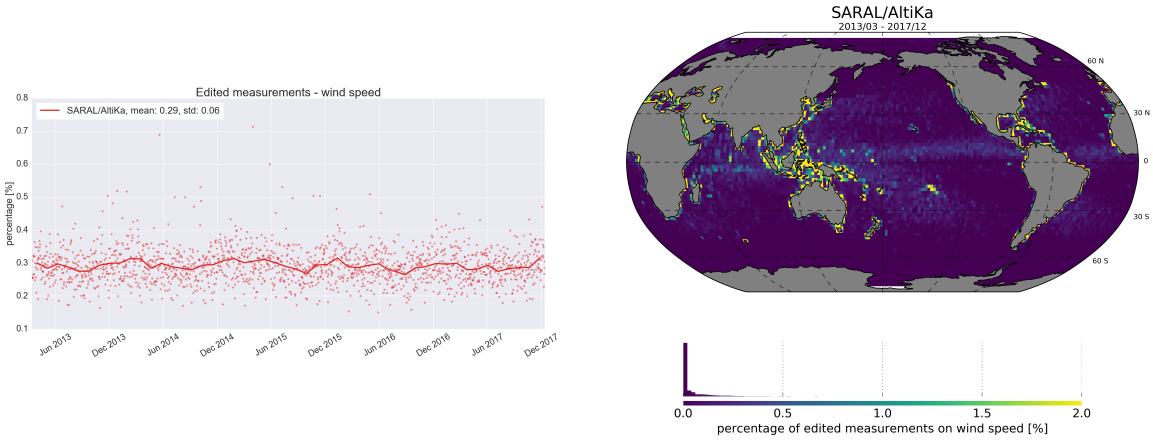

Figure 22: *Percentage of edited measurements by wind speed criterion. [left] monitoring for GDR data and [right] map since the beginning of the mission (cycles 1 to 114).*

3.2.14. Ocean, pole and earth tide corrections

No measurements are edited due to the pole tide or the solid earth tide components whereas some measurements with extreme ocean tide values (GOT 4.8) are edited. The percentage of edited measurements due to the threshold on the latter is represented in figure 23. On average 0.18% of the measurements are edited due to the ocean tide correction. The majority of these measurements correspond to the Caspian Sea. In GDR-T Patch2 version, the geocentric ocean tide is not defined over land, including enclosed water bodies which on one hand impacts the Caspian Sea, and on the other hand impacts near shore data. This is due to the equilibrium long-period tide height (included in the global ocean tide) that is computed with FES2012 algorithm in Patch 2, which previously tests wether the grid of the FES2012 tide atlas is defined or not. Consequently, the equilibrium tide is set to default values over land (and therefore also the geocentric ocean tide). This explains the presence of edited data (map 23) near coasts and in the Caspian Sea.

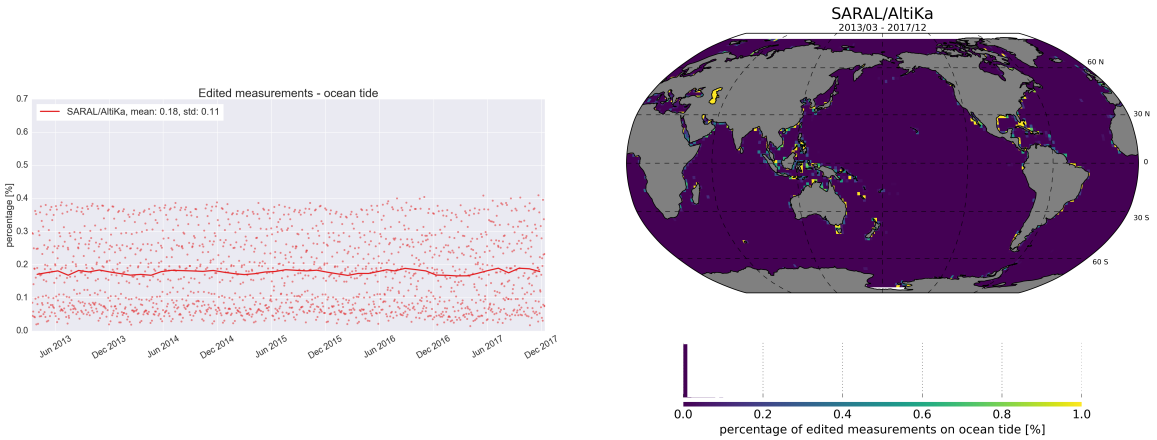

Figure 23: *Percentage of edited measurements by ocean tide criterion. [left] monitoring for GDR data and [right] map since the beginning of the mission (cycles 1 to 114).*

3.2.15. Sea surface height

The percentage of edited measurements due to sea surface height (orbit minus range, no corrections applied) criterion is represented in figure 24. On average, 0.47% of measurements are edited on this criterion. The measurements edited by sea surface height criterion are mostly found near coasts in equatorial and mid-latitude regions, as well as for regions with low significant wave heights (see map 24).

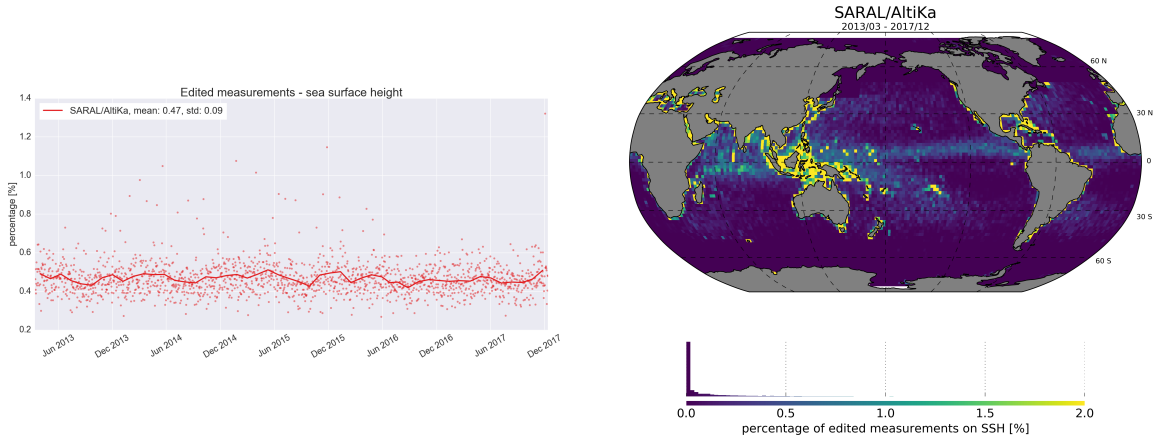

Figure 24: *Percentage of edited measurements by sea surface height criterion. [left] monitoring for GDR data and [right] map since the beginning of the mission (cycles 1 to 114).*

3.2.16. Sea level anomaly

The percentage of edited measurements due to the sea level anomaly out of thresholds is represented in figure 25. This percentage is estimated after removing ice flagged data. On average, 0.84% of data are edited by this criterion. There is a slight increase of this percentage since March 2015 approximately when the ground track was loosely maintained, resulting in higher MSS errors.
On the other hand, the map is estimated after applying all the previous editing steps, and shows very few measurements edited, mainly located at the coast. This result highlights the efficiency of the editing process in removing erroneous SLA measurements.

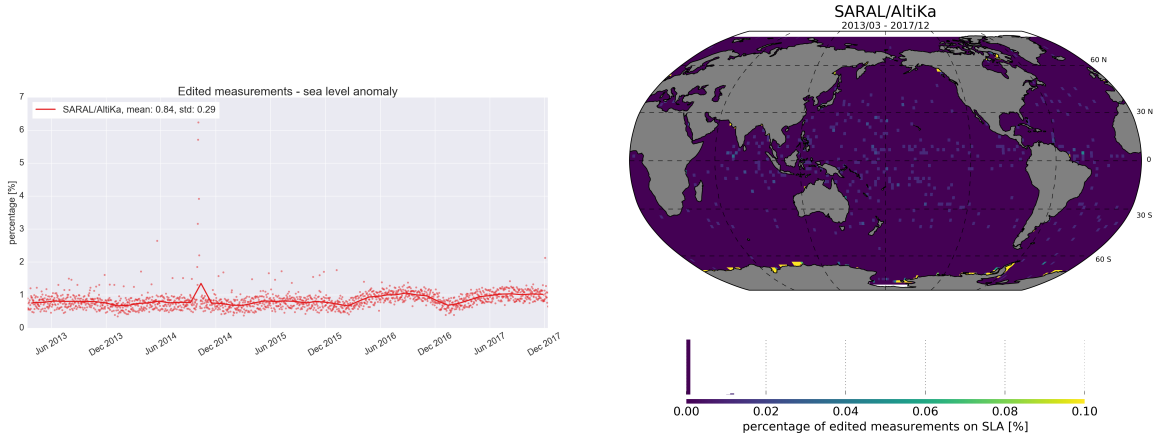

Figure 25: *Percentage of edited measurements by sea level anomaly criterion. [left] monitoring for GDR data and [right] map since the beginning of the mission (cycles 1 to 114).*

3.2.17. SLA consistency checks

The last step of the editing procedure is to check for along-track SLA consistency. Two different checks are performed:

- fitting a spline function to SLA values (after all previously mentionned editing criteria have been applied),
- checking that pass mean and standard deviation do not exceed certain thresholds.

Figure 26 shows the monitoring of the percentage of edited points by these two criteria. Very few points are edited by these two editing steps, 0.04% for splines, and 0.01% for pass statistics. In the latter case, the whole pass is edited, leaving a large gap in the data. This happened 9 times, generally when crossing very large eddies in the Southern Ocean.

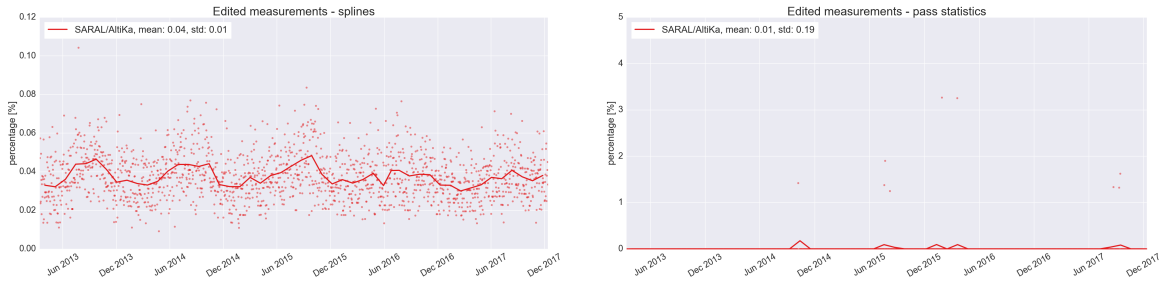

Figure 26: *Monitoring of the percentage of edited measurements by [left] spline criterion and [right] pass statistics.*

4. Monitoring of altimeter and radiometer parameters

4.1. Methodology

Statistics for the main parameters of SARAL/AltiKa have been routinely monitored since the beginning of the mission. Systematic monitoring aims at detecting changes in parameter statistics, that would indicate a problem on the mission. Comparisons with model outputs or other missions (mainly Jason-2 and Jason-3) are also performed as part of the systematic Cal/Val activities.

For SARAL/AltiKa, pass by pass, daily and cyclic statistics are computed. In this section, we mainly present results from daily and cyclic average estimates.

The measurements distribution is not homogeneous within latitudes, and can skew the statistics to values of the data in high latitudes. This can be important when comparing to other missions, like Jason-2 and Jason-3. To overcome this issue when needed, we estimate box averages (generally on a 2 degree cartesian grid) before estimating global averages. For quite a few parameters, more precise comparisons are performed by estimating short time differences at crossovers.

Note that for the same reasons as mentionned in the previous section (several SHM periods for Jason-2 in 2017), monitorings of the different parameters will include Jason-2 and Jason-3 to cover up for Jason-2's gaps and have a continuous comparisons over SARAL/AltiKa's lifetime. Also, in order to have a consistent geographical comparison, all the maps of this section are based on GDR data over the full lifetime of Jason-3, and averages are estimated over the whole oceanic domain.

4.2. 40 Hz Measurements

Number and standard deviation of 40 Hz elementary range measurements used to derive 1 Hz data are two parameters computed during the altimeter ground processing. For SARAL/AltiKa Jason-2 and Jason-3 a MQE (mean quadratic error) criterion is used to select valid 40/20 Hz measurements before performing a regression to derive the 1 Hz range from high rate (40 Hz or 20 Hz) data.

The MQE criterion checks that the high rate waveforms can be approximated by a Brown echo model (Brown, 1977 [14], Thibaut et al. 2002 [26]). Then elementary ranges too far from the regression line are discarded, through an iterative regression process, until convergence is reached. Thus, monitoring the number of 40/20 Hz range measurements and the standard deviation computed among them is likely to reveal changes at instrumental level.

4.2.1. Number of 40 Hz measurements

The mean number of elementary 40 Hz range measurements for SARAL/AltiKa is close to 38.5 (see figure 27, where Jason-2 and Jason-3 values were doubled). Before the correction of the PF/RF alignment (alignment between the platform and the radiofrequency axis) on 25th of April 2013 this

value was slightly higher (around 38.6). Jason-2 and Jason-3 have an average number of elementary 20 Hz range measurements of 19.6, which represents a higher number than SARAL/AltiKa. Jason-2 and Jason-3 also show a smaller day to day variability than SARAL/AltiKa.

Note that before Patch1 version, the MQE threshold was not applied during the 40 Hz to 1 Hz compression (IGDR data till cycle 4, pass 394). As a result, the daily mean of the number of the elementary 40 Hz range measurements was higher at 39.0.

On average 1.5 % of the 40 Hz elementary range measurements are removed during the 40 Hz to 1 Hz compression by the MQE criteria. These removed data might be due to perturbations in the footprint (rain events, sigma blooms). For these three missions, the number of elementary range measurements is correlated with the significant wave height (and, for SARAL/AltiKa, with sea ice extent). Figure 28 shows less elementary range measurements around rain areas, and also Indonesia, the Mediterranean Sea and costal areas, which are all regions of low significant wave heights (see also map of SWH 40) and therefore regions where sigma bloom may occur. High latitudes also show a lower number of range elementary measurements, due to the presence of sea-ice.

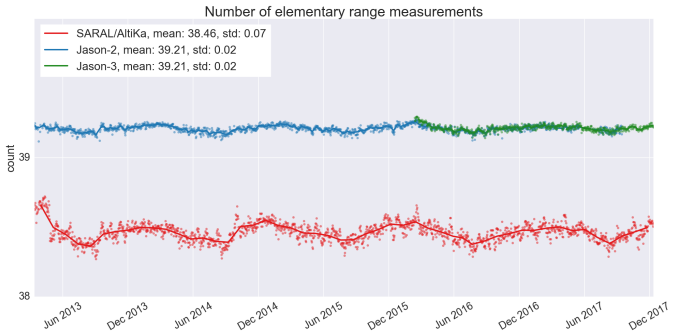

Figure 27: *Daily monitoring of mean of number of elementary measurements for SARAL/AltiKa (ref) , Jason-2 (blue) and Jason-3 (green). Dots represent daily averages, the lines correponds to cycle averages. Jason-2 and Jason-3 data are multiplied by two to account for the 40Hz/20Hz difference between the two missions.*

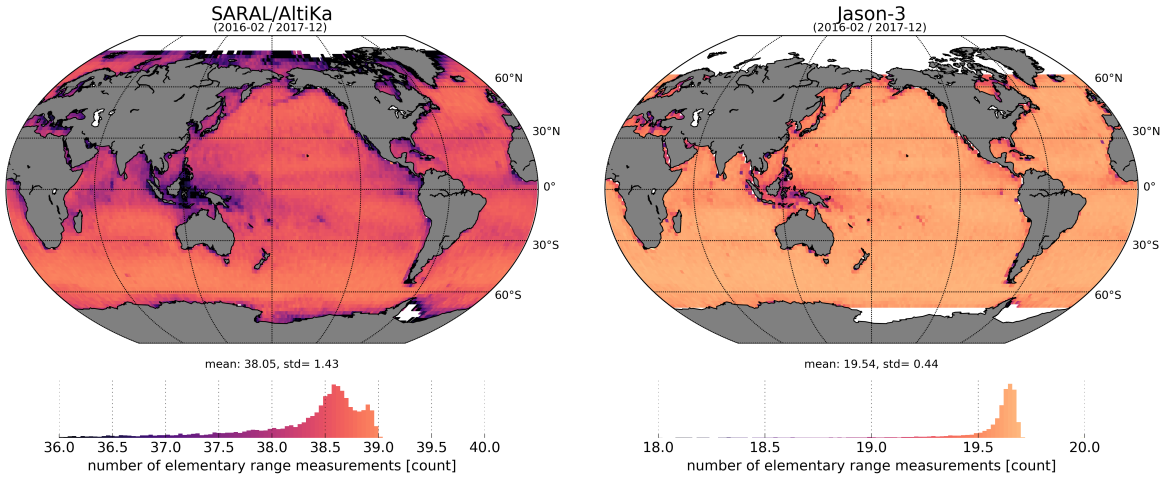

Figure 28: *Average map of number of SARAL/AltiKa elementary 40 Hz range measurements (left) and Jason-3 elementary 20 Hz range measurement (right).*

4.2.2. Standard deviation of 40 Hz measurements

Considering along-track data, SARAL/AltiKa's standard deviation of 40 Hz measurements is 5.8 *cm*, compared to 8.0 *cm* for Jason-2 and Jason-3 (right side of figure 29). When considering latitude weighted box statistics (left side of figure 29), these values decrease to respectively 5.6 and 7.7 *cm*. These values are consistent with power spectrum derived noise level estimates.

A lower value for SARAL/AltiKa compared to Jason-2 and Jason-3 is expected due to different band-widths on the two missions: 480 MHz for SARAL/AltiKa instead of 320 MHz for Jason-2 and Jason-2 (see [24]). As for the number of elementary range measurements, the standard deviation of the elementary range measurements is correlated to significant wave height (see maps on figures 30 and 40).

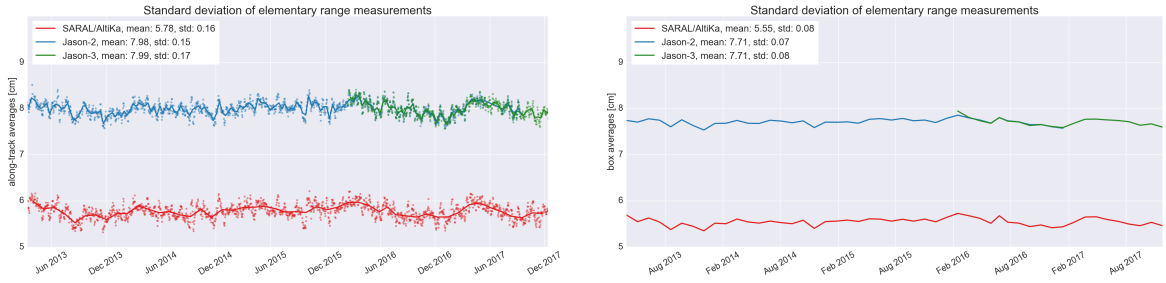

Figure 29: *Monitoring of rms of elementary 40/20 Hz range measurements for SARAL/AltiKa , Jason-2 and Jason-3, either computing latitude weighted box statistics (right) or along track averages (left).*

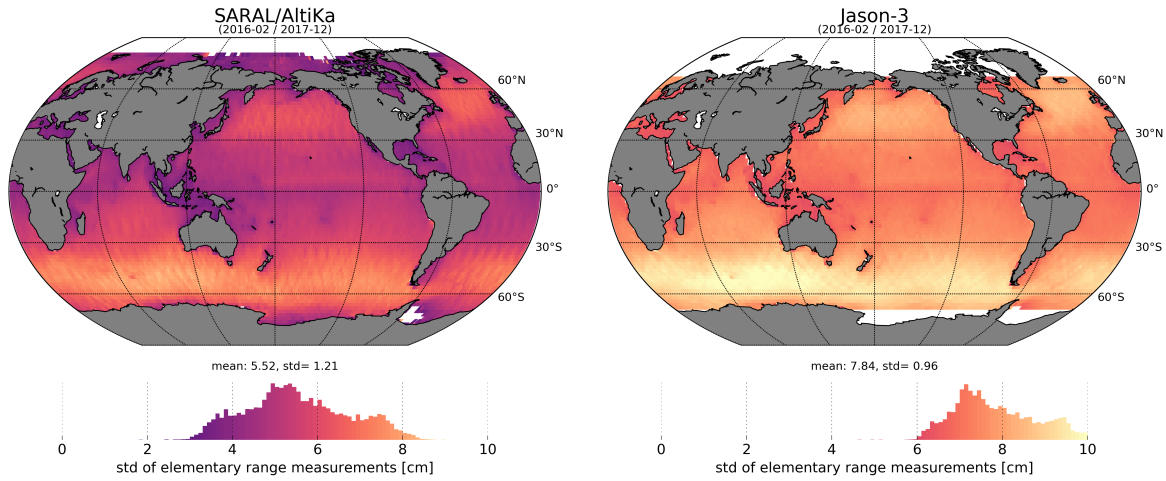

Figure 30: *Average map of rms of SARAL/AltiKa elementary 40 Hz range measurements (left) and Jason-3 elementary 20 Hz range measurement (right).*

4.3. Off-Nadir Angle from waveforms

The off-nadir angle is derived from the slope of the trailing edge of the waveform during the altimeter processing. It can either be the result of real platform mispointing or of backscattering properties of the surface. Figure 31 displays the evolution of the mean and standard deviation of this quantity over time for SARAL/AltiKa, Jason-2 and Jason-3. Jason-2 and Jason-3 show more variations of the off-nadir angle from waveforms due to its larger antenna aperture, note that these metrics are estimated on valid measurements only. Jason-2 and Jason-3 have an antenna beamwidth of 1.29°, whereas SARAL/AltiKa has only 0.6°. In addition Jason-2 and Jason-3's orbit is higher, resulting in a larger footprint radius (9.6 km) than SARAL/AltiKa (5.7 km). Therefore the probability of perturbations within the footprint - which modify the backscattering properties of the surface - is higher for Jason-2 and Jason-3 than for SARAL/AltiKa.

In the beginning of the SARAL/AltiKa mission the off-nadir angle from waveforms was slightly positive (around $0.003 deg^2$). Following an X-cross calibration maneuver ($+0.3°/-0.3°$ in pitch followed by $+0.3°/-0.3°$ in roll) done on April, 22nd 2013 (see N. Stenou [24]) a correction of $-0.045°$ in pitch direction was applied from April 25th onwards. A second X-cross calibration on April 30th, 2013 showed that the correction was successful. Off-nadir angle from waveforms stayed from this day on close to zero and very stable spatially and temporally.

During summer 2014 a rise in reaction wheel friction due to movement of lubricant resulted in an increase of the variability of the off-nadir angle. This event ended with the loss of a wheel and an important increase of the daily mean of the off-nadir angle leading to a safe-hold mode between October 6th and 9th, 2014. After the safe-hold mode, the spacecraft has been reconfigured to use only three wheels, resulting in a lower pointing accuracy at zero crossings of RW speed. A patch to the command law allowed to avoid these situations. Further mispointing events are now generally associated with random fluctuations of RW torque. A description of mispointing events can also be found in yearly report of 2015 ([10]), the main mispointing events are also mentioned in cyclic Cal/Val reports. As for further details about Jason-3's mispointing events at the begining of the mission (12 Feb- 28 MArs 2016) feel free to check out in the dedicated yearly report ([6]).

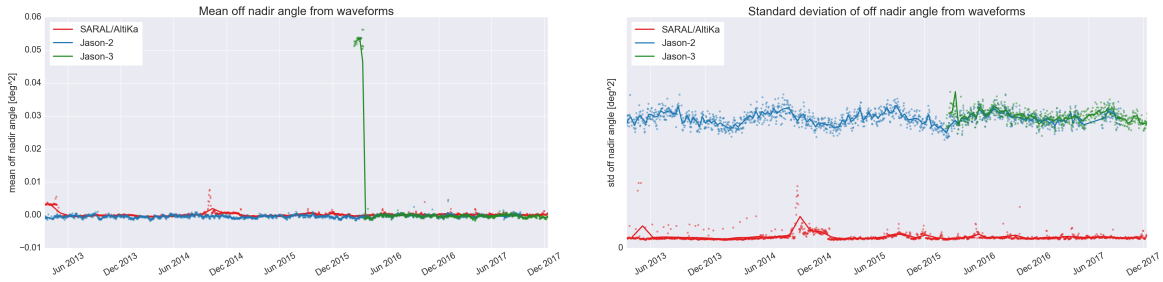

Figure 31: *Monitoring of mean (left) and standard deviation (right) of , Jason-2 and Jason-3 off-nadir angle from waveforms. Dots represent daily averages, the lines correponds to cycle averages.*

The map of SARAL/AltiKa off-nadir angle from waveforms (left of figure 32) is not homogeneous. The Indian ocean is impacted by platform mispointing due to maneuvers, and several mispointed tracks are visible due to RW issues. High mispointing values are observed at high latitudes close to sea ice, likley as a result of both platform mispointing and surface heterogeneities. Mispointing is slightly positive around Indonesia and equator and close to coasts. On the other hand, the

region around 50°S has slightly negative values. The map of Jason-3 (right of figure 32) shows a higher values of mispointing but confirms the patterns seen around Indonesia, and close to coasts. SARAL/AltiKa's map of mispointing is highly correlated to the map of backscattering coefficient (figure 36).

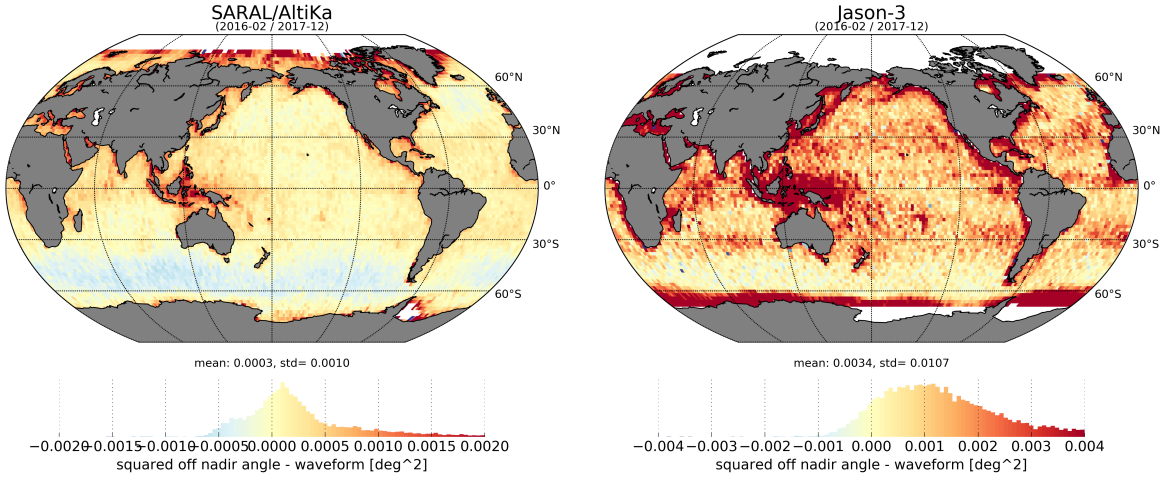

Figure 32: *Average map of off-nadir angle from waveforms for SARAL/AltiKa (left) and Jason-3 (right).*

Following the loss of the RW, ISRO has started sending platform pointing information derived from onboard star trackers. These data are routinely ingested in the SARAL/AltiKa Cal/Val database to perform comparisons between platform and waveform mispointing. Figure 33 compares waveform and plaftorm mispointing estimates. Over time, there is a good agreement between waveform and platform estimation. However the map of plaform mispointing is mush more homogeneous than the one derived from waveforms (32), as it is not impacted by pseudo mispointing due to heterogeneous surface properties in the radar footprint.

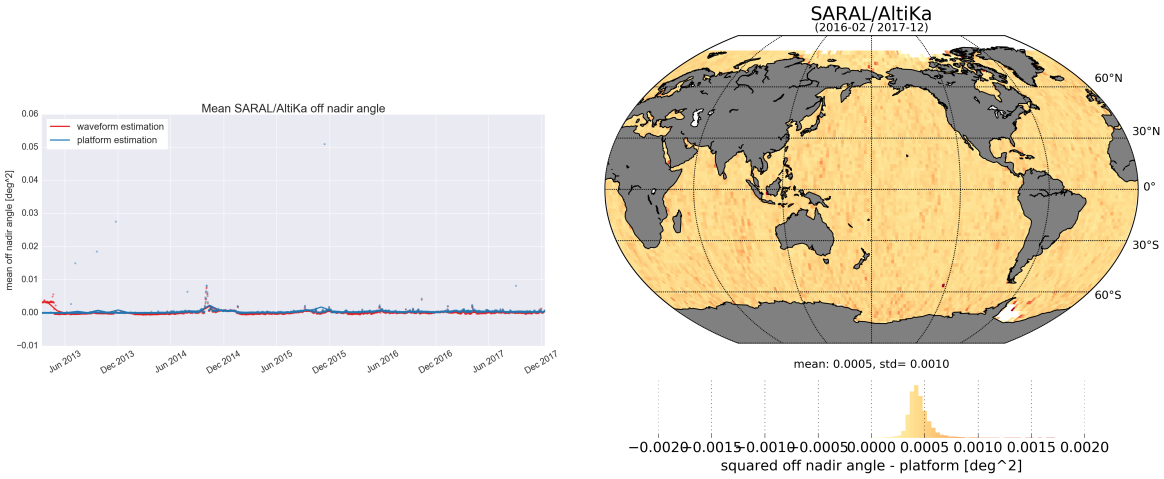

Figure 33: *Monitoring of off-nadir angle from waveform and platform for SARAL/AltiKa (left) and map of platform off-nadir angle (right).*

In order to get a better picture of SARAL/AltiKa mispointing events, we detect mispointed track sections. Track sections are defined as 15 consecutive measurements with mispointing values greater

than 0.015 deg^2. Results of this detection algorithm are presented in figure 34. There is an excellent agreement between the number of mispointed sections detected from waveforms and platfom data, indicating that, when consecutive measurements are affected by mispointing, this is likely a real platform pointing issue. Before October 2014, small peaks are associated with maneuvers. From October 2015 to February 2015, mispointed sections are associated with zero crossings of the RW speed. The command low was changed to avoid zero crossings and mispointing events occur randomly since then. No long term evolution of the number of these events is observed.

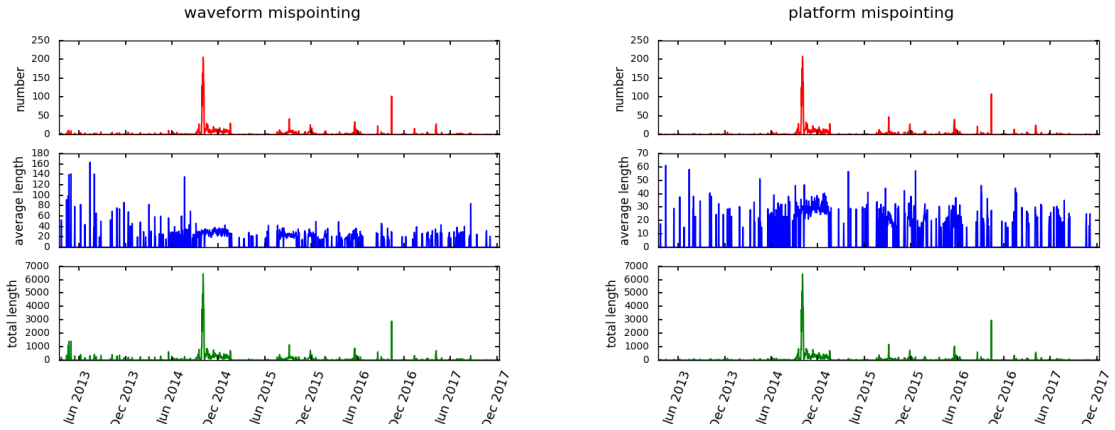

Figure 34: *Monitoring of mispointed track sections from waveform (left) and platform (right) data.*

4.4. Backscatter coefficient

SARAL/AltiKa is the first altimeter mission using the Ka-band frequency and was expected to show a different behavior than altimeters using Ku-band frequency. Several preparatory studies were done before launch, predicting that the Ka-band backscattering coefficient would be about 3.5 dB smaller than the Ku-band backscattering coefficient (see [24]). Note that the backscattering coefficient used here is corrected for atmospheric attenuation.

In flight assessment shows that the difference with respect to Ku-band backscattering coefficient is smaller than expected: 2.5 dB in average (see bottom of figure 35). The daily evolution of SARAL/AltiKa backscattering coefficient shows the same signals as the one of Jason-2 and of Jason-3 (top left of figure 35), the dispersion diagram of backscattering coefficients at 3h crossover points with Jason-3 (38) shows also a good correlation , and maps show consistent patterns (36)

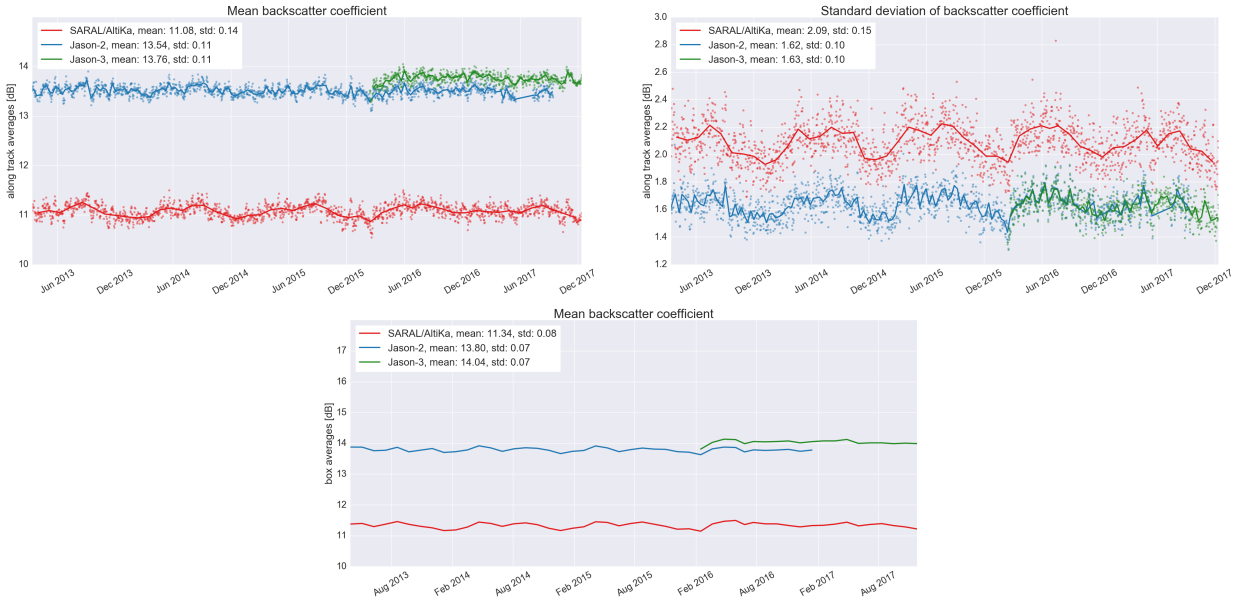

Figure 35: *Daily monitoring of mean and standard deviation of SARAL/AltiKa, Jason-2 and Jason-3 backscattering coefficient (top) and cyclic monitoring of box averaged latiude weighted mean (bottom).*

However the backscattering standard deviation is higher for SARAL/AltiKa than for Jason-2 and Jason-3 (top right of figure 35). While maps of backscattering coefficient show the same structures (see figure 36), the amplitudes of the observed structures are slightly larger for SARAL/AltiKa than for Jason-3. Indeed the difference between Ka- and Ku-band backscattering coefficient is not a simple bias, as shown on the map (right of figure 37), which shows a latitude dependency and/or signals related to waves and rain events. Note that the differences between the two missions are highly related to the sea surface temperature so that hot surface temperature of low latitude implies a stronger difference between the two bands ([3]).

Figure 38 displays the dispersion diagram between SARAL/AltiKa and Jason-3 backscatter, estimated at 3h crossovers, as well as the histogram of backscatter. While a good correlation between the two missions is observed, the relation is not strictly linear. The population distribution is different for the Ka- and Ku-band frequencies: the SARAL/AltiKa histogram is tilted with a larger

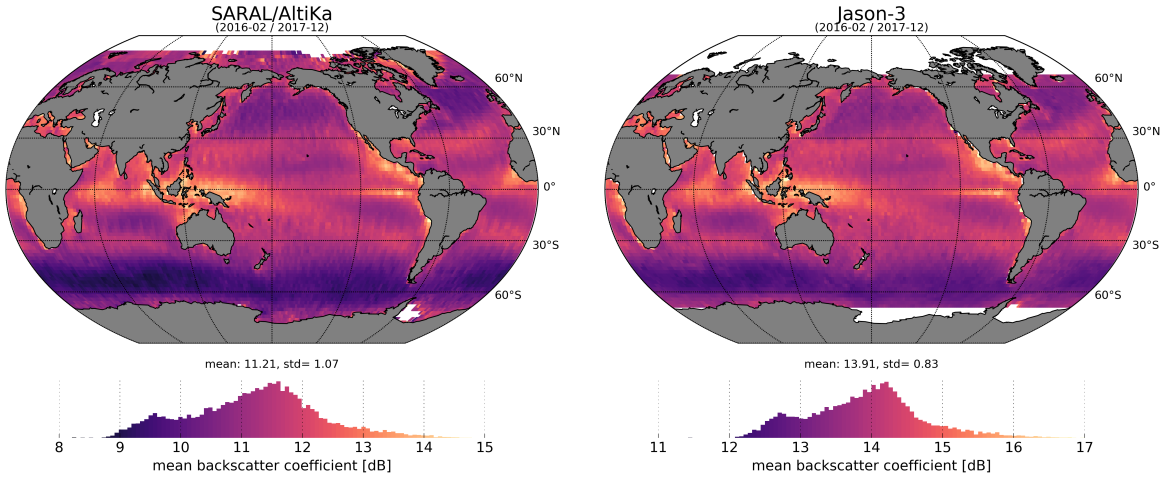

Figure 36: *Average map of backscattering coefficient for SARAL/AltiKa (left) and Jason-3 (right).*

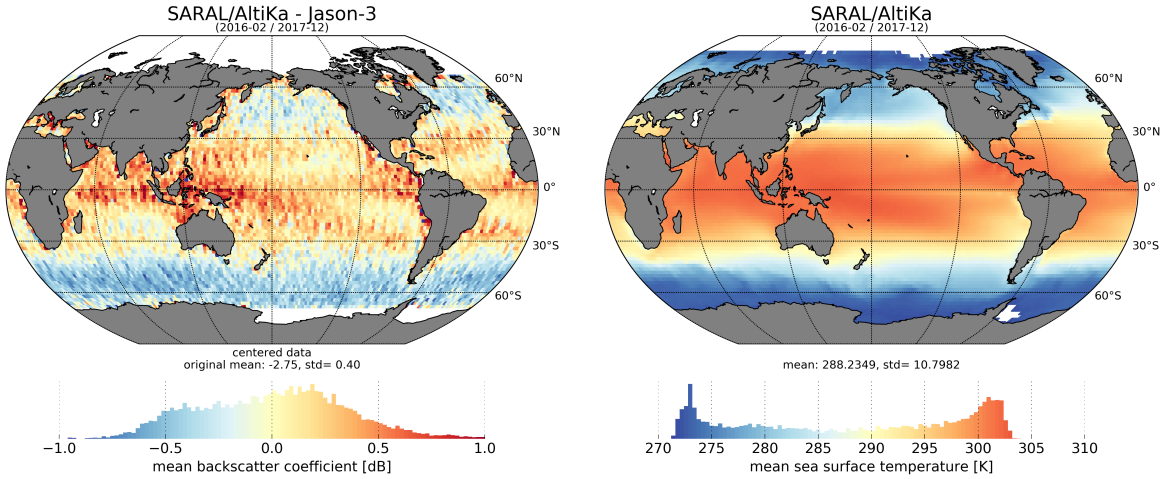

Figure 37: *Difference map of SARAL/AltiKa and Jason-3 backscattering coefficient (left) and map of sea surface temperature (right) .*

number of measurements at low backscatter values.

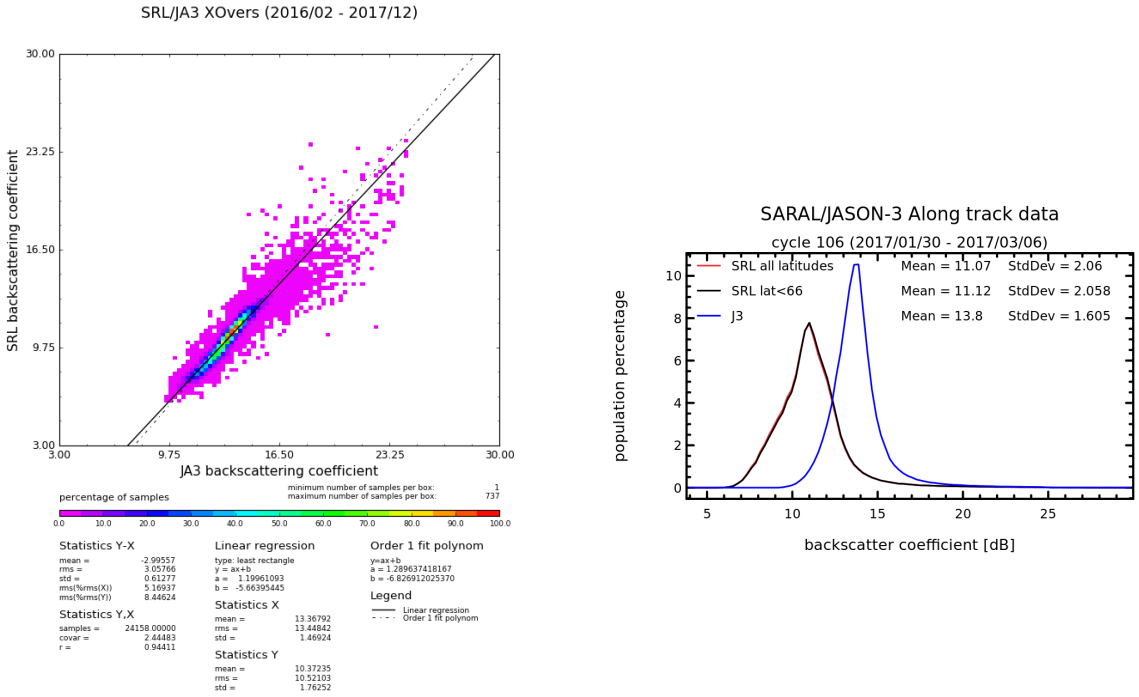

Figure 38: *Dispersion diagram of backscattering coefficient between SARAL/AltiKa and Jason-3 at 3h crossover points (left) and histogram of along-track data computed over SARAL/AltiKa 106 (right).*

4.5. Significant wave height

The significant wave height (SWH) is one of the parameters derived from the waveforms. Monitoring of mean and standard deviation of SWH show a very good agreement between SARAL/AltiKa Jason-2 and Jason-3 (see top of figure 39). When accounting for the different data distribution with latitude (see bottom of figure 39), the difference between SARAL/AltiKa and the Jason's missions is in average only of 1 cm. When taking into account all latitudes, SWH is largely reduced for SARAL/AltiKa as small SWH occur in very high northern latitudes when the sea ice recedes (see also left map of figure 40). The maps of SWH show the same structures: low SWH around Indonesia, in the Mediterranean Sea and the Gulf of Mexico and high SWH around 50°S (as well as in North Atlantic). The difference map between the two satellites (bottom of figure 40) is centered around a difference of 4 cm, with slightly higher values for SARAL/AltiKa. Although this might appear to contradict top left of figure 39, it is only the result of different ways to estimate the mean. Stronger differences occur in high latitudes (in regions, where SWH is higher than 2-3 m). When considering the dispersion diagram between SARAL/AltiKa and Jason-3 SWH at 3 hours crossovers (left of figure 41), a strong correlation coefficient ($r > 0.99$) is obtained, with an almost perfectly linear relationship between the two missions.

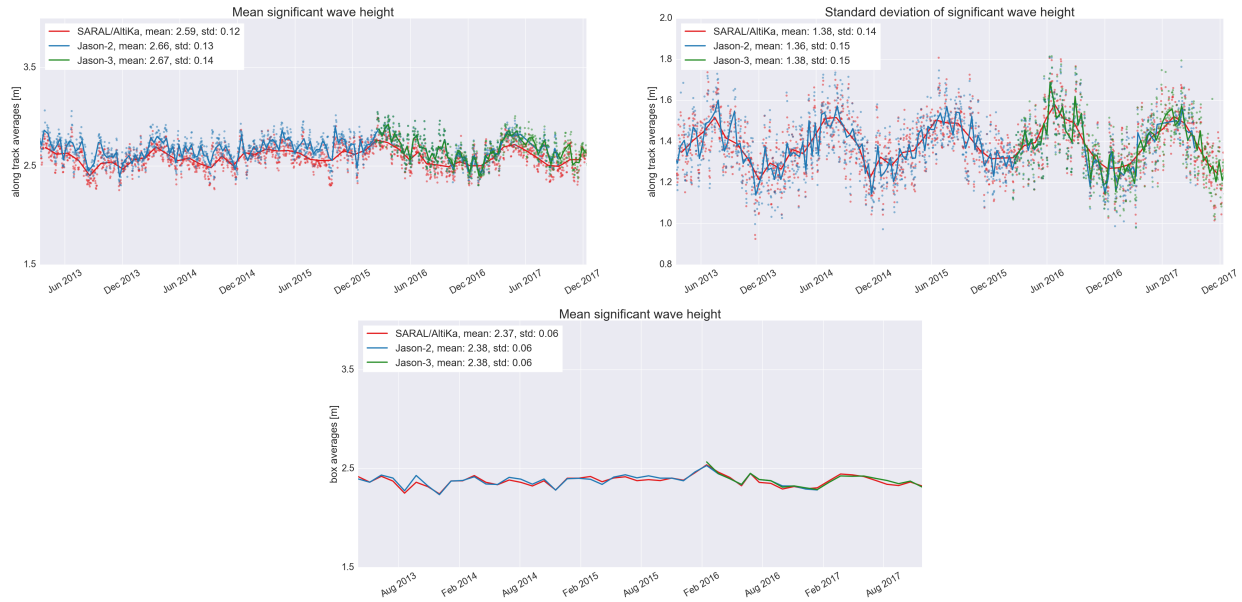

Figure 39: *Daily monitoring of mean and standard deviation of significant wave height for SARAL/AltiKa, Jason-2 and Jason-3 (top) and cycle per cycle monitoring of box averaged latitude weighted mean (bottom).*

When considering crossover points between SARAL/AltiKa and Jason-3 (figure 41, left) mean SWH values are 3.15 m for SARAL/AltiKa and 3.09 m for Jason-3. This is much higher than the mean values of daily along-track SWH (around 2.60 m), and results from the geographical distribution of 3h crossover points: most crossover points are located in high SWH areas (latitudes around 50°), which biases the mean towards high SWH. Nevertheless, this diagnosis shows that for the same positions (SARAL/AltiKa/Jason-3 crossovers) with a time difference lower than 3h, SARAL/AltiKa SWH is slightly higher than Jason-3's. This is also the case when computing latitude weighted box statistics (in order to compensate for uneven data distribution), as shown on bottom of figure 39,

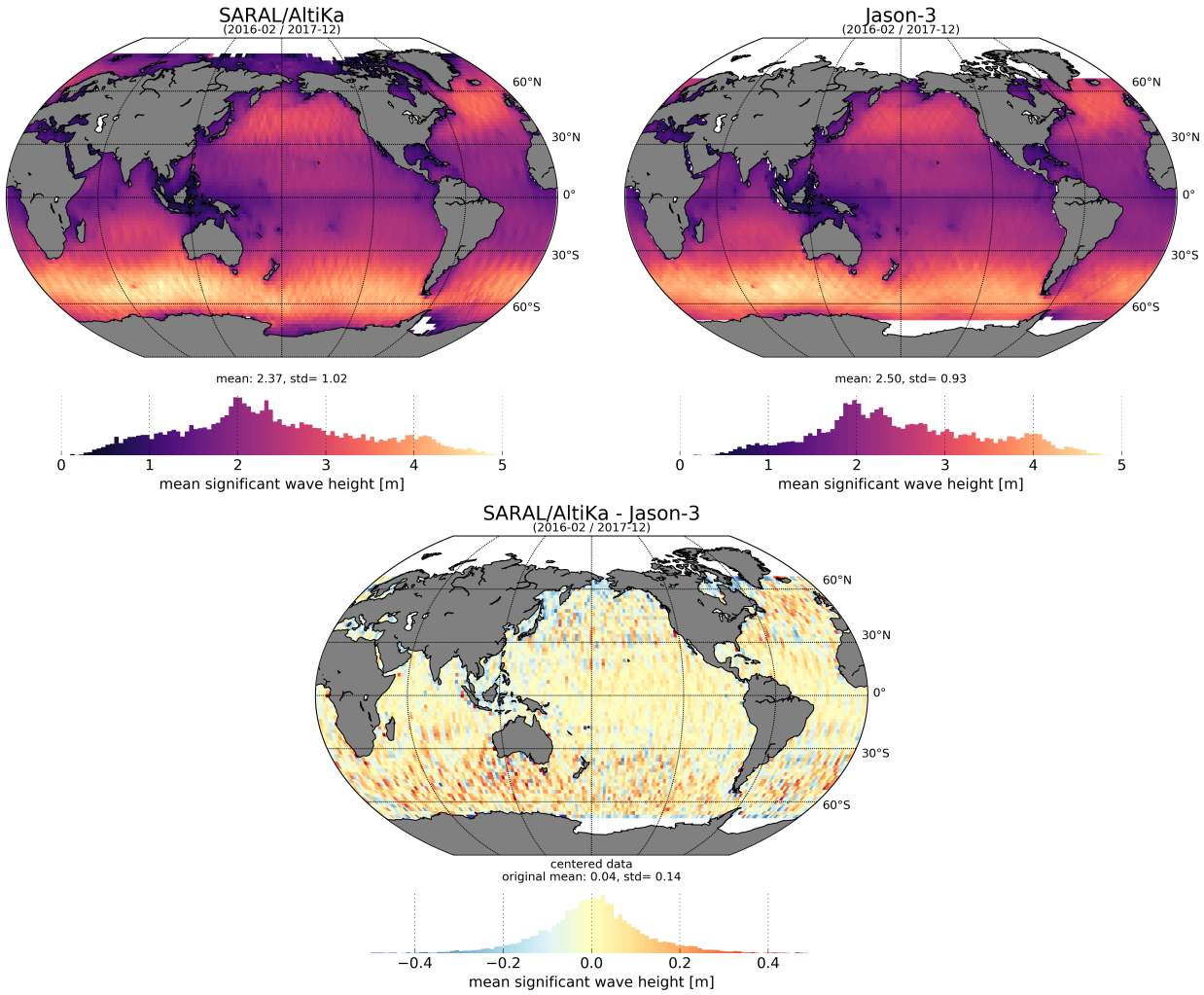

Figure 40: *Average map of significant wave height for SARAL/AltiKa (left) and Jason-3 (right) . Difference map of SARAL/AltiKa and Jason-3 significant wave height.*

where Jason-2's and Jason-3's SWH is generally slightly lower than SARAL/AltiKa's. When considering along-track statistics (top of figure 39), Jasons' SWH appears higher than SARAL/AltiKa SWH, this is again an effect of geographical data distribution.

The shapes of the histograms are very similar (see right side of figure 41) for Jason-3 and SARAL/AltiKa, except for small SWH. The minimum SWH value of SARAL/AltiKa SWH is around 12 cm (related to the look-up table), it is 0 for Jason-3. Nevertheless, small SWH of current Jason-2 and Jason-3 data are not precise (errors of about 15 cm), as the look-up table correction for small SWH is not accurate, whereas the SARAL/AltiKa look-up tables were updated in Patch2. Furthermore, the histogram for SARAL/AltiKa shows a small bump for SWH around 50 cm. Note that in the wave forecasting systems of Meteo-France, altimeter significant wave height from SARAL/AltiKa are only assimilated for values higher than 50 cm. According to L. Aouf, the SARAL/AltiKa SWH data have a positive impact on the wave analysis and forecast of the Meteo-France wave analysis model ([13]).

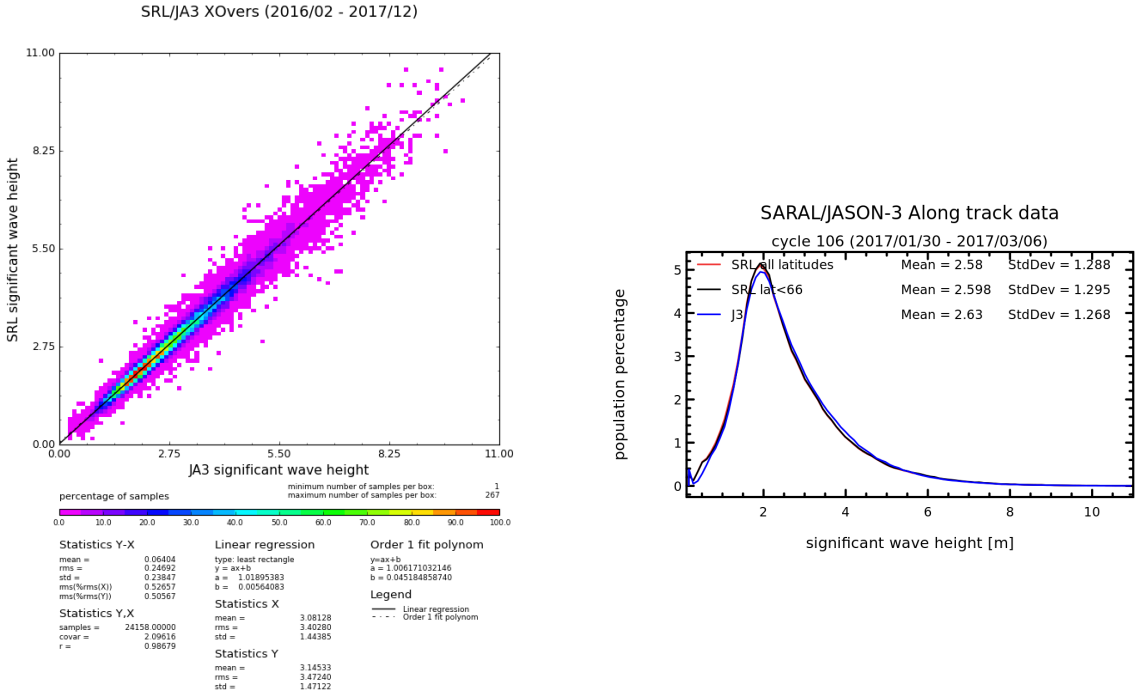

Figure 41: *Dispersion diagram of significant wave height between SARAL/AltiKa and Jason-3 at 3h crossover points on the left and histogram of along-track data computed over SARAL/AltiKa cycle 106 the right.*

4.6. Ionosphere correction

As SARAL/AltiKa uses a single frequence, no dual frequency ionosphere correction is available, GIM model is used instead. This is not an issue as the SARAL/AltiKa altimeter uses a frequency of 35.75 GHz (Ka-band), and ionospheric effects are therefore very small (divided by roughly seven compared to Ku-band frequency). In this section, Jason-2 and Jason-3 ionospheric correction values were scaled to be compared to SARAL/AltiKa ones. The scaling factor is based on the radar frequency ratio: $\frac{(f_{ku})^2}{(f_{ka})^2} = \frac{(13.575)^2}{(35.75)^2} \approx 0.14$ between instruments. Monitoring the evolution of the ionospheric correction on SARAL/AltiKa, Jason-2 and Jason-3 shows very similar evolution (42), with a slightly higher variability for Jason-2 and Jason-3, likely related to small scale features the GIM model is unable to reproduce. Effects of varying local times on Jason-2 and Jason-3 are also visible.

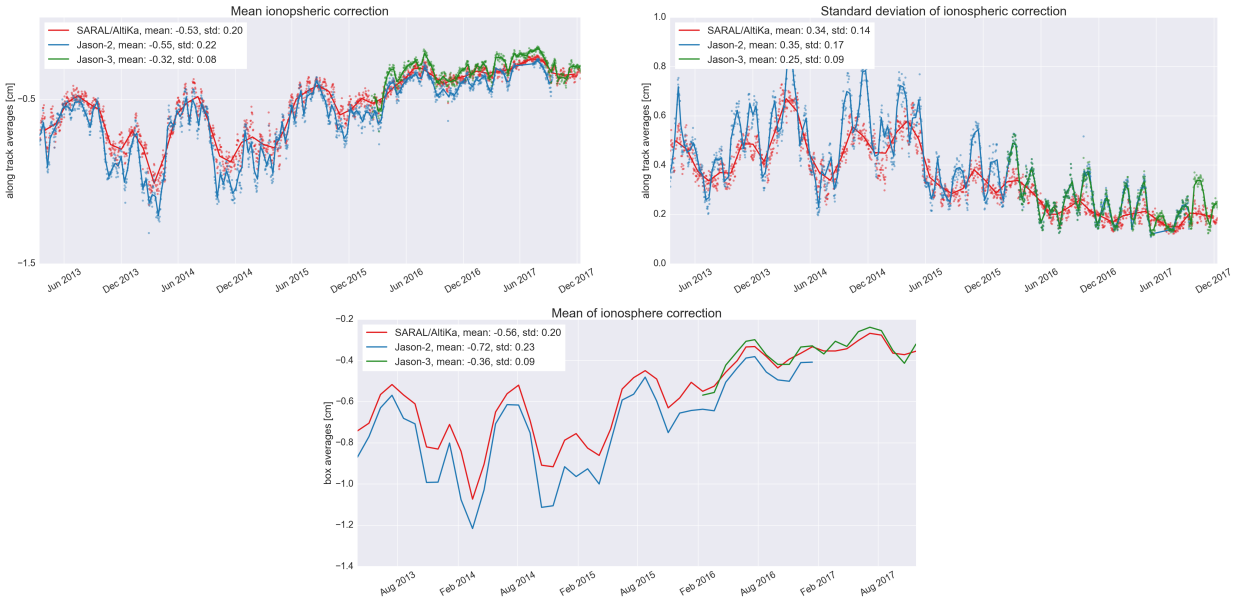

Figure 42: *Daily monitoring of mean and standard deviation ionosphere correction for SARAL/AltiKa (GIM), Jason-2 and Jason-3 (filtered dual-frequency ionosphere correction with scale factor 0.14418 for mean computation).*

Small differences between the missions are still observed, which may also be due to the fact that SARAL/AltiKa is a sun-synchronous satellite with 6:00 local time for ascending node and 18:00 local time for descending node. As ionosphere correction varies with local time, it is very small for ascending (morning) passes and has absolute values up to 2 cm in the equatorial region for descending (evening) passes. Jason-2 and Jason-3 on the other hand are not sun-synchronous and revisits only every 12 cycles the same local hours. Different altitudes between Jasons and SARAL/AltiKa might also impact the observed ionospheric content.

Highest ionosphere correction (absolute values) can be found in the same regions (equatorial region) for SARAL/AltiKa and Jason-3 (see maps of figure 43, where Jason-3 data are not scaled), but the amplitude is of course very different (due to the different frequencies).

The dispersion diagram of ionosphere corrections (figure 44, Jason-3 is rescaled to Ka-band frequency) at 3h crossovers shows a correlation level of 0.90 between the two missions. Histograms are

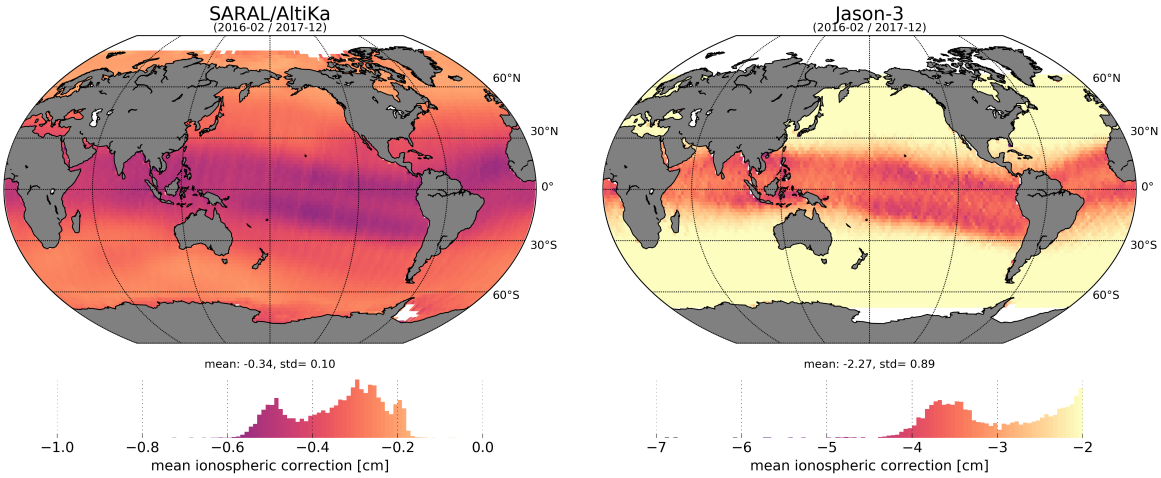

Figure 43: *Average map of ionosphere correction for SARAL/AltiKa (GIM, left) and Jason-3 (filtered dual-frequency ionosphere correction, right). Note that color scales are different for SARAL/AltiKa and Jason-3.*

slightly different, with a bi-modal distribution for Jason-3 that is less visible on SARAL/AltiKa.

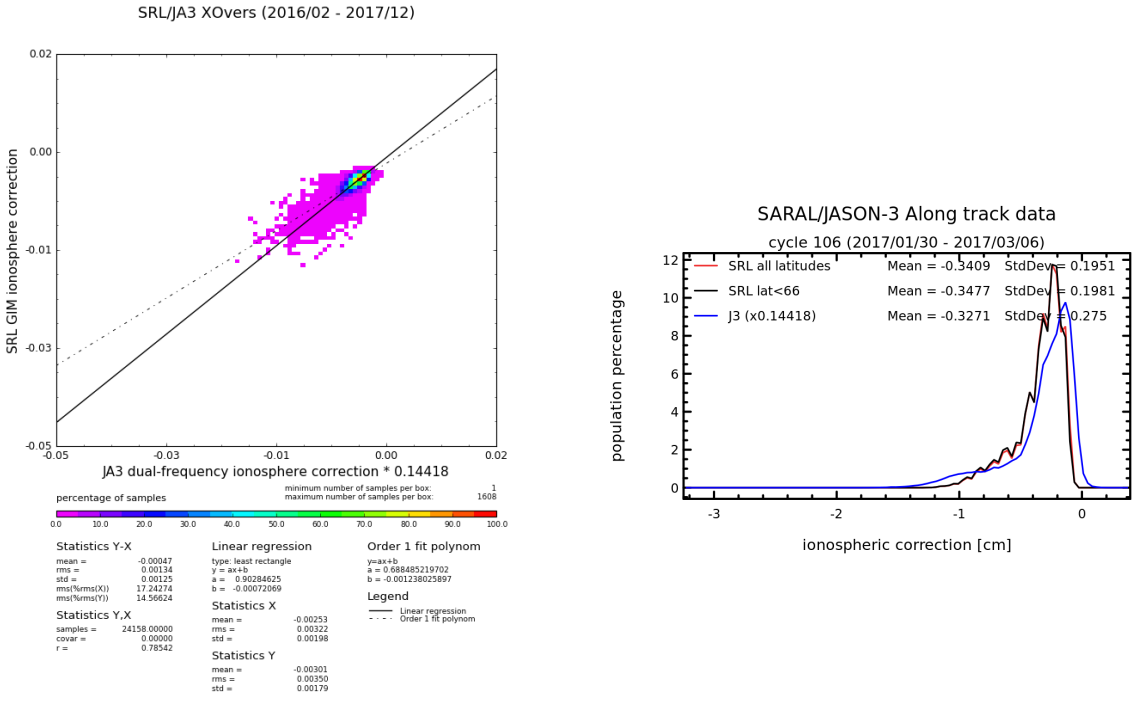

Figure 44: *Dispersion diagram of ionosphere correction between SARAL/AltiKa (GIM) and Jason-3 (filtered dual-frequency with scale factor of 0.14418 for Jason-3) at 3h crossover points on the left and histogram of along-track data computed over SARAL/AltiKa cycle 106 on the right.*

4.7. Radiometer wet troposphere correction

4.7.1. Overview

In order to have access to radiometer wet troposphere correction, liquid water content, water vapor content and atmospheric attenuation, SARAL/AltiKa uses a dual-frequency radiometer (23.8 GHz +/- 200 MHz & 37 GHz +/- 500 MHz), whereas Jason-2 and Jason-3 have a similar three-frequency radiometer (18.7, 23.8 and 34.0 GHz). Figure 45 shows the daily mean and standard deviation of radiometer wet troposphere correction for SARAL/AltiKa, Jason-2 and Jason-3. With Patch2, the standard deviation is smaller for SARAL/AltiKa than for Jasons. Concerning the mean of radiometer wet troposphere correction, Jason-2 and Jason-3 has dryer values than SARAL/AltiKa. This is on the one hand related to different radiometer wet troposphere correction retrieval algorithms, but on the other hand, this can also be related to different local times of the satellites (sun-synchronous 6h/18h for SARAL/AltiKa). During several months the radiometer wet troposphere correction of SARAL/AltiKa went dryer, this is related to the saturation of the hot calibration counts, which was corrected on 22 October 2013 (explaining the jump of around 5 mm amplitude visible on the monitoring of figure 46). The safe-hold mode of SARAL/AltiKa did generate a 1 mm bias on the daily mean which is documented in a previous yearly report [10]. Both anomalies will be corrected in the next GDR-E reprocessing, foreseen late 2018.

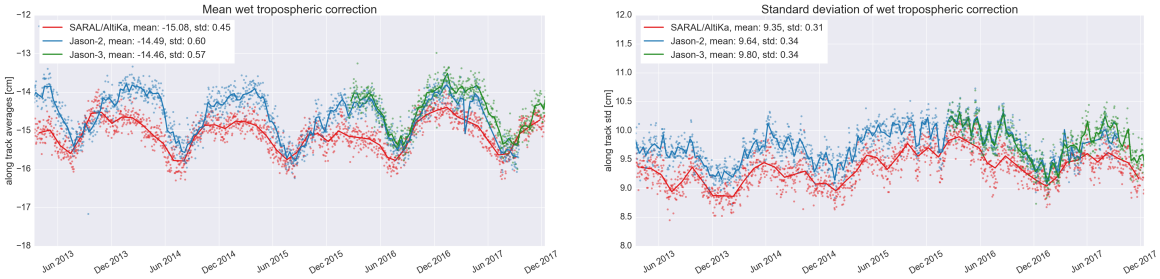

Figure 45: *Monitoring of mean and standard deviation of radiometer wet troposphere correction for SARAL/AltiKa (red) Jason-2 (blue) and Jason-3 (green).*

4.7.2. Comparison with the ECMWF model

The ECWMF wet troposphere correction is used as a reference to investigate small differences between SARAL/AltiKa Jason-2 and Jason-3 radiometer corrections. Daily differences are calculated and plotted in figure 46. The drift in the radiometer wet troposphere correction of SARAL/AltiKa due to the saturation of the hot calibration count is clearly visible on the left part of figure 46. In avarage the difference between radiometer and ECMWF wet troposphere correction for SARAL/AltiKa and Jason-3 is around 6 mm. As for Jason-2 it's performance regarding the wet troposphere correction has been severely impacted by the several SHM modes experienced since Mars 2016. The two ECMWF model updates that occurred during the observed period (June and November 2013), which might have an impact on the model wet troposphere correction, did not show any impact on the data.
The standard deviation of radiometer minus model wet troposphere correction is higher for SARAL/AltiKa (around 1.6 cm) compared to Jasons (around 1.2 cm), shown on left of figure 46 and also on the histogram on figure 48. Work is ongoing to provide a more accurate wet tropospheric correction for the future GDR-E version.

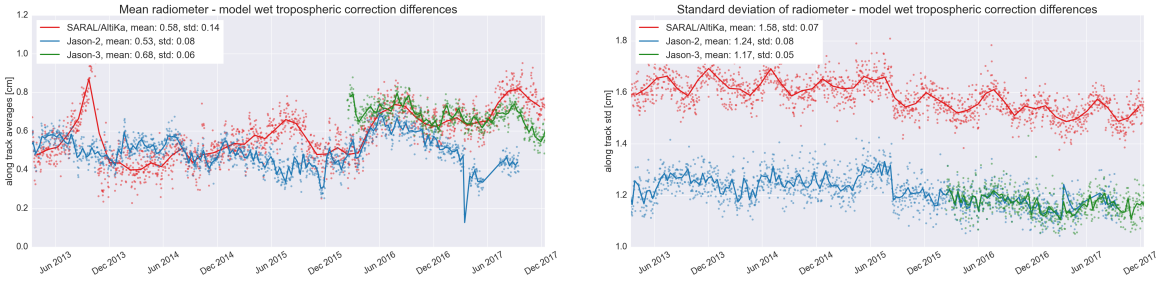

Figure 46: *Monitoring of mean and standard deviation of radiometer minus model wet troposphere correction differences for SARAL/AltiKa Jason-2 and Jason-3.*

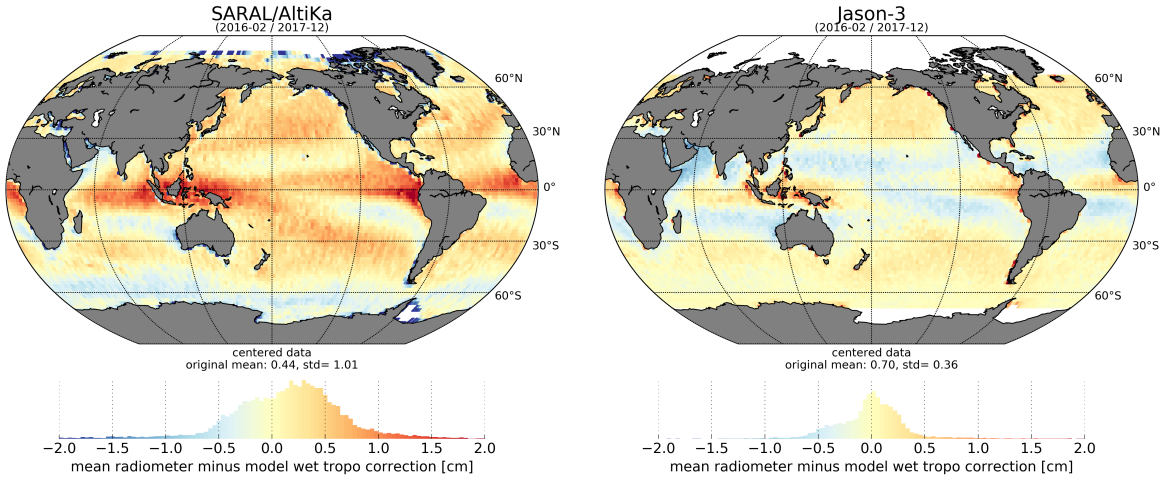

Figure 47: *Average map of radiometer minus ECMWF model wet troposphere correction for SARAL/AltiKa (left) and Jason-3 (right).*

The maps of radiometer minus ECMWF model wet troposphere correction (figure 47) are centered around the mean value (7 mm for Jason-3, 4.4 mm for SARAL/AltiKa). The mean of the SARAL/AltiKa map is impacted on the one side by the saturation of the hot calibration counts (which tends to overestimate the difference) and on the other side by some boxes near the frontier between sea-ice and free water (which tends to underestimate the mean). These boxes with strong negative values are an indication that probably not all sea ice cases are edited. In the frame of the PEACHI project, a new ice flagging procedure was tested, and will be implemented in the upcoming GDR-E. Geographical structures of the radiometer minus model wet troposphere corrections are similar for the two satellites in high latitudes (around $\pm$ 50°), but quite different for low latitudes. This is also observed on the histogram of wet troposphere differences (figure 48) which is slightly wider for SARAL/AltiKa than for Jason-3.

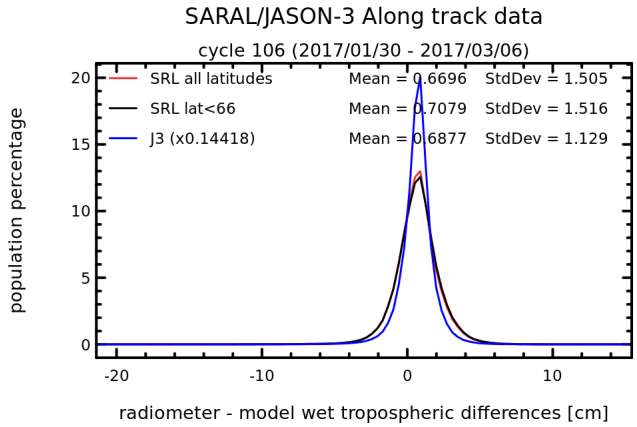

Figure 48: *Histogram (of along-track data) of radiometer minus ECMWF model wet troposphere correction between SARAL/AltiKa and Jason-3 computed for SARAL/AltiKa cycle 106.*

4.8. Altimeter wind speed

The Patch1 version of the products used the wind look-up table from Jason-1 which, with the Ka-band backscattering coefficient produced erroneous wind speeds. In the Patch2 version, the altimeter wind speed algorithm developed by [20] for Ka-band altimetry is used. Figure 49 shows the daily monitoring of the mean and standard deviation of altimeter wind speed for SARAL/AltiKa, Jason-2 and Jason-3. The SARAL/AltiKa Patch2 altimeter wind speed has values similar to Jason-2's altimeter wind speed while still on its nominal period (before October 2016) and to Jason-3's wind speed all along. It should be noted that in the current products, the SARAL/AltiKa wind speed is impacted by the saturation of the radiometer hot calibration counts through the estimation of the atmospheric attenuation which is applied on the backscatter coefficient used in the computation of wind.
The maps of altimeter wind speed for SARAL/AltiKa and Jason-3 are consistent (see 50). Figure 51 shows a good correlation of wind speed data between the two missions ($r = 0.94$), yet the relationship between Jason-3 and SARAL/AltiKa remains not truly linear. SARAL/AltiKa's wind speed seems to saturate for values greater than 16 m/s which tends to underestimated the wind speed compared to Jason-3. This might be related either to the wind retrieval algorihtm or can be an effect of the SST signal in the Ka band backscatter coefficient that alters the wind speed computation. This specific behavior will be investigated for the upcoming GDR-E products. The distribution of SARAL/AltiKa wind speed values shows two modes, this feature is less present on Jason-3 data. SARAL/AltiKa's histogram has sudden decline above 16 m/s which is not observed on Jason-3 data.

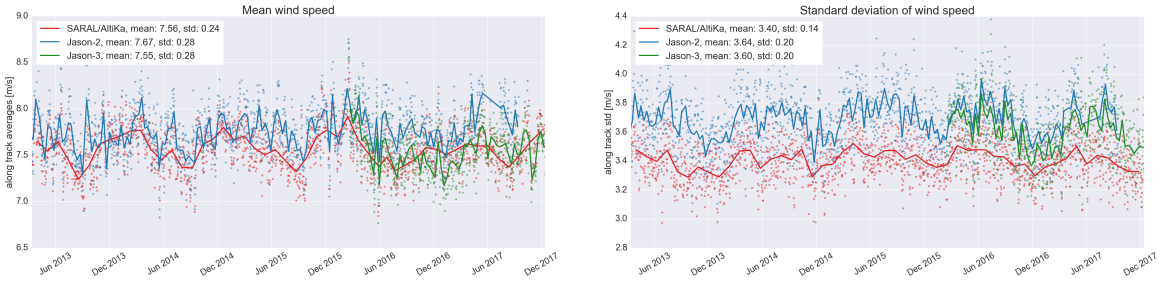

Figure 49: *Monitoring of mean and standard deviation of altimeter wind speed for SARAL/AltiKa and Jason-3.*

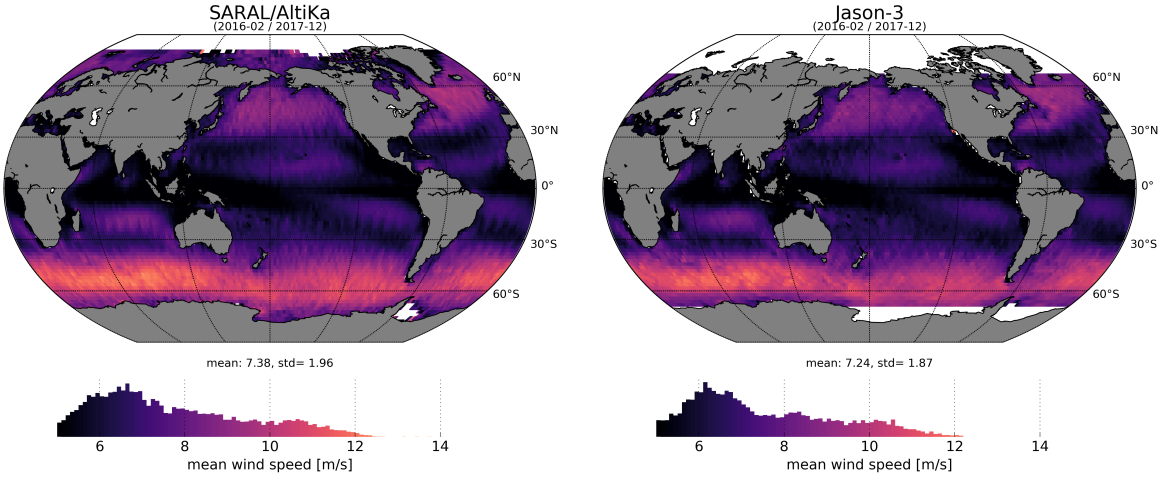

Figure 50: *Average map of altimeter wind speed for SARAL/AltiKa (left) and Jason-3 (right).*

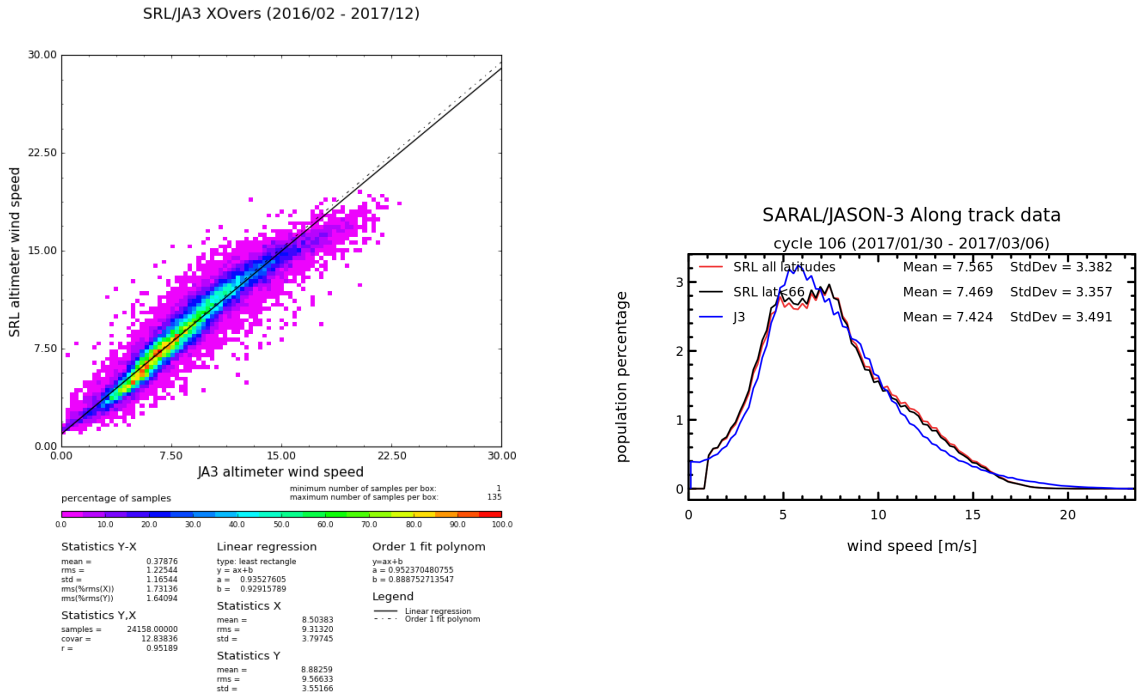

Figure 51: *Dispersion diagram of altimeter wind speed between SARAL/AltiKa and Jason-3 at 3h crossover points (left) and histogram of along-track data computed for SARAL/AltiKa cycle 106 (right).*

4.9. Sea state bias

In Patch1 version, the sea state bias was as a first approximation set to -3.5% of SWH.
For Patch2 a hybrid SSB solution developed by R. Scharroo was used (this SSB was computed using the same method as in [23]). The Patch2 SSB solution is in absolute values around 1.8 cm stronger (which increases the Patch2 SLA) than the Patch1 solution. The daily monitoring of the along-track sea state bias for SARAL/AltiKa Jason-2 and Jason-3 shows a similar temporal evolution, but SARAL/AltiKa SSB has higher absolute values (around 2.5 cm higher) than Jason-2 and Jason-3 (see left side of figure 52). This is also the case when considering latitude weighted box statistics (bottom of figure 52). The bias between SARAL/AltiKa and Jasons' SSB is not homogeneous but varies geographically, as shown on bottom of figure 53. Furthermore the daily standard deviation is also slightly larger for SARAL/AltiKa compared to Jasons (see right side of figure 52).

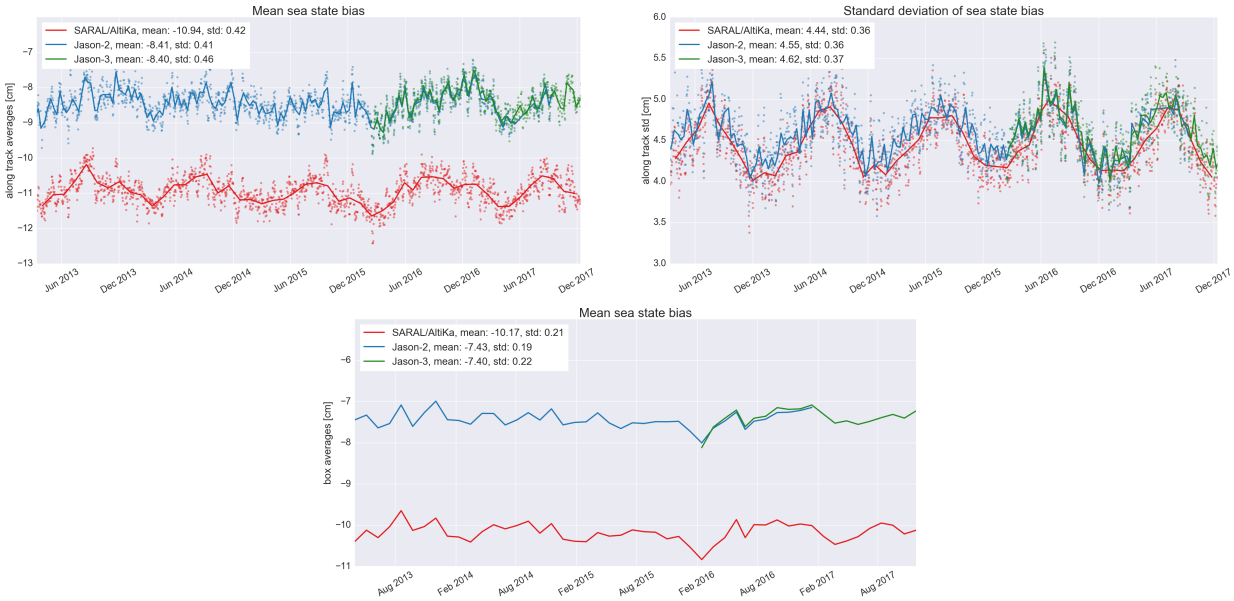

Figure 52: *Monitoring of mean and standard deviation of (along-track) sea state bias of SARAL/AltiKa Jason-2 and Jason-3 on the top. Cycle per cycle monitoring of latitude weighted box averaged mean on the bottom.*

The map of SARAL/AltiKa sea state bias shows higher values in the region of 50°S (where SWH is strong) than the map of Jason-3 (top of figure 53). The dispersion diagram of SARAL/AltiKa and Jason-3 sea state bias at 3h multi-mission crossovers confirms that the SARAL/AltiKa SSB is overestimated for high SSB (i.e. for high SWH). The different nature of the SSB models used for SARAL/AltiKa and Jason-3 (dedicated model) is also visible on the right side of figure 54, showing very different shapes of histograms. An updated SSB solution for SARAL/AltiKa is available through the PEACHI project and will be used in the upcoming GDR-E products.

This difference in sea state bias between the two missions has also an impact on the geographically correlated biases between the two missions, as shown in chapter 5.3., concerning maps of sea surface height differences at multi-mission crossover points.

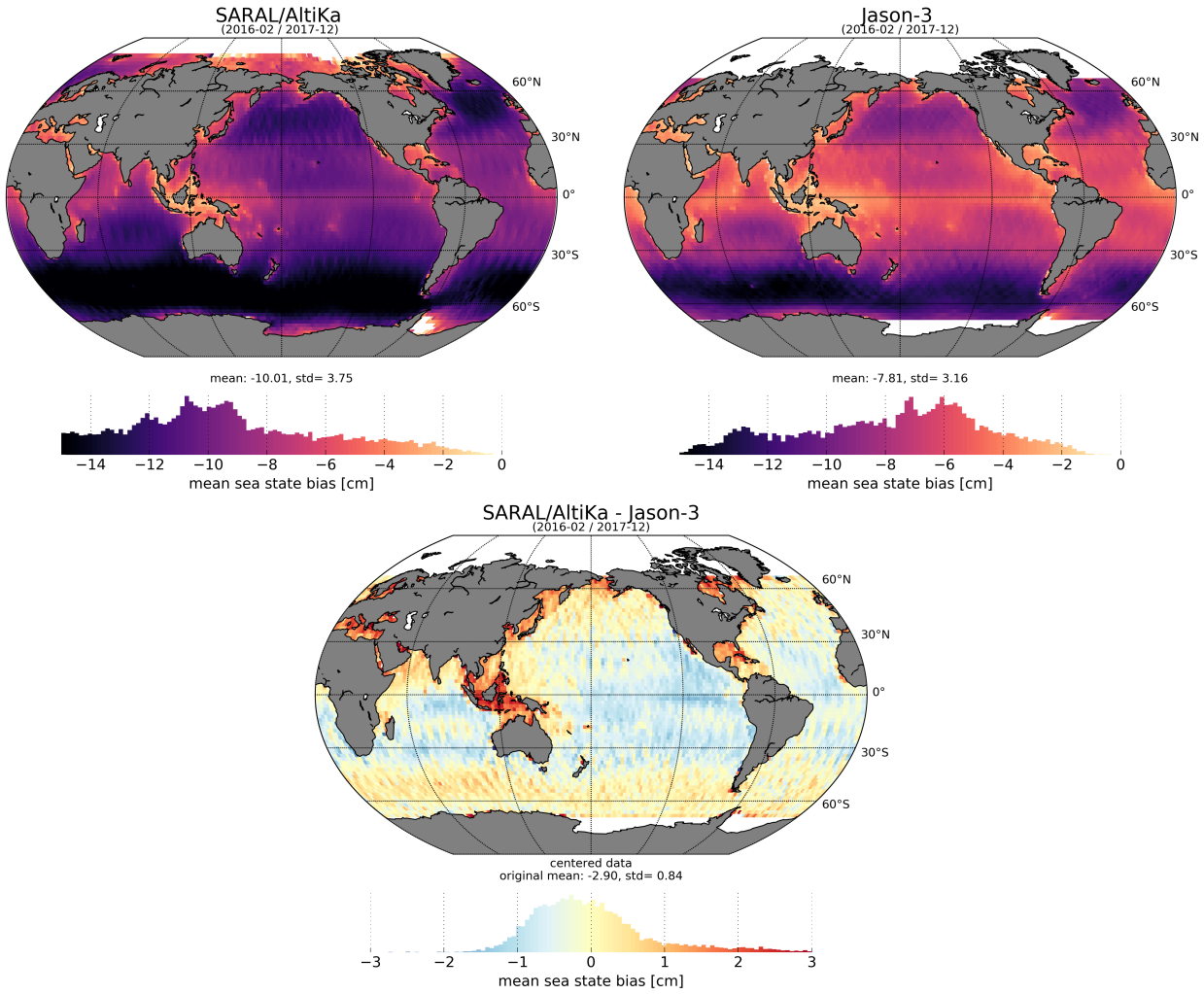

Figure 53: *Average map of sea state bias for SARAL/AltiKa (left) and Jason-3 (right). Map of differences of gridded SARAL/AltiKa and Jason-2 sea state bias.*

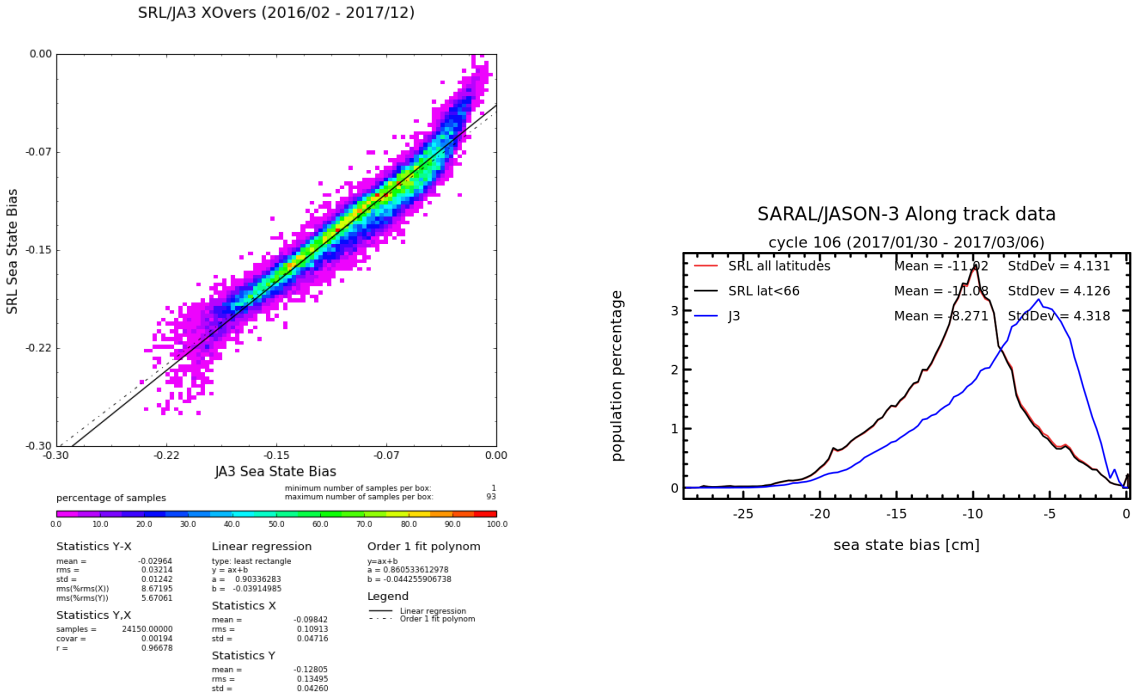

Figure 54: *Dispersion diagram of sea state bias between SARAL/AltiKa and Jason-3 at 3h crossover points (left). Histogram (of along-track data) computed for SARAL/AltiKa cycle 106 (right).*

5. SSH crossover analysis

5.1. Overview

SSH crossover differences are the main tool to analyze the whole altimetry system performance. Crossovers measure the SSH consistency between ascending and descending passes. At each crossover, the observed difference of SSH measurements between ascending and descending arcs results from the sum of errors in the system and ocean variability. In order to reduce the impact of ocean variability, only crossovers with a maximum time difference of 10 days are selected. This gives a measure of the mission performance on mesoscale time/space scales. Mean and standard deviation of SSH crossover differences are computed from the valid data set to estimate maps and cycle per cycle monitoring over the altimeter period. In order to monitor the performances over stable surfaces, additional editing is applied to remove shallow waters (bathymetry above -1000 m), areas of high ocean variability (variability above 20 cm rms) and high latitudes ($|lat| < 50\,\mathrm{deg}$). Under these conditions, SSH performances are always estimated with equivalent conditions.

The formula used to estimate a fully corrected SSH for SARAL/AltiKa and Jason-3 is defined below:

$$SSH = Orbit - Altimeter\ Range - \sum_{i=1}^{n} Correction_i \tag{1}$$

where the sum of corrections expands as:

$$\begin{aligned} \sum_{i=1}^{n} Correction_i \;=\; & Dry\ troposphere\ correction \\ & + \; Dynamical\ atmospheric\ correction \\ & + \; Radiometer\ wet\ troposphere\ correction \\ & + \; Ionospheric\ correction \\ & + \; Sea\ state\ bias\ correction \\ & + \; Ocean\ tide\ correction\ (including\ loading\ tide) \\ & + \; Earth\ tide\ height \\ & + \; Pole\ tide\ height \end{aligned}$$

The corrections effectively used to generate the metrics presented in this report are summarized in table 6 for SARAL/AltiKa and Jason-3. The standards correspond to the current version of the GDR products: GDR-T Patch2 for SARAL/AltiKa and GDR-D for Jason-3.

Parameter	SARAL/AltiKa	Jason-3
Orbit	CNES POE-D until cycle 24, POE-E afterwards	CNES POE-D (Doris/Laser/GPS)
Dynamic atmospheric correction	Computed from ECMWF atmospheric pressures after removing S1 and S2 atmospheric tides (for inverse barometer) + Mog2D High Resolution ocean model	
Radiometer wet troposphere correction	MWR using P2	AMR
Ionospheric correction	GIM model	dual-frequency altimeter ionosphere correction
Sea State Bias	Hybrid SSB model	MLE4 version derived from 1 year of MLE4 Jason-2 altimeter data with version 'd' geophysical models
Global ocean tide	GOT 4.8 ocean tide	
Earth tide	From Cartwright and Taylor tidal potential	
Pole tide	Wahr [1985]	
Mean Sea Surface	CNES_CLS_2011 untill cycle 34, CNES_CLS_2015 afterwards	

Table 6: *S*tandards used for SSH estimation on SARAL/AltiKa and Jason-3

When not otherwise stated, the standards from table 6 are used.

5.2. Mean of SSH mono-missioon crossover differences

The map of SSH mean ascending/descending differences at crossovers should ideally be close to zero: only time differences shorter than 10 days are selected in order to be as close as possible to the steady ocean hypothesis while maintaining a global sampling by crossovers. Of course this is untrue due to quickly evolving mesoscale ocean features, yet, large geographically correlated patterns on such maps indicate systematic differences between ascending and descending passes, which are generally errors. This can indicate either problems in the orbit computation or in geophysical corrections. Figure 55 shows the map of mean SSH differences at crossovers for SARAL/AltiKa and Jason-3, computed over the same period in a similar way (based on SARAL/AltiKa cycles).

Both missions show geographically correlated patterns of low amplitudes. The mean difference

is slightly negative on SARAL/AltiKa and Jason-3, with a larger mean difference observed on SARAL/AltiKa. Locally differences can reach 2 *cm* on SARAL/AltiKa while they remain below 1 *cm* on Jason-3.

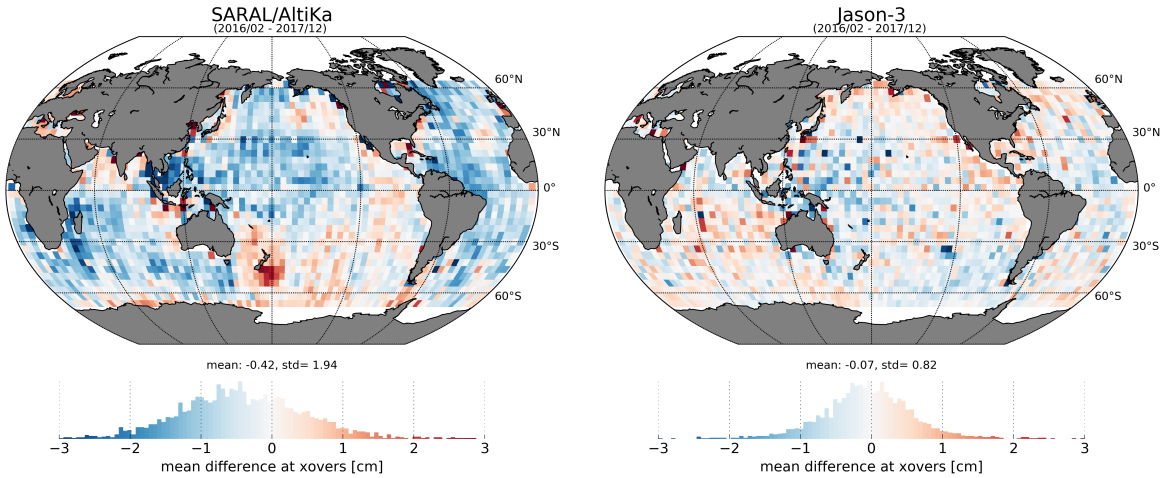

Figure 55: *Map of mean of SSH crossovers differences for [left] SARAL/AltiKa and [right] Jason-3.*

In addition to mapping the differences accumulate over several cycles, the global mean of SSH differences at crossovers is estimated for each cycle. This quantity is monitored over time to detect any issue on the mission.

Over SARAL/AltiKa lifetime, the evolution of the cycle-average mean SSH difference at crossovers is plotted on figure 56 for SARAL/AltiKa, Jason-2 and Jason-3. The left and right panels correspond to two different selections of crossovers used to estimate the mean (no selection at all and selection on bathymetry, latitude and oceanic variability), while plain and dotted lines correspond to two ways of averaging the SSH differences at crossovers (a simple ensemble mean and a latitude weighted mean based on the crossovers theoretical density). The weighted averaging method was described in the SARAL/AltiKa yearly report 2014 [29]. For SARAL/AltiKa, the mean difference is slightly negative $\approx -2/-4$ *mm* depending on the averaging method and the crossovers selection, Jason-2 and Jason-3 being closer to zero, around ≈ -1 *mm*. The mean value is very stable over time for the three missions, with a slightly larger cycle to cycle variability on Jason-2 and Jason-3 than on SARAL/AltiKa, but note that the samples used for Jason-2 and Jason-3 are smaller than those for SARAL/AltiKa due to different cycle lengths. One can also note a periodic signal around one year on SARAL/AltiKa, which is related to the β angle (see [9] for an in-depth analysis of such signals).

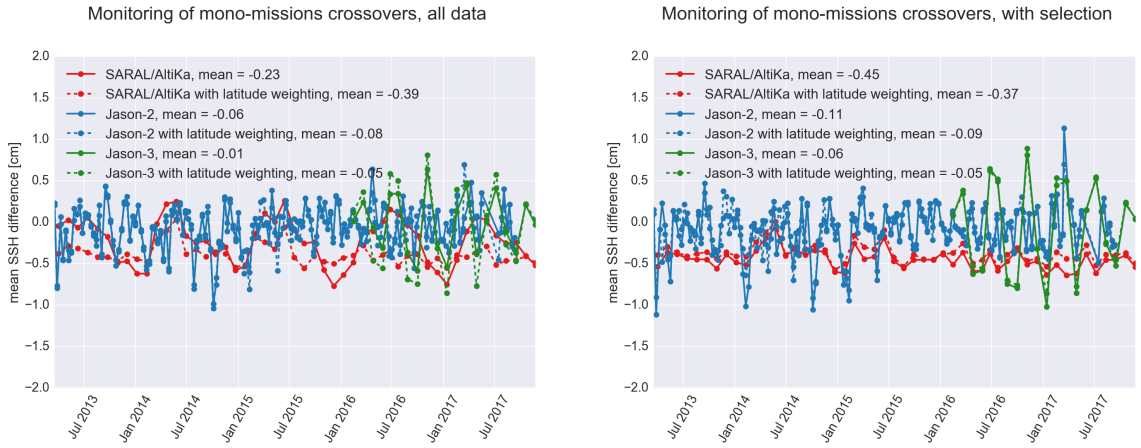

Figure 56: *Cycle per cycle monitoring of ascending/descending SSH differences at mono-mission crossovers for SARAL/AltiKa Jason-2 and Jason-3 for Saral cycles 1 to 114.*

5.3. Mean of SSH multi-mission crossover differences

On top of monomission crossovers that permits to detect systematic biases on one mission, crossovers differences are also estimated between different missions. In this case they are used to check for geographically correlated biases or drifts that could happen between two missions. Here SARAL/AltiKa is compared to Jason-2 and Jason-3 through their SSH differences at crossovers.

The temporal evolution of the mean of SARAL/AltiKa minus Jason-2 and SARAL/AltiKa minus Jason-3 SSH differences at crossovers is shown on figure 57. A selection for latitudes lower than 50°, deep ocean and low oceanic variability areas is used here, along with a mean estimation based on a latitude weighted average. The bold lines were computed using the radiometer wet tropospheric correction while the dotted lines are based on the model correction. In all cases the temporal evolution of SSH differences at crossovers is very steady for both SARAL/AltiKa / Jason-2 and SARAL/AltiKa / Jason-3 crossovers:

- the mean bias between SARAL/AltiKa and Jason-2 is around 46 *mm*,
- the mean bias between SARAL/AltiKa and Jason-3 is around 18 *mm*,
- there is no significant drift between SARAL/AltiKa and Jason-2 nor SARAL/AltiKa and Jason-3.

At some periods, differences up to 2 *mm* can be found when comparing the radiometer and model wet tropospheric corrections. There are two explanations for these differences:

- saturation of hot calibration counts, resulting in a drift of the SARAL/AltiKa radiometer wet tropospheric correction around October 2013,
- a 1 *mm* shift in wet tropospheric path delay after the SHM on SARAL/AltiKa (October 2014, [10]).

Rather than looking at the temporal evolution, mapping the SSH differences between SARAL/AltiKa and Jason-3 provides information about geographically correlated biases between the two missions. Such maps are shown on figure 58, they are both computed over the whole available period of

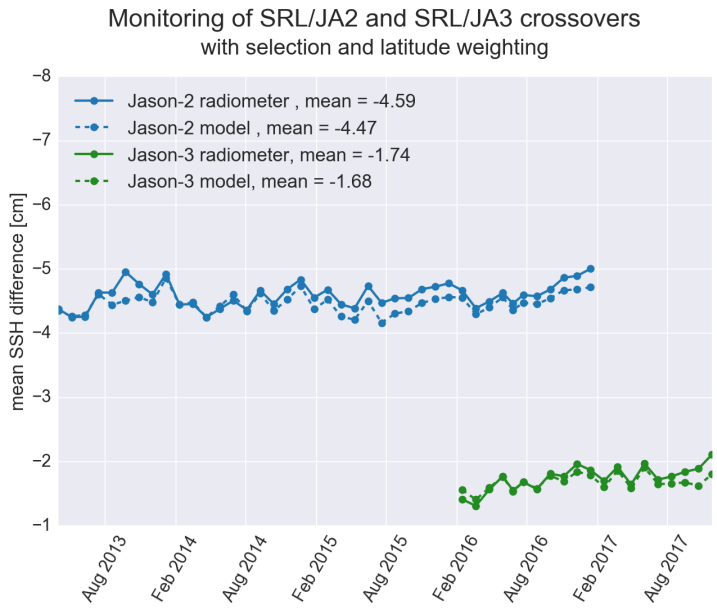

Figure 57: *Monitoring of mean of SARAL/AltiKa minus Jason-2 and SARAL/AltiKa minus Jason-3 differences at crossovers using radiometer wet troposphere correction (bold line) or ECMWF model wet troposphere correction (dotted line) for GDR data, ensemble mean (left) and latitude weighed mean (right).*

Jason-3 to have a suitable comparison and both maps are centered before plotting. Large scale biases are visible between the two missions with amplitudes up to ±3 cm. Using the radiometer on both missions (left of figure 58) shows a negative patch in the western tropical Pacific Ocean centered on Indonesia and a large positive patch in the Southern Ocean, which extends towards the north in Atlantic Ocean. As observed for mono-mission crossover differences, part of the observed pattern might come from orbit related issues and/or from geophysical corrections. Using the model wet tropospheric correction on both missions (right of figure 58) reduces the Southern Ocean patch and to a lesser extent the negative Indonesian patch, as well as a positive patch at the southern tip of Greenland. However the positive patch in the southern Atlantic Ocean remains. Improvements are expected from a new radiometer retrieval algorithm, as well as a new SSB model for SARAL/AltiKa as part of the futur GDR-E prducts.

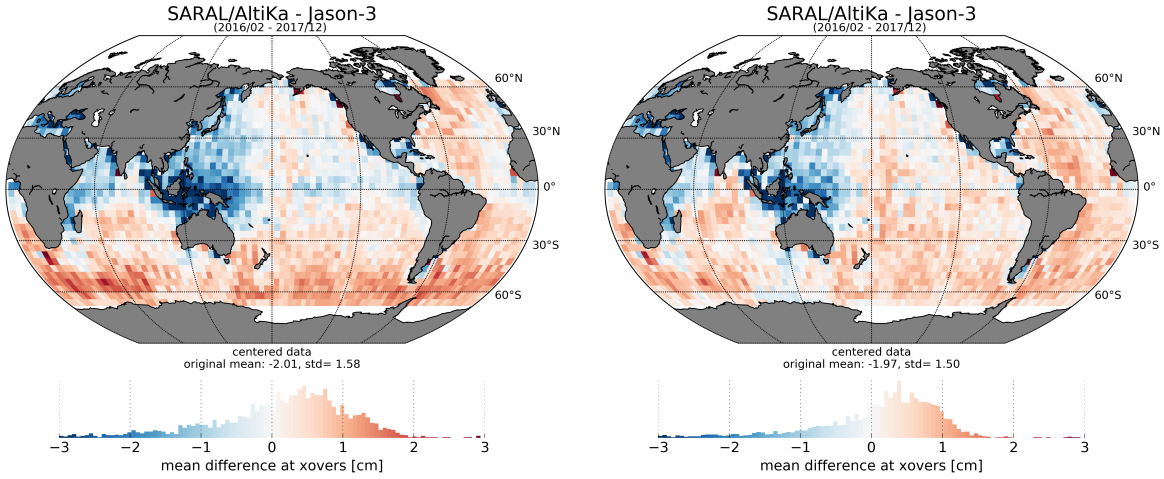

Figure 58: *Map of mean of SSH crossovers differences between SARAL/AltiKa and Jason-3 using the radiometer wet tropospheric correction (left) or the ECMWF model wet troposphere correction (right) for both missions. The maps are centered around the mean.*

5.4. Standard deviation of SSH crossover differences

The standard deviation of SSH differences at crossovers is a key performance metric for satellite altimetry missions. In this section the standard deviation of SSH differences at crossovers is investigated for SARAL/AltiKa and compared to Jason-2 and Jason-3.

The cycle per cycle standard deviation of SSH differences at crossovers is plotted on the left of figure 59 for different selections and averaging methods:

- solid black: no selection is applied, and the ensemble standard deviation is estimated without any weighting. In this case the standard deviation amounts to 6.88 cm and its temporal evolution is impacted by an annual signal due to varying sea ice extent.
- dotted black: no selection is applied on the crossovers, but the standard deviation is estimated after weighting the crossovers following the method described in [29]. This process slighlty reduces the standard deviation (6.33 cm) due to downweighting of crossovers at high latitudes and it also reduces the amplitude of the annual signal.
- solid red: shallow waters (bathymetry $< -1000\ m$), high latitudes and high variability areas have been removed. This is as close as possible to the steady ocean hypothesis and the standard deviation of SSH differences drops to 5.31 cm, no more annual cycle is observed.
- dotted red: uses the same selection as above, combined to a latitude weighting of the crossovers before estimating the standard deviation. Using this method leads to a small increase of the standard deviation of SSH differences at crossovers (at 5.49 cm)

The right part of figure 59 displays the geographical distribution of the standard deviation of SSH differences at crossovers. This map shows the expected patterns with high standard deviation observed in high ocean variability areas and in the Arctic Ocean (where some geophysical corrections such as tides, are less accurate).

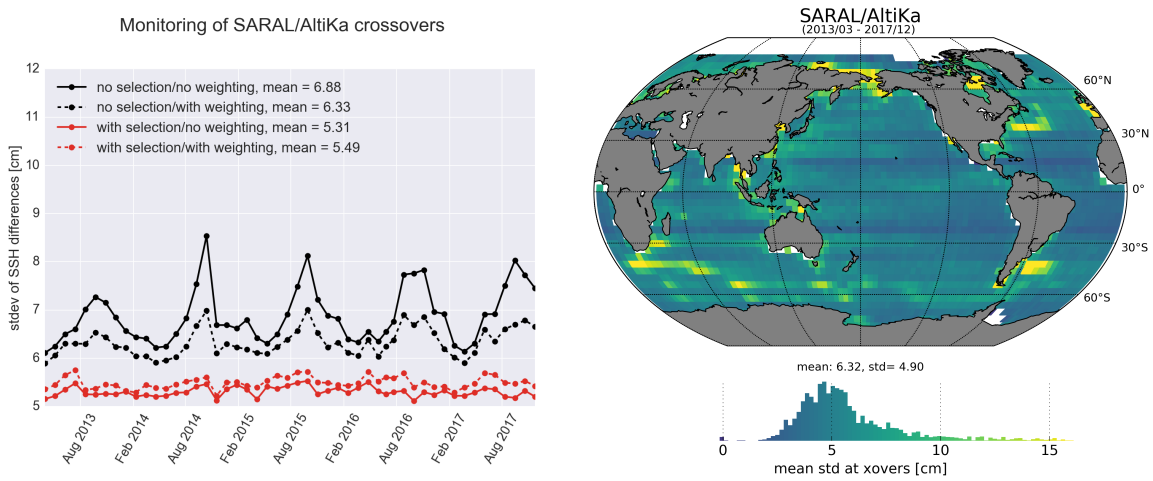

Figure 59: *Cycle by cycle standard deviation of SSH crossover differences for SARAL/AltiKa using different selections and averaging methods (left) and map of standard deviation at crossover points. In both cases the radiometer wet tropospheric correction is used.*

As part of the routine Cal/Val activities, the performance of SARAL/AltiKa is compared to Jason-2 and Jason-3 through the use of the standard deviation of SSH differences at crossovers. Figure 60 display comparisons between SARAL/AltiKa Jason-2 and Jason-3 performance at crossovers for different selections. In each case the performance using the radiometer and the model are displayed.

To account for the uneven distribution of crossover points, we estimate weighted statistics (figure 60) where the weights applied are based on the crossovers density. This allows to better compare two missions that do not share the same ground track. Similar results are obtained with these weighted statistics: depending on the wet troposphere correction choosen, SARAL/AltiKa's performance is equivalent to Jason's.

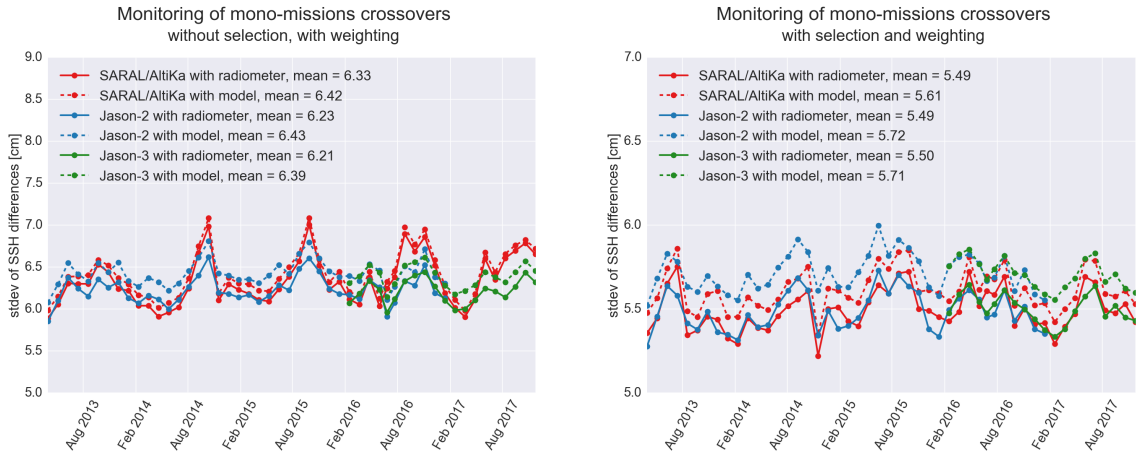

Figure 60: *Monitoring of the standard deviaiton of SSH differences at crossovers for SARAL/AltiKa Jason-2 and Jason-3 without any selection (left) and after removing high latitudes, shallow waters and high variability areas (right). A weighting based on crossovers density is applied.*

5.5. Performances of the different product types

Saral/AltiKa data are also available as OGDR and IGDR products, which are more rapidly available than GDR products. The main differences between the different data products are listed in table 7.

Auxiliary Data	Impacted Parameter	OGDR	IGDR	GDR
Orbit	Satellite altitude, Doppler correction, ...	DORIS Navigator	Preliminary (Doris MOE)	Precise (Doris + Laser POE)
Meteo Fields	Dry/wet tropospheric corrections, U/V wind vector, Surface pressure, Inverted barometer correction,...	Predicted	Restituted	Restituted
Pole Location	Pole tide height	Predicted	Predicted	Restituted
Mog2D	HF ocean dealiasing correction	Not available	Preliminary	Precise
GIM	Ionosphere correction	Predicted	Restituted	Restituted

Table 7: *D*ifferences between the auxiliary data for the O/I/Gdr products (from [15])

Figure 61 displays the monitoring of the cycle per cycle mean and standard deviation of SSH differences at crossovers for the OGDR, IGDR and GDR products. Regarding the mean, all three products show a good stability, of course the temporal variablity is greater for OGDR and IGDR than for GDR data. As expected GDR products provide the best performance with a standard deviation of the differences at crossovers of 5.3 cm. But IGDR data also exhibit a very good performance, with an average standard deviation of the differences of 5.4 *cm*, very close to the GDR value despite degraded standards (GDR-T and GDR-T Patch1) at the beginning of the period and a less accurate orbit solution (MOE vs. POE). OGDR data show a higher standard deviation at $\approx$ 6.8 cm.

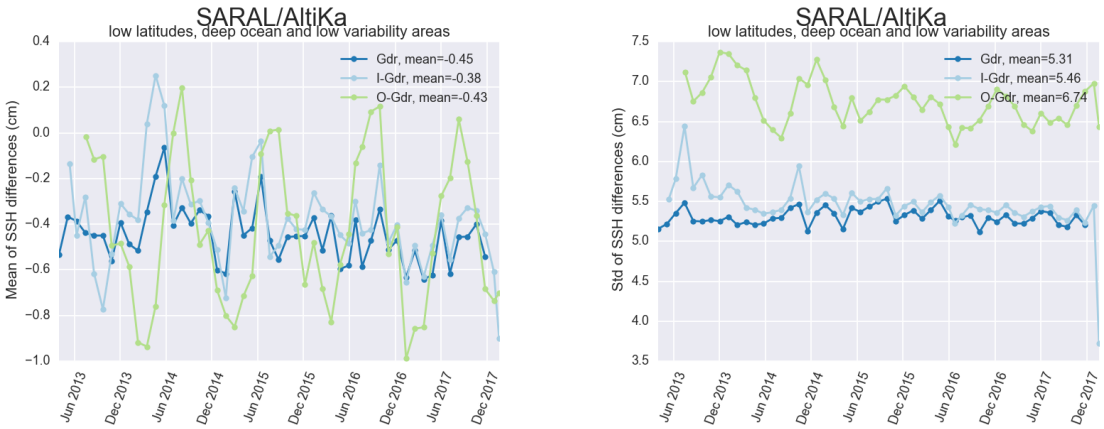

Figure 61: *Cycle per cycle monitoring of mean and standard deviation of SSH crossover differences for SARAL/AltiKa using radiometer wet troposphere correction and geographical selection (|latitude| < 50°, bathymetry < -1000 m and ocean variability < 20 cm rms).*

5.6. Estimation of pseudo time-tag bias

The pseudo time tag bias is found by computing at crossovers the regression between SSH differences and orbital altitude rate ($\dot{H}$), also called satellite radial speed :

$$\Delta SSH = \alpha \dot{H}$$

This method allows to estimate the time tag bias but also absorbs other errors correlated with $\dot{H}$ as for instance orbit errors. Therefore it is called "pseudo" time tag bias.

Figure 62 shows the monitoring of the pseudo datation bias for SARAL/AltiKa Jason-2 and Jason-3 on a cyclic basis. On average SARAL/AltiKa has a slightly lower pseudo time-tag bias than Jason-2 and Jason-3, around -0.02 ms, and appears to be more stable over time.

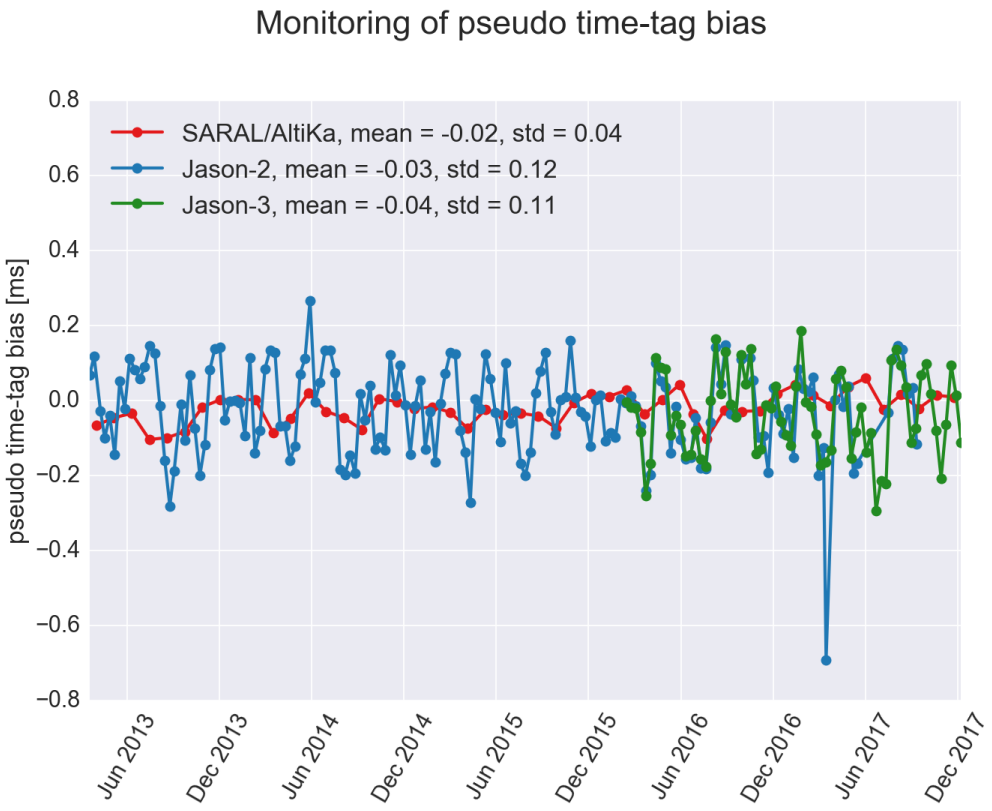

Figure 62: *Cycle per cycle monitoring of the pseudo time tag bias for SARAL/AltiKa and Jason-2*

6. Sea Level Anomalies along-track analysis

6.1. Overview

The Sea Level Anomalies (SLA) are computed along track from the SSH minus the mean sea surface where the SSH is estimated as defined in the previous section (5.1.):

$$SLA = SSH - MSS$$

where the mean sea surface used here is the CNES/CLS 15 model all along (cycle 1 to 114).

Figure 63 shows two maps of SLA from SARAL/AltiKa and Jason-3 over one cycle of SARAL/AltiKa (here cycle 106). The two maps show very similar patterns.

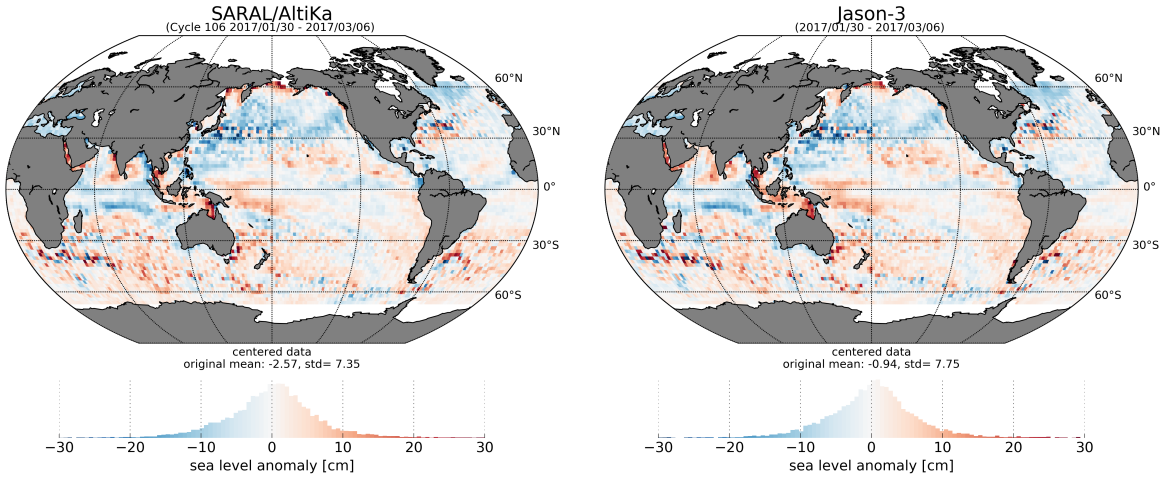

Figure 63: *SLA map for SARAL/AltiKa 106 cycle using the radiometer wet tropospheric correction (left) from SARAL/AltiKa data, and (right) from Jason-3 data over the same period.*

Computing differences between SARAL/AltiKa and Jason-3 allows a better appreciation of potential discrepancies between the two missions than individual maps. Figure 64 displays the average SLA differences between SARAL/AltiKa and Jason-3, for the radiometer and the modeled wet tropospheric correction. Both maps show geographically correlated differences with amplitudes up to ≈ 2 cm. The patterns are very similar to the ones observed at SARAL / Jason-3 crossovers with a positive patch in the Atlantic Ocean and a negative one around Indonesia. The amplitude of the differences is slightly reduced when using the model wet tropospheric correction on both missions.

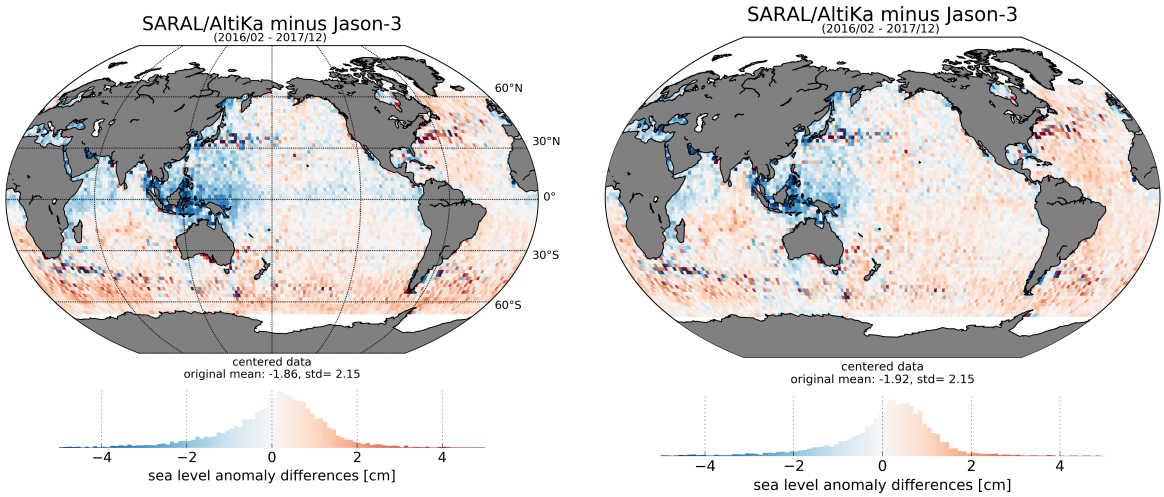

Figure 64: *Map of mean SLA differences between SARAL/AltiKa and Jason-3 using (left) the radiometer and (right) model wet tropospheric correction.*

6.2. Along-track SLA performances compared to Jason-2 and Jason-3

Looking at along-track SLA provides additionnal metrics to estimate the altimetry system performances. The evolution of the mean SLA allows the detection of shifts, drifts or geographically correlated biases, while looking at the SLA variance may also highlight changes in the long-term stability of the altimeter's system performance. Figure 65 displays the temporal evolution of the mean and standard deviation of SARAL/AltiKa Jason-2 and Jason-3 SLA, while figure 66 shows the SLA difference between SARAL/AltiKa and both Jason-2 and Jason-3.

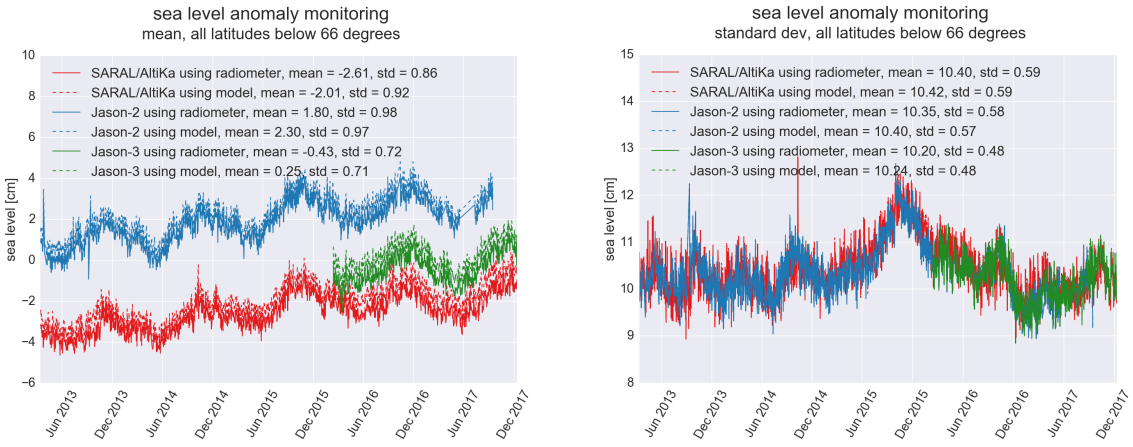

Figure 65: *Monitoring of daily mean (left) and daily standard deviation (right) of SLA of GDR data using the radiometer (plain lines) and the model (dotted lines) wet tropospheric corrections. Global statistics are estimated for all latitudes between* $-66°$ *and* $66°$.

SARAL/AltiKa Jason-2 and Jason-3 daily mean of SLA show similar signals and evolution.
There is an offset between SARAL/AltiKa and Jason-3 of around 1.8 *cm* (see figure 66), which is consistent with multi-mission crossovers analysis. The standard deviation of daily averages of SLA differences is below 5 *mm*. No statistically significant drift is observed between SARAL/AltiKa and

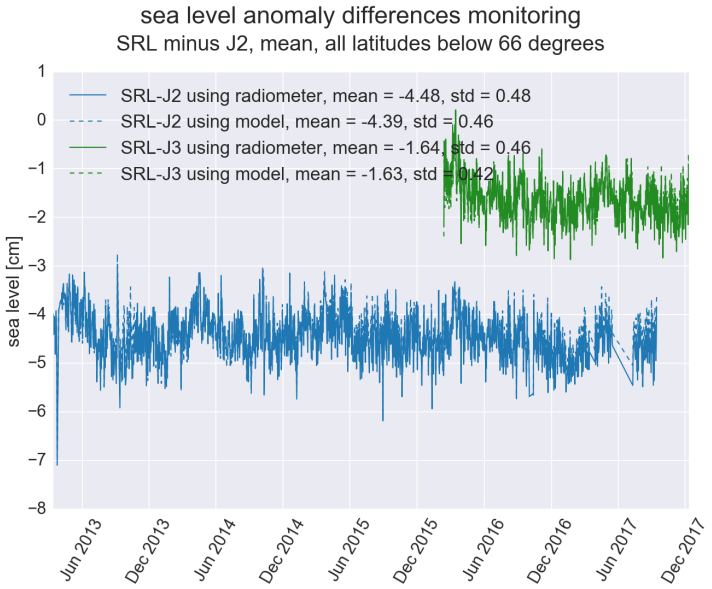

Figure 66: *Monitoring of the daily mean SLA difference between SARAL/AltiKa and Jason-2 / SARAL/AltiKa and Jason-3, using the radiometer and model wet tropospheric corrections.*

Jason-2 nor with Jason-3. Switching from the radiometer to the model wet tropospheric correction has little impact on daily averages of SLA differences between SARAL/AltiKa and Jason-2 or Jason-3, as daily SLA variations are much larger than the difference between wet tropospheric corrections.

6.3. Along-track performances of the different product types (OGDR/IGDR/GDR)

SARAL/AltiKa products are available for three data types (with different latency and precision): OGDR, IGDR and GDR. These products show somes differences in the product content which are summarized in table 7). Figure 67 displays the evolution of the mean and standard deviation of global SLA, as it is in the different products currently available. There are several shifts on the mean OGDR and IGDR values:

- in Feb 2014, when OGDR and IGDR, changed from Patch 1 to Patch 2,
- in July 2014, due to mean sea surface and editing changes.

There is one shift on the mean GDR timeseries corresponding to a mean sea surface standard change from the 2011 to 2015 CNES/CLS MSS in June 2016. Regarding standard deviation, GDR products show the lower standard deviation with 10.7 *cm*, while IGDR and OGDR data show a higher SLA variability, which is expected from less accurate orbit solutions and some geophysical corrections.

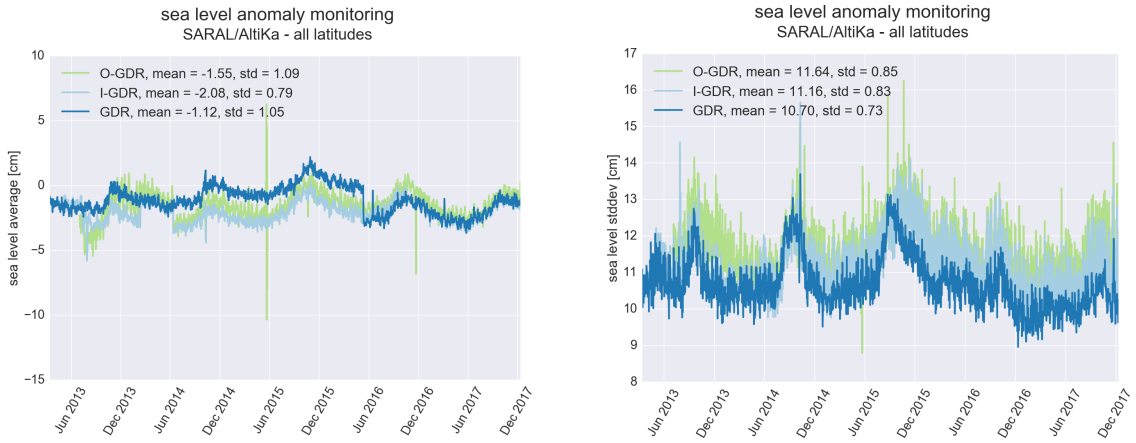

Figure 67: *Daily monitoring of the mean (left) and standard deviation [right] of global average SARAL/AltiKa SLA, using the radiometer wet tropospheric correction, for OGDR, IGDR and GDR products.*

6.4. SARAL/AltiKa as part of the GMSL record

SARAL/AltiKa data can easily be merged to the global Global Mean Sea Level (GMSL) record. Figure 68 presents two ways to do this. Left displays how SARAL/AltiKa blends in with the reference GMSL record while right is a zoom on the SARAL/AltiKa period where actual biases between missions are kept. Even though SARAL/AltiKa is not used to build the reference GMSL indicator (see [4] for further details) , with now more than 4 years of data, and Jason-2 available over the same period, we can give some credit to SARAL/AltiKa's global sea level trends estimates. Over the same period SARAL/AltiKa and Jason-2 show very similar global mean sea level rise rates indeed, around $4,6$ and $4,4$ mm/yr respectively.

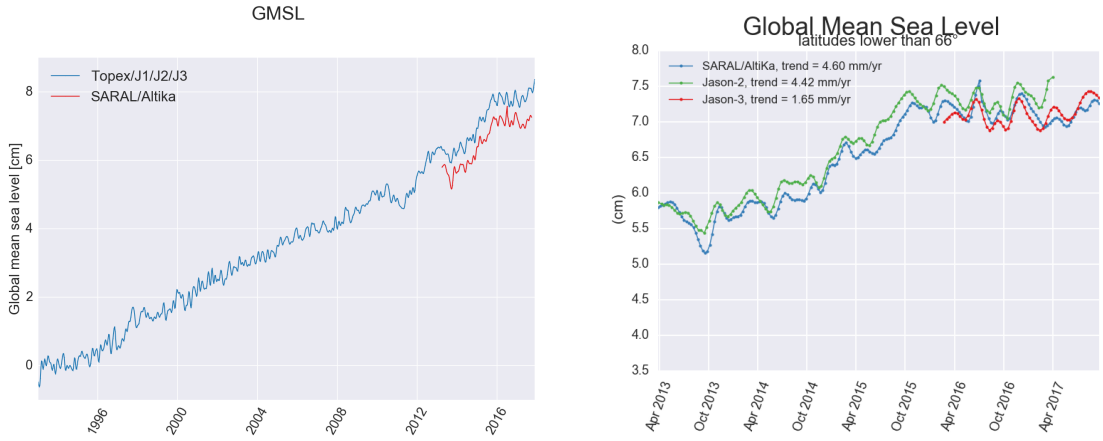

Figure 68: *[left] SARAL/AltiKa global mean record compared to the reference global mean sea level from TOPEX/Poseidon, Jason-1 and Jason-2 and Jason-3, and [right] a zoom on the SARAL/AltiKa period with biases between missions retained*

As for tide gaude comparison, figure 69 shows the SLA differences between the altimeters and the GLOSS/CLIVAR tide gauge network for Jason-2 (left) and SARAL/AltiKa (right). For more details about the calculation methods and the data used to have such comparisons, please feel free to check it out in the annual report of MSL activities [4]. As shown in the right panel of figure 69, the difference between SARAL/AltiKa's and tide gauge's SLA estimation is lower than $4mm$, which is highly satisfying and a comparable performance to Jason-2 (left). Moreover, thanks to tide gauge comparison, we can confirm that no significant drift affects SARAL/AltiKa's SLA.

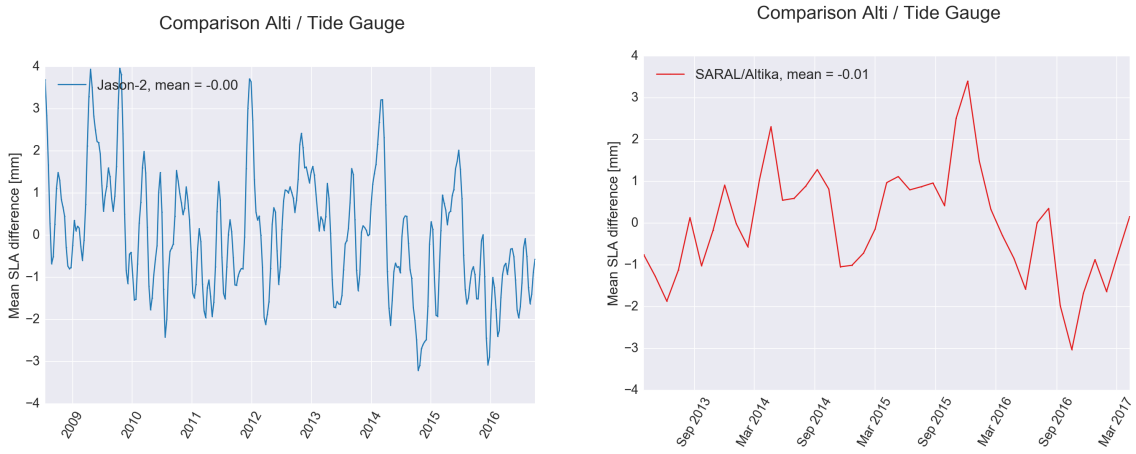

Figure 69: *SLA differences between the altimeters and the GLOSS/CLIVAR tide gauge network for Jason-2 (left) and SARAL/AltiKa (right).*

7. Conclusion

SARAL/AltiKa was launched on February, 25th 2013 and has been providing high quality sea surface height measurements for more than 4 years.

This report summarizes a variety of results, including comparisons with Jason-2 and Jason-3 to demonstrate the excellent quality of SARAL/AltiKa data. The main points of this performance assessment are summarized below:

- SARAL/AltiKa provides an excellent coverage of the ocean, with more than 99% of measurements available over ocean.
- Data quality is excellent, with only 2.6% of edited measurements, a value lower than the one of Jason-2.
- Global bias is of 18 mm with Jason-3 and of 46 mm with Jason-2.
- SLA statistics show no long term drifts, SARAL/AltiKa and Jason-2 and Jason-3 observe very similar SLA features when considering temporal evolution of global averages and also geographical patterns.
- Standard deviation of daily SLA averages differences between SARAL/AltiKa and both Jasons is below 5 mm.
- At crossovers SARAL/AltiKa shows a performance similar to Jason-2 with a standard deviation of 5.49 cm.

All these metrics confirm the excellent data quality of SARAL's data record, enventhough there is still some room for further improvement with updated wet tropo and SSB algorithm. One should bear in mind that 2016 was marked by a milestone for SARAL/AltiKa: the start of the drifting phase on July, 4th. As shown throughout the report, the orbit change does not have any measureable impacts on the instrument's performance. Besides, after 18 months on an unmaintained but slowly decaying altitude (see [2] for further details about the altitude decay of SARAL/AltiKa during its drifting phase), SARAL/AltiKa provides an extremely dense, albeit random, yearly coverage for geodetic applications (Mean Sea Surface or Bathymetry) and yields an enhanced mesoscale monitoring capability ([2]&[1]).

Mispointing events are still affecting the platform, resulting from random anomalies in reaction wheel friction. However there is no noticeable change in the occurence of these events, which are easily edited and do not affect the data quality. So far, SARAL/AltiKa data quality remains excellent.

The GDR dataset is not homogeneous (change of orbit standard at cycle 25 and change of mean sea surface model at cycle 34) for now, a reprocessing is planed in 2019.

8. Glossary

AMR Advanced Microwave Radiometer

CLS Collecte Localisation Satellites

CNES Centre National d'Etudes Spatiales

CNG Consigne Numerique de Gain (= Automatic Gain Control)

DEM Digital Elevation Model

DIODE Détermination Immédiate d'Orbite par Doris Embarqué

ECMWF European Centre for Medium-range Weather Forecasting

EDP Earliest Detection Part

GDR Geophysical Data Record

GDR-T Geophysical Data Record version T (test)

GIM Global Ionosphere Maps

GOT Global Ocean Tide

IGDR Interim Geophysical Data Record

JPL Jet Propulsion Laboratory (Nasa)

MLE Maximum Likelyhood Estimator

MOE Medium Orbit Ephemeris

MQE Mean Quadratic Error

MWR MicroWave Radiometer

MSS Mean Sea Surface

NSIDC National Snow and Ice Data Center

PF/RF PlatForm / RadioFrequency

PLTM PayLoad TeleMetry

POE Precise Orbit Ephemeris

OGDR Operational Geophysical Data Record

SALP Service d'Altimétrie et de Localisation Précise

SARAL Satellite with ARgos and ALtika

SSH Sea Surface Height

SLA Sea Level Anomaly

SLR Satellite Laser Ranging

SSB Sea State Bias

SWH Significant Wave Height

TEC Total Electron Content

TM TeleMetry

9. References

References

[1] Mercator Ocean Journal #56, 2017, *Special Issue CMEMS* section : High-level data processing and observation products (TACs), available at: https://www.mercator-ocean.fr/en/science-publications/mercator-ocean-journal/mercator-ocean-journal-56-special-issue-cmems/

[2] Dibarboure, G., Lamy, A., Pujol, M-I, 2018, The drifting phase of SARAL/AltiKa: securing a stable mesoscale sampling with an unmaintained decaying altitude, **in preparation**,will be submitted to *Remote Sensing*

[3] Vandemark, D., Chapron, B., Feng, H., Mouche, A., 2016, Sea surface reflectivity variation with ocean temperature at Ka-band observed using near-nadir satellite radar data, submitted to *Remote Sensing*

[4] Ablain, M., Taburet, N., Zawadzki, L., Jugier, R., Vayre, M., 2017, SALP annual report (2017) of Mean Sea Level Activities SALP-RP-MA-EA-23189-CLS available from http://www.aviso.altimetry.fr/fileadmin/documents/calval/annual_report_****.pdf

[5] Roinard, H., 2017, Jason-2 validation and cross calibration activities (Annual report 2017) SALP-RP-MA-EA-23186-CLS available from http://www.aviso.altimetry.fr/fileadmin/documents/calval/annual_report_****.pdf

[6] Lauret, O., 2016, Jason-3 validation and cross calibration activities (Annual report 2016) SALP-RP-MA-EA-23060-CLS available from https://www.aviso.altimetry.fr/fileadmin/documents/calval/validation_report/J3/annual_report_j3_2016.pdf

[7] Dibarboure, G. and A. Lamye, 2017, The drifting phase of SARAL/AltiKa: securing a stable mesoscale sampling with an unmaintained decaying altitude, submitted to *Remote Sensing*

[8] Prandi, P., S. Philipps, V. Pignot and N. Picot, 2015, SARAL/AltiKa Global Statistical Assessment and Cross-Calibration with Jason-2 *Marine Geodesy*, 38, DOI: 10.1080/01490419.2014.995840

[9] Ollivier, A. 2016, Assessment of Orbit Quality through the Sea Surface Height calculation - Yearly report 2016 - SALP activities, SALP-RP-MA-EA-23080-CLS

[10] Prandi, P., V. Pignot, 2015, Saral/ Altika validation and cross calibration activities (Annual report 2015) SALP-RP-MA-EA-22957-CLS available from http://www.aviso.altimetry.fr/fileadmin/documents/calval/annual_report_al_2015_01.pdf

[11] Philipps, S., P. Prandi and V. Pignot, 2013, Saral/ Altika validation and cross calibration activities (Annual report 2013) SALP-RP-MA-EA-22271-CLS available from http://www.aviso.altimetry.fr/fileadmin/documents/calval/annual_report_Altika_2013.pdf

[12] Frery, M.-L. *et al.*, 2014, Correction du canal 37GHz du radiomètre AltiKa, CLS/DOS/NT-14-115

[13] Aouf, L. and J.-M. Lefèvre, 2013, The impact of Saral/Altika wave data on the wave forecasting system of Météo-France : update, Oral presentation at SARAL/AltiKa 1st Verifica-

tion Workshop, Toulouse, France, available at http://www.aviso.oceanobs.com/fileadmin/documents/ScienceTeams/Saral2013/24_wave_lotfi.pdf

[14] Brown, G.S., 1977, The average impulse response of a rough surface and its application", *IEEE Transactions on Antenna and Propagation*, Vol. AP 25, N1, pp. 67-74

[15] SARAL/AltiKa Products handbook, 2013, *SALP-MU-M-OP-15984-CN* edition 2.3, available at: http://www.aviso.oceanobs.com/fileadmin/documents/data/tools/SARAL_Altika_products_handbook.pdf

[16] Boy, F. and J.-D. Desjonqueres, 2010, Note technique datation de l'instant de reflexion des échos altimètres pour POSEIDON2 et POSEIDON3, *TP3-JPOS3-NT-1616-CNES*

[17] Desjonquères, J. D. , G. Carayon , N. Steunou and J. Lambin, 2010, Poseidon-3 Radar Altimeter: New Modes and In-Flight Performances, *Marine Geodesy*, 33:1, 53–79, available at http://pdfserve.informaworld.com/542982__925503482.pdf

[18] Faugere, Y., A. Delepoulle, F.Briol, I. Pujol, N. Picot, E. Bronner; 2013, Altika in DUACS: Status after 2 months (and perspectives), oral presentation at SARAL/AltiKa 1st Verification Workshop, Toulouse, France, available at http://www.aviso.oceanobs.com/fileadmin/documents/ScienceTeams/Saral2013/34_Altika_in_Duacs_Faugere.pdf

[19] Griffin, D. and M. Cahill, 2013, Use of AltiKa NRT sea level anomaly in the Australian multi-mission analysis, Oral presentation at SARAL/AltiKa 1st Verification Workshop, Toulouse, France, available at http://www.aviso.oceanobs.com/fileadmin/documents/ScienceTeams/Saral2013/33_multi_mission_gridding_GRIFFIN.pdf

[20] Lillibridge, J., R. Scharroo, S. Abdalla, and D. Vandemark, 2013, One-and Two-Dimensional Wind Speed Models for Ka-band Altimetry, *Journal of Atmospheric and Oceanic Technology*, doi: http://dx.doi.org/10.1175/JTECH-D-13-00167.1

[21] Picot, N., A. Guillot, P. Sengenès, J. Noubel, N. Steunou, S. Philipps, P. Prandi, G. Valladeau, M. Ablain, S. Desai, B. Haines and S. Fleury, 2013, Data Quality Assessment Of The SARAL/AltiKa Ka-band Mission, Oral presentation at OSTST, Boulder, USA, available at http://www.aviso.oceanobs.com/fileadmin/documents/OSTST/2013/oral/Picot_SARAL_Data_Quality_Assessment.pdf

[22] Philipps, S. and V. Pignot, 2014, Saral/AltiKa reprocessing GDR-T Patch2, SALP-RP-MA-EA-22345-CLS/CLS.DOS/NT/14-031

[23] Scharroo, R., and J. L. Lillibridge, 2005, Non-parametric sea-state bias models and their relevance to sea level change studies, in *Proceedings of the 2004 Envisat & ERS Symposium*, Eur. Space Agency Spec. Publ., ESA SP-572, edited by H. Lacoste and L. Ouwehand

[24] Stenou, N., P. Sengenes, J. Noubel, N. Picot, J.D. Desjonquères, J.C. Poisson, P. Thibaut, F. Robert and N. Tavenea, 2013, AltiKa Instrument : In-Flight Stability And Performances, Oral presentation at OSTST, Boulder, USA, available at http://www.aviso.oceanobs.com/fileadmin/documents/OSTST/2013/oral/Steunou_OSTST2013_AltiKa_Instrument.pdf

[25] SARAL System Requirements, *SRL-SYS-SP-010-CNES*

[26] Thibaut, P., O.Z. Zanifé, J.P. Dumont, J. Dorandeu, N. Picot, and P. Vincent, 2002, Data editing: The MQE criterion, *Paper presented at the Jason-1 and TOPEX/Poseidon Science Working Team Meeting, New-Orleans (USA), 21-23 October*

[27] Tolman, H. L., 2014, User manual and system documentation of WAVEWATCH III version 4.18. *NOAA / NWS / NCEP / MMAB Technical Note 316, 194 pp.* available at http://polar.ncep.noaa.gov/waves/wavewatch/manual.v4.18.pdf

[28] The WAVEWATCH III Development Group., 2016, User manual and system documentation of WAVEWATCH III version 5.16. *NOAA / NWS / NCEP / MMAB Technical Note 329, 326 pp.* available at http://polar.ncep.noaa.gov/waves/wavewatch/manual.v5.16.pdf

[29] Prandi, P., V. Pignot and S. Philipps, 2015, Saral/ Altika validation and cross calibration activities (Annual report 2014), SALP-RP-MA-EA-22418-CLS

[30] Roinard, H., S. Philipps and O. Lauret, 2016, Jason-2 validation and cross calibration activities (Annual report 2015), SALP-RP-MA-EA-XXXXX-CLS available at http://www.aviso.altimetry.fr/en/data/calval.html

[31] Roinard, H., P. Matton and S. Philipps, 2015, Jason-2 validation and cross calibration activities (Annual report 2014), SALP-RP-MA-EA-22409-CLS available at http://www.aviso.altimetry.fr/en/data/calval.html

[32] Pujol, M.-I., Y. Faugere, G. Dibarboure, P. Schaeffer, A. Guillot and N. Picot, 2015, The recent drift of SARAL: an unexpected MSS experiment, oral presentation at the 2015 OSTST, Reston, VA

[33] - Dibarboure, G., F. Boy, J. D. Desjonqueres, S. Labroue, Y. Lasne, N. Picot, J. C. Poisson, and P. Thibaut, 2014: Investigating short-wavelength correlated errors on low-resolution mode altimetry. *J. Atmos. Oceanic Technol.*, **31**, 1337–1362, doi:10.1175/JTECH-D-13-00081.1

[34] - Dufau, C., M. Orsztynowicz,G. Dibarboure, R. Morrow, and P.-Y. Le Traon (2016), Mesoscale resolution capability of altimetry:Present and future, *J. Geophys. Res.Oceans*, **121**, doi:10.1002/2015JC010904.

[35] Edward D. Zaron , Robert deCarvalho, 2016. Identification and Reduction of Retracker-Related Noise in Altimeter-Derived Sea Surface Height Measurements. *Journal of Atmospheric and Oceanic Technology*, p201-210, doi:10.1175/JTECH-D-15-0164.1

10. Annex

10.1. Content of Patch 1

Hereafter the content of Patch 1 is recalled. All GDR data up to cycle 7 included were initially produced with this patch. It was used to produce IGDR data from cycle 4 pass 395 to cycle 10 pass 565.

Altimeter calibration file : The altimeter calibration stability has been analysed. Based on the actual data, we have implemented an averaging of the calibrations over a 7 days window for the low pass filter (identical to Jason-2) and 3 days for the internal path delay and total power (not used on Jason-2). This will slightly reduce the daily noise observed in the altimeter calibration data.

Altimeter characterization file : We have updated the altimeter characterization file using the flight calibration of the gain values (4 calibrations performed). The impact is very small (of the order of 0.01 dB).

Retracking look-up tables : We have updated the ocean retracking look-up tables using the flight calibration data (PTR). The impact is very small on the range and sigma0 values but of the order of 15 cms on SWH for low sea states.

MQE : We have analyzed the altimeter flight data and based on the observed MQE values over ocean a threshold of 2.3E-3 (Jason-2 value is 8E-3) is used for the 1Hz data computation.

Neural network : A first linear relation has been computed between the measured BT and the simulated one. This linear relation is applied on the 23.8 GHz only – the same analysis will be conducted on the 37 GHz and sigma0. This generates a bias on the radiometer wet tropospheric correction which is now much more consistent with the model one.

Atmospheric attenuation : The value outputted by the neural algorithm is now recorded in the level2 products (it was set to 0 at the beginning of the mission). Rad_water_vapor and rad_liquid_water: The values have been corrected to comply with the actual unit in the level2 products (kg/m^2). But the rad_liquid_water remains not reliable as an anomaly has been noticed in the neural network.

SSHA : The radiometer wet tropospheric correction is now used to compute this value (the model value was used at the beginning of the mission).

Controls parameters : The threshold values have been updated with in-flight data. This is a first tuning – additional work is necessary.

10.2. Content of Patch 2

Hereafter the content of Patch 2 is recalled. GDR data were produced using Patch 2 from cycle 8 onwards. Cycles 1 to 7 were reprocessed with the Patch 2 to provide a consistent dataset

Wind look-up table : The table provided by NOAA is used. This table is only based on the measured sigma0, taking into account the atmospheric attenuation (sigma0 at the surface). (Reference: Lillibridge et al. [20])

SSB look-up table : The table provided by R. Scharroo is used (same method as in [23]). We use only the significant wave height to compute the SSB.

Radiometer neural algorithm : Taking into account several months of AltiKa measurements, the neural network coefficients have been updated. Note that this modifies the radiometer related parameters (radiometer wet troposphere correction, atmospheric attenuation, radiometer liquid water content and radiometer water vapor content).

Ice-2 retracking algorithm : The algorithm has been updated taking into account the AltiKa Ka band specificities (ice2 algorithm was based on ENVISAT Ku band experience).

FES2012 tide model : This new tide model is included, improving the SSH accuracy in coastal zones. (Reference : http://www.aviso.oceanobs.com/en/data/products/auxiliary-products/global-tidefes2004-fes99/description-fes2012.html)

Matching pursuit algorithm : The algorithm based on J. Tournadre proposal has been tuned to comply to AltiKa Ka band specificities.

MQE parameter scale factor : The scale factor of the MQE has been modified.

Update of the altimeter characterization file : The altimeter characterization file has been modified in order to account for 63 values of altimeter gain control loop (AGC). This has impacts over sea ice and land hydrology, in some cases the AGC was set to default value in current P1 products.

Doris on ground processing (Triode) : The Doris navigator ground processing has been upgraded to reduce the periodic signal observed on the altitude differences with MOE/POE.